Differential gene expression screening uncovers downregulation of the cell cycle regulator BTG2 as an important step in renal tumor biology

Inauguraldissertation

zur Erlangung der Würde eines Doktors der Philosophie

vorgelegt der

Philosophisch-Naturwissenschaftlichen Fakultät

der Universität Basel

von

Kirsten Struckmann

aus Deutschland

Basel, 2003

Genehmigt von der Philosophisch-Naturwissenschaftlichen Fakultät

auf Antrag von

Prof. Dr. med Christoph Moroni (Fakultätsverantwortlicher)

Prof. Dr. Nancy Hynes (Korreferentin)

Basel, den 21.10.2003

Prof. Dr. Matthias Tanner (Dekan)

Meinen Eltern Dieter und Christel Struckmann

CONTENTS

I ACKNOWLEDGEMENTS 6

II ABBREVIATIONS 7

III ABSTRACT 8

1 INTRODUCTION 10

1.1 EPIDEMIOLOGY OF RENAL CELL CANCER 10
1.2 ETIOLOGY OF RCC 11
1.3 PROGNOSIS OF RCC 11
1.4 THERAPEUTICAL APPROACHES FOR RCC 12
1.5 PROGNOSTIC PARAMETERS IN RCC 12
1.6 CLEAR CELL RENAL CELL CARCINOMA (CRCC) 16
1.6.1 Histopathology of cRCC 16
1.6.2 Cytogenetic and molecular alterations in cRCC 16
1.6.3 Molecular carcinogenesis of cRCC 19
1.7 CDNA AND TISSUE MICROARRAY TECHNOLOGIES FOR THE IDENTIFICATION OF CRCC RELEVANT GENES 20
1.8 AIM OF THE THESIS 21

2 MATERIAL AND METHODS 23

2.1 CELL CULTURE 23
2.2 RNA EXTRACTION 23
2.3 CDNA ARRAY EXPERIMENTS 25
2.4 RNA *IN SITU* HYBRIDIZATION ON FROZEN RENAL TISSUE MICROARRAYS 26
2.5 CLONING OF *BTG2* AND *G3PDH* SEQUENCES 29
2.6 NORTHERN BLOT ANALYSIS 32
2.7 QUANTIFICATION OF *BTG2* MRNA COPY NUMBERS USING THE LIGHTCYCLER 34
2.7.1 General aspects of quantitative PCR using the LightCycler system 34
2.7.2 Generation of standard curves from BTG2 and G3PDH in vitro transcripts 36
2.8 BTG2 MRNA EXPRESSION IN PRIMARY CRCC AND NORMAL RENAL TISSUE 39
2.9 INDUCIBILITY OF *BTG2* MRNA EXPRESSION IN CRCC CELL LINES 40

3 RESULTS 41

3.1 CDNA ARRAY ANALYSIS 41
3.2 RNA *IN SITU* HYBRIDIZATION 43
3.3 MOLECULAR STUDIES ON *BTG2* TO EVALUATE ITS IMPORTANCE FOR CRCC BIOLOGY 50
3.3.1 Northern blot analysis 52
3.3.2 BTG2 mRNA expression in primary cRCC and normal renal tissue evaluated by quantitative RT-PCR 53
3.3.3 Modulation of BTG2 mRNA expression in cRCC cell lines 56

4 DISCUSSION 61

4.1 COMBINATION OF CDNA AND TISSUE MICROARRAY TECHNOLOGIES FOR THE IDENTIFICATION OF CRCC RELEVANT GENES 61

4.2 *BTG2* – A NEW CANDIDATE GENE FOR RENAL TUMOR BIOLOGY? 66
4.3 CONCLUSION 74

5 APPENDIX 76

6 LITERATURE 78

7 CURRICULUM VITAE 98

I Acknowledgements

First of all, I want to thank Prof. Dr. med. Michael J. Mihatsch for hosting and supporting my work at the Institute of Pathology.

I am very grateful to Prof. Dr. med Holger Moch for giving me the opportunity to work in his group, for his excellent supervision during the whole time of my PhD work, and for informative discussions about the pathobiology of renal cancer.

My special thanks go to the members of my thesis committee, Prof. Dr. med. Christoph Moroni and Dr. Nancy Hynes for providing excellent advice and for very helpful discussions.

I am deeply thankful to Dr. Peter Schraml and Dr. Ronald Simon because they teached me so many things about research work, they always had time for fruitful discussion, and they supported me during the whole time of my PhD thesis.

Thanks to all of the members of the laboratory for their friendship, collegiality, and technical assistance. In particular, I would like to thank Alexander Rufle for informative discussions about molecularbiological techniques and his professional assistance and also Martina Mirlacher, Martina Storz, and Yvonne Knecht for preparing frozen sections and histological stainings needed in my thesis.

I also would like to thank Dr. Heide Tullberg who gave me very helpful instructions for my work in the cell laboratory.

Finally, I would like to thank my whole family, in particular my parents Dietrich and Christiane Struckmann, and Daniele Calvano Forte for supporting me during the whole time of my PhD studies.

II Abbreviations

AJCC	**A**merican **J**oint **C**ommitte on **C**ancer
bp	**b**ase **p**air
CAP	**C**ollege of **A**merican **P**athologists
CGH	**C**omparative **G**enomic **H**ybridization
chRCC	**Ch**romophobe **R**enal **C**ell **C**ancer
cRCC	**C**lear **C**ell **R**enal **C**ell **C**ancer
E	Amplification **E**fficiency
FISH	**F**luorescence ***in situ*** **H**ybridization
H&E staining	**H**emalaun & **E**osin Staining
IHC	**I**mmuno**h**isto**c**hemistry
kb	**k**ilo**b**ase
LOH	**L**oss **o**f **H**eterozygosity
NCBI	**N**ational **C**enter for **B**iotechnology **I**nformation
pRCC	**P**apillary **R**enal **C**ell **C**ancer
RCC	**R**enal **C**ell **C**ancer
RISH	**R**NA ***in situ*** **H**ybridization
RT-PCR	**R**everse **T**ranscription – **P**olymerase **C**hain **R**eaction
pT category	**P**athological **T**umor category (extension of primary tumor mass)
TMA	**T**issue **M**icro**a**rray
TNM system	**T**umor, (Lymph -)**n**ode, (distant) **M**etastases system (pathological tumor classification system)
TPA	12-O-**t**etradecanoyl**p**horbolester-13-**a**cetate
UICC	**U**nion **N**ationale **C**ontre le **C**ancer

III Abstract

Renal cell cancer (RCC) is the most common malignancy affecting the adult kidney. The most prevalent RCC subtypes is clear cell RCC (cRCC), which accounts for 75% of all malignant lesions. RCC is characterized by an unpredictable clinical course and a poor prognosis. Very little is known about molecular alterations involved in initiation and progression of RCC. Identification of molecular markers might facilitate diagnosis and outcome predictions and help to develop innovative and novel treatment options. For this reason, it was the aim of this thesis to identify RCC associated genes. In a first part, potentially renal tumor relevant genes were uncovered using a combination of cDNA and tissue microarray technology. In a second part, one gene was selected to further evaluate its impact on RCC biology using Northern blot analysis, quantitative RT-PCR, and functional studies in cRCC cell lines.

To uncover renal cancer associated genes, gene expression profiles of four cRCC cell lines and normal renal tissue were compared using BD Atlas™ Human Cancer 1.2 cDNA microarrays. Twenty-five genes were found significantly differentially expressed. To evaluate the relevance of those genes for RCC, mRNA expression levels were further studied by RNA *in situ* hybridization on a tissue microarray generated from 61 snap frozen primary RCC and 12 normal renal tissues. Five genes (*VIM*, *CD74*, *CHES1*, *LITAF*, and *BTG2*) appeared to be highly interesting renal carcinogenesis relevant genes. Of those genes, three (*CHES1*, *LITAF*, and *BTG2*) have never been associated with renal cancer before.

BTG2, a negative cell cycle regulator, which was expressed in normal renal tissue but downregulated in cRCC cell lines and primary cRCCs, was chosen for further experiments. Northern blot analysis confirmed the results obtained by cDNA and tissue microarray analysis. Quantitative RT-PCR analysis in 42 primary cRCCs and 17 normal renal tissues revealed up to 44-fold reduced *BTG2* mRNA expression in the tumor tissues. Decrease of *BTG2* mRNA expression was not associated with advanced disease indicating that reduction of *BTG2* mRNA expression is rather an early event in renal carcinogenesis. In cRCC cell lines, *BTG2* mRNA expression was weakly inducible by the phorbolester TPA in one of four cultures. In contrast, increasing cell densities lead to slightly elevated *BTG2* mRNA expression in three of four cRCC

cell lines. Importantly, in both experiments *BTG2* mRNA levels did not reach values observed in normal renal tissue by far. The results obtained in the second part of this thesis strongly suggest that downregulation of *BTG2* is an important step in renal cancer development. Further experiments (allelic deletion, mutation and methylation analysis and also re-expression of *BTG2* in cRCC cell lines) are necessary to show whether *BTG2* is a new renal tumor suppressor gene.

In summary, application of high throughput cDNA microarray analysis in combination with tissue microarray technology allowed the identification of five genes, which might play a role in renal tumor biology. Further studies on *BTG2*, the most interesting candidate gene, indicate that downregulation of *BTG2* mRNA expression is an early and important step in renal carcinogenesis. More experiments will show whether *BTG2* is a new renal tumor suppressor gene.

1 Introduction

1.1 Epidemiology of renal cell cancer

Renal cell cancer (RCC) is the umbrella term for a family of very heterogenous tumors, which were primarily classified based on cytomorphological characteristics and their site of origin (1). All RCC subtypes have in common that they are derived from epithelial cells of the renal tubulus system (nephron). The most prevalent RCC subtypes are clear cell RCC (cRCC), papillary RCC (pRCC), and chromophobe RCC (chRCC) which account for 75%, 10%, and 5% of all malignant lesions of the kidney, respectively. Duct-Bellini carcinomas, a very rare and aggressive subtype, account for 1% of all renal tumors. Three to five percent of all renal carcinomas remain unclassified since they do not fit into any of the mentioned categories. Not only malignant lesions but also benign tumors derive from the nephron. Oncocytoma, the most common benign lesion, arises from the distal tubulus epithel and accounts for 5% of all renal lesions (2).

Referring to the data provided by Globocan 2000 (www-dep.iarc.fr/globocan/globocan.html), RCC accounts for about 2% of all human cancers. It is the most common malignancy affecting the adult kidney. For the year 2000, the estimated world-wide incidence was about 189.000 and the world-wide mortality was about 91.000. About two-thirds of these cases are diagnosed in more developed countries. In Switzerland, the estimated incidence for the year 2000 was about 880 and the mortality was about 440. Men are more frequently affected by cRCC and pRCC than women. In contrast, chRCC is more frequently found in women than in men (3).

There has been a strong increase in the incidence rate of RCC within the past decades. Frequent usage of modern abdominal imaging modalities lead to incidental detection particularly of small, asymtomatic renal tumors and explain the increasing incidence of RCC. In 1970 merely 10% of the renal tumors were diagnosed incidentally whereas in 1998 already 61% were found by accident in a routinous check-up (4-6).

1.2 Etiology of RCC

According to Dhôte et al. (7), who reviewed more than 100 publications released between 1987 and 1998, accepted risk factors for renal cancer are heavy smoking and severe obesity. Interestingly, both risk factors are sex-linked since smoking leads to a higher incidence of RCC in men whereas severe obesity is significantly associated with renal cancer in women. Several types of exposure are also thought to be associated with RCC. For instance, workers in the iron, steel, glas, and petrol industry are at higher risk of developing RCC. Also, intake of phenacetin (analgesic) and thiazidic (antihypertensive drug) has been shown to be associated with renal cancer.

1.3 Prognosis of RCC

Among the most common RCC subtypes, cRCCs have the worst prognosis, directly followed by pRCCs (5-year-survival-rates 50% and 58%, respectively). In contrast, chRCCs show a significantly better outcome. Seventy-eight % of patients affected by chRCC are still alive 5 years after diagnosis (3).

The prognosis for patients suffered from RCC largely depends on the development of metastases. Due to the lack of early symptoms, the percentage of advanced already metastatic tumors at first presentation is rather high. Additionally, 40 to 50% of non-metastatic tumors at first presentation will metastasize during the course of disease. In 80 to 85% of these cases, metastases occure within three years after presentation (8, 9). Frequent sites for dissemination are lung, bone, liver, and brain but additional, uncommon sites are typical for renal cancer (8, 10).

Late recurrance after long-term, disease free survival is another peculiarity of renal cancer. McNichols et al. (11) found a recurrence rate of 11% in a group of 506 10-year-survivors. Therefore, a patient with proven RCC can never be considered cured.

1.4 Therapeutical approaches for RCC

Therapy of choice for localized tumors is nephrectomy, which implies the excision of the tumor containing kidney and, in case of total nephrectomy, the adrenal gland and auxiliary lymphnodes (12). After nephrectomy, the 5-year survival rate of localized, organ-confined RCC is between 88% and 100% (13).

Once the tumor becomes metastatic, therapy remains a challenge for the oncologist. RCC has been shown to be nearly insensitive towards conventional chemo-, hormonal, and radiation therapy (14-17). The resistance towards chemotherapeutical agents might be explained by (i) presence of the transmembrane drug-transporting p170 glycoprotein (*MDR1*), which causes efflux of the therapeutical drugs from the tumor cells, in a large subset of RCC (18, 19) and (ii) the low growth fraction and long doubling time of RCC resulting in a reduced susceptibility of renal carcinoma cells to the effects of chemotherapeutic agents (19, 20).

In contrast to conventional therapies, immunotherapy seems to have at least some effect on disease progression. The principal cytokines used for RCC therapy are interferon-α and interleukin-2 (19). Recently, the overall response rate for interferon-α was 11 to 16% (21, 22). Although, duration of response is less than 2 years, some long term survivors have been described (21). The objective respones rates for interleukin-2 were between 15% and 20% (23-25). Among patients with complete or partial response, 60% and 18% were alive 5 years after diagnosis, respectively (24).

1.5 Prognostic parameters in RCC

Prognostic factors are used to predict the course of a disease, to choose among different treatment options, and to determine patient eligibility for entry into a study. Prognostic parameters have to meet many criteria like significant association with clinical course of disease, reproducibility in large clinical trials, and independent predictive potential in multivariate statistical analysis before they become applicable for clinical purposes. The *College of American Pathologists* (CAP) working classification (26) allows the graduation of prognostic markers into different groups based on the respective state of research (Table 1).

Table 1: CAP working classification.

Category	Definition
I	Well supported by the literature; generally used in patient managment
II	Extensively studied biologically and/or clinically **A**: Tested in clinical trials **B**: Biologic and correlative studies performed; few clinical outcome studies
III	Currently do not meet criteria for Category I or Category II

According to the CAP working classification there are only a few Category I prognostic parameters for RCC. Those include patient related criteria like symptomatic presentation (hematuria, pain, palpable tumor mass) and more than 10% body weight loss and also conventional macro- and microscopical parameters like for instance occurance and localization of metastasis, tumor stage and grade of nuclear differentiation (27).

To date, the most significant factor in prognosis of RCC continues to be tumor stage, which reflects the anatomical spread of the disease at presentation (28). Two staging systems, one developed by Robson et al. (29) and the TNM system provided and regularly revised by the *Union Nationale Contre le Cancer* and *the American Joint Committee on Cancer* (AJCC) (30) are frequently used in pathological institutions worldwide. The TNM system, which is applied at our institute, divides renal tumors into four different groups (I-IV) depending on tumor size and extension (pT category) and occurance of lymphnode (pN category) and/or distant metastasis (pM category). Following the TNM guidlines (Table 2), 5-year and 10-year survival rates are 94% and 91.6% in stage I tumors, 89.7% and 78% in stage II, 63.4% and 46.4% in stage III, and 28% and 16.3% in stage IV lesions (31). However, assessment of the metastatic status is often impossible. For those cases tumor extension (T category) alone is also a reliable marker for outcome predictions due to its significant association with the survival time (3).

Second in importance, but also significantly associated with patient survival, is the grade of nuclear differentiation or tumor grade (3, 28). Already in 1971 Skinner et al. has directed attention to the correlation of nuclear features, like size, content, and shape, with patient survival

(4). Today, the 4-tired grading system developed by Fuhrman (32) and the 3-tired system provided by Thoenes (1) are the most frequently used systems for the grading of renal tumors. At our institute the Thoenes grading system is used, which separates RCC in highly differentiated (grade 1), moderately differentiated (grade 2), and poorly differentiated (grade 3) tumors. Grade 1 lesions have a significantly better prognosis than grade 2 and grade 3 tumors (3).

The prognostic potential of tumor stage and grade is universally accepted in the literature and both parameters are generally applied in clinical practice. However, these conventional histopathological markers obviously have limitations since unfavourable clinical courses of renal tumors that were originally thought to have a good prognosis are common (13, 33-35).

Table 2: TNM staging system.

pT-, pN-, and pM-category	**Definition** [1]
pTX	Primary tumor cannot be assessed
pT0	No evidence of primary tumor
pT1	Tumor < 7 cm, limited to the kidney
pT2	Tumor > 7 cm limited to the kidney
pT3	Tumor extends into major veins, adrenal gland or perinephric tissues but not beyond *Gerota facia*
pT4	Tumor invades beyond *Gerota facia*
pNX	Regional lymph nodes cannot be assessed
pN0	No regional lymph node metastasis
pN1	Metastasis in a single regional lymph node
pN2	Metastasis in more than one regional lymph node
pMX	Distant metastasis cannot be assessed
pM0	No distant metastasis
pM1	Distant metastasis
Tumor stage	**pT; pN; pM combination**
I	pT1; pN0; pM0
II	pT2; pN0; pM0
III	pT1; pN1; pM0 pT2; pN1; pM0 pT3; pN0 or pN1; pM0
IV	pT4; pN0 or pN1; pM0 any pT; pN2; pM0 any pT; any pN; pM1

[1] *Gerota facia*: tough, fibrous membrane surrounding the perinephric fat.

In addition to the limited number of histopathological markers, identification of molecular markers may help to individually predict disease outcome in RCC. The Ki-67 antigene is widely used as a proliferation marker in histopathology. The nuclear protein is not detectable during G0 and early G1 phase but accumulates during G1 to M phase (36). Ki-67 is suggested to play a role in chromosome condensation, sister chromatid separation, and in the control of higher order chromatin structure (36-38). Its applicability as an independent prognostic parameter has already been shown for prostate and breast cancer (36). Plenty of studies have been done concerning the usability of Ki-67 as a prognostic parameter for RCC. Some groups could show that increased expression of Ki-67 is also a powerfull, independent prognostic marker associated with adverse disease outcome (39-41). In contrast, other groups demonstrated that Ki-67 does not provide additional information beyond what tumor stage and grade are already telling the pathologists/clinicians (20, 42). Thus, the prognostic value of Ki-67 immunostaining remains uncertain.

Matrix metalloproteinases (MMP) and their inhibitors (tissue inhibitors of matrix metalloproteinases; TIMP) are thought to play an important role in tumor progression. Beside their well-known function in extracellular matrix organization newer studies have shown that MMPs and TIMPs also might have influence on cell proliferation, apoptosis, angiogenesis and immune response (43). Altered expression levels of individual MMPs and TIMPs have already been associated with disease progression in a variety of human tumors (44). Recently, increased TIMP1 expression was shown to be an independent (assessed in a multivariate analysis including tumor stage, grade and expression of other MMPs/TIMPs) predictor of shortened survival in cRCC (45). This finding is corroborated by other groups, which have linked increased TIMP1 expression to shortened survival in colorectal, breast, and non-small cell lung cancer (46-48). By analyzing a subset of 153 archival, paraffin embedded primary cRCCs with patient follow-up data, we found that strong MMP3 immunopositivity is significantly associated with adverse outcome in advanced (pT3/pT4) tumors and that expression of TIMP3 protein is linked to occurance of lymphnode metastasis in this RCC subtype (own unpublished observations).
Thus, altered expression levels of MMPs and TIMPs might be of importance for renal tumor biology and further studies in this field would be worthwhile.

The list of molecular markers tested for their value as prognostic parameters in RCC is endless. Although there are some promising candidates, tumor grade and stage are still the parameters of choice.

1.6 Clear cell renal cell carcinoma (cRCC)

As already mentioned in the previous sections, cRCC is the most common RCC subtype by far. Consequently, most previous studies have been done on cRCC and also the tissue material and cell lines used for the experiments in this thesis are stemming from cRCC. On this account, the histo- and molecularpathology of cRCC will be addressed in the following sections.

1.6.1 Histopathology of cRCC

As illustrated in figure 1, cRCCs arise from epithelial cells of the proximal tubulus (1). Prominent characteristics of cRCC are large plantcell-like cells with a clear cytoplasma due to the high contents of cholesterol, lipid, and glycogen which are eluted during routine processing of the tumor tissue (Figure 1). Clear cell RCCs generally show a solid growth pattern (28). Sarcomatoid differentiation and occurance of necrosis have been associated with adverse outcome (3).

1.6.2 Cytogenetic and molecular alterations in cRCC

First insights into the pathogenesis of RCC have been aquired using conventional cytogenetic analysis. Already in the late eighties and early nineties it could be demonstrated that loss of 3p sequences is fundamental to cRCC development occuring in up to 95% of the analyzed cases (49-53).

Introduction of Comparative Genomic Hybridization (CGH) analysis in 1992 facilitates the detection of DNA copy-number losses and gains in a given tissue sample (54, 55). To generate a CGH profile of a tumor, equal amounts of tumor and normal DNA are labelled with two different fluorochromes prior cohybridization to human metaphase chromosomes. The fluorescence intensity ratio of the two fluorochromes along the length of the chromosome is measured to calculate the DNA copy number changes within the tumor specimen. Many groups have studied

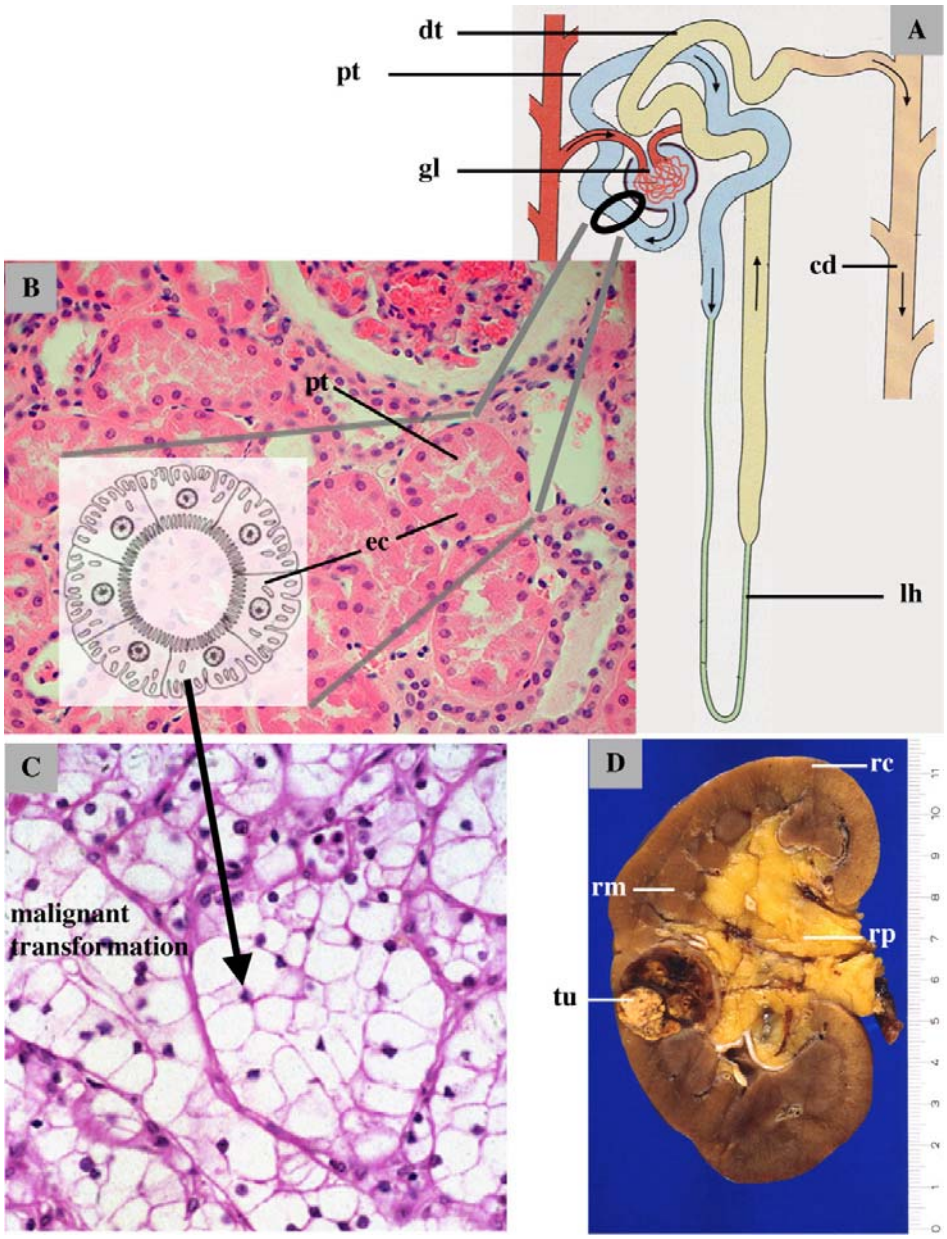

Figure 1: Point of origin and histopathology of cRCC.

(A) cRCC arise from the functional unit (nephron) of the kidney. Point of origin are epithelial cells of the proximal tubule (circle). cd = collecting duct; ct = collecting tubule; dt = distal tubule; gl = glomerulus; lh = loop of Henle; pt = proximal tubule. (B) H&E stained section of normal renal tissue with a schematic display of a cross section through the proximal tubule. ec = epithelial cell; pt = proximal tubule. (C) H&E stained section of cRCC showing the typical plantcell-like character of cRCC cells. (D) Cross section through kidney containing a cRCC. rc = renal cortex; rm = renal medulla; rp = renal pelvis; tu = tumor.

cRCC using this technology and found that this RCC subtype is characterized by frequent losses of chromosomes 3p, 4q, 6q, 8p, 9p, 13q, 14q, and Xq and gains of 5q, 7, and 17 (56-58). Figure 2 shows an example of a CGH profile of cRCC. Using CGH data, Jiang et al. (57) have constructed

evolutionary trees for cRCC thereby gaining insight into the order of occurance of genetic alterations. Beside 3p, whose loss already was considered to be an early event in renal tumor biology (50, 59), they also found loss of 4q to be important in the initiation of cRCC. Additionally, due to their analysis, they suggested two distinct subclasses of cRCC from which one is characterized by successive loss of 13q, 9p, and 18q and the other one by successive loss of 6q, and gain of 17q and 17p.

Certain cytogenetic alterations have already been implicated with progression of cRCC. For instance, loss of 9p, 13q, and 14q have been associated with shortened survival in advanced (Stage III and IV disease) cRCCs (56, 57, 60, 61).

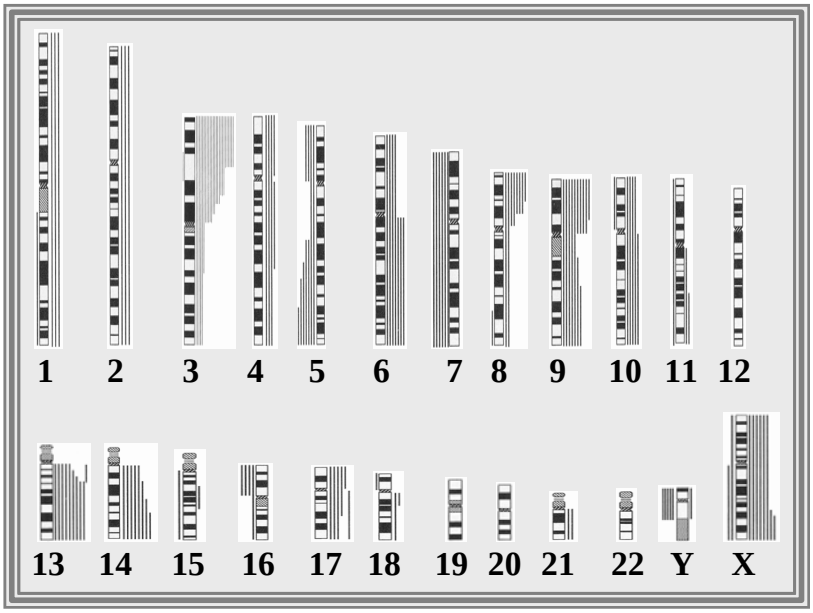

Figure 2: CGH profile of cRCC generated from 41 primary cRCCs (Moch et al. 1996).

Bars on the right site of the chromosome: DNA sequence losses; bars on the left site of the chromosome: DNA sequence gains.

Two important points can be summarized from the findings described above:

(1) DNA sequence losses are much more frequent than DNA sequence gains suggesting that renal pathogenesis is mainly driven by loss of function of genes (potential tumor suppressor genes) located in these regions.

(2) No amplified DNA sequences (harboring potential oncogenes) have been identified in primary cRCC.

1.6.3 Molecular carcinogenesis of cRCC

Obviously, loss of 3p sequences is the most common event in cRCC (50, 62, 63) indicating that genes localized in this chromosomal region are of particular importance for renal tumor biology. Interestingly, loss of 3p is also frequent in other solid human cancers, i. e. lung, breast, ovarian, and head and neck tumors (64-69). At least three separate regions of 3p, 3p25-26, 3p21-22, and 3p12-14, are critical in the development of cRCC (62, 70-75).

One of the first genes associated with sporadic cRCC was the *Von Hippel-Lindau* (*VHL*) gene, which is located at 3p25 and mutated in VHL syndrome (dominantly inherited familial cancer syndrome) families (76). Introduction of the *VHL* cDNA into renal cancer cell lines has functionally confirmed that this gene has tumor suppressive properties (77). Somatic mutations in all 3 exons and hypermethylation of the *VHL* promoter have been described in 34-85% (78-80) and 15-19% (80, 81) of the analyzed cRCCs indicating the importance of *VHL* in renal tumor biology. The *VHL* protein plays a role in the regulation of the cellular response towards hypoxia. Hypoxia activates the transcription factor *HIF-α*, which regulates expression of genes involved in angiogenesis, cell adhesion, extracellular matrix regulation, proliferation, and apoptosis (reviewed in (82-85). Under normal oxygen conditions, binding of *VHL* to *HIF-α* causes the ubiquitylation and degradation of *HIF-α* (86, 87). It has been shown that *VHL* inactivating mutations lead to stabilization of *HIF-α* in cRCC (86-88). According to this, *HIF-α* protein is abundant in primary cRCC in contrast to normal renal tissue (and other RCC subtypes) where *HIF-α* levels were very low or even undetectable (89, 90). Turner et al. could show that strong *HIF-α* expression is associated with increased *vascular endothelial growth factor* (*VEGF*) expression and microvessel density in cRCC (90). These findings indicate that impaired *VHL* function could promote cRCC development by constitutive activation of *HIF-α,* which leads to increased vascularization, paving the way for boundless tumorgrowth and metastasis.

Beside *VHL*, other genes located at 3p may be of importance for renal tumor biology. Dammann et al. (91) have identified a human *RAS effector homologue* (*RASSF1*), on 3p21.3, through its interaction with the human DNA repair protein *XPA* in a yeast 2-hybrid screen. Three splice variants of the *RASSF1* gene (*RASSF1A-C*), of which *RASSF1A* seems to play a key role in tumorigenesis, are existing. Epigenetic silencing of the *RASSF1A* promotor has been described in 24-91% of the analyzed primary cRCCs and in 100% of evaluated cRCC cell lines (92, 93). In contrast to *VHL*, which is strictly associated with cRCC, *RASSF1A* promoter methylation has also been obseved in pRCC (93). *RASSF1A* promoter methylation is also common in other human cancers, including breast, lung, prostate, ovarian, and skin tumors (94-98). Re-expression of *RASSF1A* resulted in growth suppression and reduced colony formation in a cRCC cell line corroborating the tumor suppressive function of this gene in renal pathogenesis (92). However, the mechanism by which *RASSF1A* contributes to renal tumorigenesis is yet unclear. The presence of a RAS association domain and a strong homolgy to *Nore1* (a mouse RAS effector protein which in vivo interacts with *Ras* in a GTP-dependent manner following receptor activation (99)) suggest that *RASSF1A* functions in a Ras signalling pathway, possibly as a negative regulator of cell growth (91).

By introducing a chromosomal fragment, encompassing 3p14-p12, into a highly malignant cRCC cell line Sanchez et al. (100) obtained dramatically reduced tumor growth in athymic nude mice suggesting another renal cancer relevant tumor suppressor gene on the short arm of chromosome 3. In 1998, the region containing the tumor suppressor gene(s) was confined to 3p12 and designated nonpapillary renal carcinoma-1 (NRC-1) locus (101). Introduction of NRC-1 locus into different renal cancer cell lines showed that the tumor suppressive properties of 3p12 are independent of histological phenotype and VHL mutation status (102). The tumor suppressor gene(s) located at 3p12 remain to be identified.

1.7 cDNA and tissue microarray technologies for the identification of cRCC relevant genes

Because cancer is a multistep process it is unlikely that alterations of genes located at 3p are sufficient to induce and promote renal carcinogenesis. By CGH analysis it has been shown that virtually all chromosomes are affected in cRCCs (56-58) strongly suggesting that many more

genes are playing a role in renal tumor biology. Further studies are necessary to identify renal tumor relevant genes and evolve the molecular pathways leading to renal cancer initiation and progression. Those genes could than be used as diagnostic and prognostic parameters or as new targets for innovative and effective therapies.

Recently, cDNA array technology was developed which allows expression analysis of thousands of genes in parallel thus accelerating and facilitating target gene identification. This technology offers the possibility to generate gene-expression profiles of each tissue of interest in a very short time enabling to uncover the molecularbiological processes leading not only to cancer but also to other diseases (103, 104). In cancer research, cDNA arrays have been employed to elucidate the molecular pathogenesis of tumor diseases (105-107), to promote the molecular subclassification of pathohistologically similar tumor entities (108, 109), to identify new diagnostic and prognostic markers and therapeutical targets (110-112), and to evaluate the response of tumor cells to different chemotherapeutical drugs (113, 114).

Interpreting the multiparametric data, validating results, and prioritizing the candidate markers are the major challenges for microarray-based cancer profiling efforts. To assess the clinical significance of prognostic or diagnostic marker genes, large numbers of tissue samples have to be analyzed. This is rather cumbersome and time-consuming if large conventional histological sections are used. Recently, tissue microarrays (TMA) have been designed to analyze simultanously new cancer related genes in hundreds of tumors on the DNA, RNA, and protein level (115, 116). Consequently, a combination of cDNA microarray and TMA technology is particularly suitable for rapid identification and subsequent validation of potential novel cancer markers and prognostic parameters (117-120).

1.8 Aim of the thesis

Despite many efforts, the genetical background of renal carcinogenesis largely remains unclear. As a result of this, there is a lack of diagnostic and prognostic markers allowing reliable prediction of the clinical course of a renal tumor. Furthermore, there are virtually no therapeutical options for advanced renal cancer. Consequently, this tumor entity is still a challenge for pathologists and oncologists and the identification of genes with impact on renal tumor biology is

of great importance. Recently developed microarray technologies, like cDNA and tissue microarrays, allow rapid identification and validation of potentially tumor relevant genes.

The aims of this thesis were to

- uncover yet unknown cRCC associated genes (**first part of this thesis**)
- further characterize a selected candidate gene (**second part of this thesis**)

First part: High-throughput technologies for identification of differentially expressed genes.

- Identification of potentially renal tumor relevant genes by comparing gene expression profiles of cRCC cell lines and normal renal tissue with each other using cDNA microarrays.
- Verification of significantly differentially expressed genes by oligo-based RNA *in situ* hybridization (RISH) on tissue microarrays constructed from 61 fresh frozen primary RCCs and 12 normal renal tissues.

Second part: Further studies on the highly differentially expressed gene *BTG2* to assess its role in cRCC biology.

- Confirmation of results from precedent cDNA and tissue microarray experiments using Northern blot analysis and quantitative RT-PCR on the LightCycler instrument (Roche).

- Gain insight in the regulation of *BTG2* gene transcription in renal cancer by analyzing *BTG2* mRNA expression levels in cRCC cell lines under certain conditions (TPA treatment, increasing cell density) with the help of quantitative RT-PCR.

2 Material and Methods

2.1 Cell culture

Human cRCC cell lines (Caki-1, Caki-2, 786-O, and 769-P) and the human cervix carcinoma cell line HeLa were obtained from American Type Culture Collection (ATCC). Caki-2, 786-O, and 769-P cells derive from different primary cRCCs whereas Caki-1 was established from a skin metastasis of a cRCC. All cell lines were cultured in Optimem medium (Gibco) which was supplemented with 10% foetal calf serum (Amimed) and Penicillin/Streptomycin (100 IU/ml and 100 µg/ml, respectively; Amimed). Medium renewal was done three times per week.

Cells were detached using Trypsin-EDTA (0.05% Trypsin/0.02% EDTA; Amimed) following standard protocols (121). In order to store cells, cultures were detached and resuspended in 2-5 ml culture medium. Cells were pelleted by centrifugation at 1000 rpm for 10 min at 4°C. Pellets were resuspended in culture medium containing 10% DMSO (Sigma) to a concentration of 1 x 10^6 cells per ml and stored at –75°C.

For cell counting, cells were stained with one volume trypan blue (Appendix) to visualize apoptotic cells and counted using a hemocytometer (Neubauer chamber), according to standard protocols (121).

2.2 RNA extraction

Extraction of total RNA from cell lines

To extract RNA for cDNA array experiments, cells were quickly thawed at 37°C and pelleted at 1000 rpm for 10 min at 4°C prior addition of TRIzol® reagent (Invitrogen). For Northern blot and quantitative RT-PCR experiments cells were detached by directly adding TRIzol® reagent (Invitrogen) to the culture vessel.

Total RNA was extracted according to the instructions given in the TRIzol® reagent manual (http://www.invitrogen.com/content/sfs/manuals/15596026.pdf). To eliminate contaminating DNA, RNA was treated using the DNAse I system of Qiagen.

Extraction of total RNA from human lymphocytes

Lymphocytes were isolated from human whole blood of healthy donors using Histopaque-1077 (Sigma). In brief, whole blood (20-30 ml) was carefully pipetted onto one volume of Histopaque-1077 and centrifuged at 1600 rpm for 10 min at room temperature to separate the lymphocytes from the erythrocytes. After centrifugation the lymphocyte-containing interphase was transferred into a 50 ml Falcon tube. Lymphocytes were washed with 20-30 ml PBS (Gibco). Cells were pelleted by centrifugation at 1600 rpm for 10 min at room-temperature. The pellet was resuspended in 2 ml TRIzol® reagent (Invitrogen) and total RNA was extracted as described above.

Extraction of total RNA from snap-frozen tissues

H&E stained histological sections (122) were prepared from each tissue prior RNA extraction. Representative tissue areas, identified on the H&E stained histological sections, were used for RNA extraction. One ml TRIzol® reagent (Invitrogen) was added to 15-20 frozen sections (each 20-30 µm) of each sample and total RNA was extracted as described above.

Extraction of polyA$^+$ mRNA

PolyA$^+$ mRNA was extracted from total RNA using the polyA$^+$ mRNA extraction kit of Qiagen according to the instructions of the manufacturer.

Evaluation of RNA quantity and quality

Total RNA concentrations were determined using a spectrophotometer (Genequant). To assess quality of total RNA, 0.5–1 µg was separated under denaturating conditions using agarose/formaldehyd gels as described in section 2.6.

2.3 cDNA array experiments

Generation of cDNA array probes

For each experiment, 5 µg of total RNA from cRCC cell lines Caki-1, Caki-2, 786-O, and 769-P and normal renal tissue (Invitrogen) were reverse transcribed and thereby labeled with (α-^{32}P)dATP (Amersham Pharmacia) using the Atlas™ Pure Total RNA Labeling System (BD Clontech). Unincorporated nucleotides were removed using the QIAquick Nucleotide Removal Kit according to the instructions of the manufacturer (Qiagen).

cDNA array hybridization

Atlas™ Human Cancer 1.2 cDNA Arrays (BD Clontech) were used for cDNA array analysis. These arrays contain cDNA spots of 1176 genes known to have impact on initiation and progression of human cancers.
Prehybridization, hybridization, and washing of the cDNA microarrays was done according to the recommendations of the manufacturer. After hybridization, arrays were exposed to high resolution Phosporimager screens (Packard) for 24 h and scanned using the Cyclone Phosphorimager (Packard).

Evaluation of cDNA array data

AtlasImage software 1.01a (BD Clontech) was used for digital image analysis. Background corrected signal density (sDens) values were calculated for each arrayed spot and were normalized according to the AtlasImage sum method. Only those spots showing sDens values $\geq$ 4500 were clearly distinguishable from background noise. Therefore, spots with sDens values $<$ 4500 were excluded from analysis.

sDens ratios were calculated between each cRCC cell line showing gene expression (sDens $\geq$ 4500) and normal renal tissue. We also included genes in our analysis, which were not expressed in normal renal tissue (sDens $<$ 4500) but which were strongly expressed (sDens $\geq$ 13500; 3x threshold value) in at least two cell lines (and vice versa). In those cases sDens ratios were calculated as described above.

Genes showing expression alterations > 0.5-fold and < 2-fold were considered to be equally expressed. Expression alterations ≤ 0.5-fold and ≥ 2-fold in at least two cell lines were defined as decreased or increased, respectively, in cRCC cell lines compared to normal renal tissue.
Only genes with expression alterations ≤ 0.25-fold and ≥ 4-fold in at least two cell lines were further studied by RISH on renal TMAs.

2.4 RNA *in situ* hybridization on frozen renal tissue microarrays

TMA construction

Sixty-one renal cancer samples and 12 normal renal tissues were used for TMA construction. All tissue samples derived from the tumorbank of the Institute of Pathology in Basel. Renal tumor subtypes were defined according to Thoenes et al. (1). Histological grade and the pT category of the tumors were determined according to Thoenes and recommendations of the UICC, respectively (1, 29). Table 3 shows an overview of the renal tissues arrayed on the frozen TMA.

Table 3: Composition of renal TMA.

		pT category				grade			
tissue[1]	n	1	2	3	ni[2]	1	2	3	ni[2]
cRCC	51	32	4	15	-	12	30	7	2
pRCC	4	1	-	3	-	2	2	-	-
chRCC	4	1	3	-	-	1	2	-	1
oncocytoma	2	1	-	-	1	-	-	1	1
normal kidney	12	-	-	-	-	-	-	-	-

[1] cRCC = clear cell RCC; pRCC = papillary RCC; chRCC = chromophobe RCC
[2] ni = no information available

Conventional H&E stained histological sections were prepared from each tissue (122). All sections were reviewed by a pathologist to select representative tissue areas which were than used for TMA construction. Tissue microarray construction was largely done according to Schoenberg et al. (116). At our laboratory, frozen TMA manufacturing was optimized by using a drill (0.6 mm diameter) instead of a hollow needle to bore wholes into the recipient block. Figure 3 briefly illustrates the construction of a TMA. Conventional H&E stainings (122) were made from the TMA sections to ensure integrity of every single tissue spot. Generated TMA blocks as well as TMA sections were stored at –75°C.

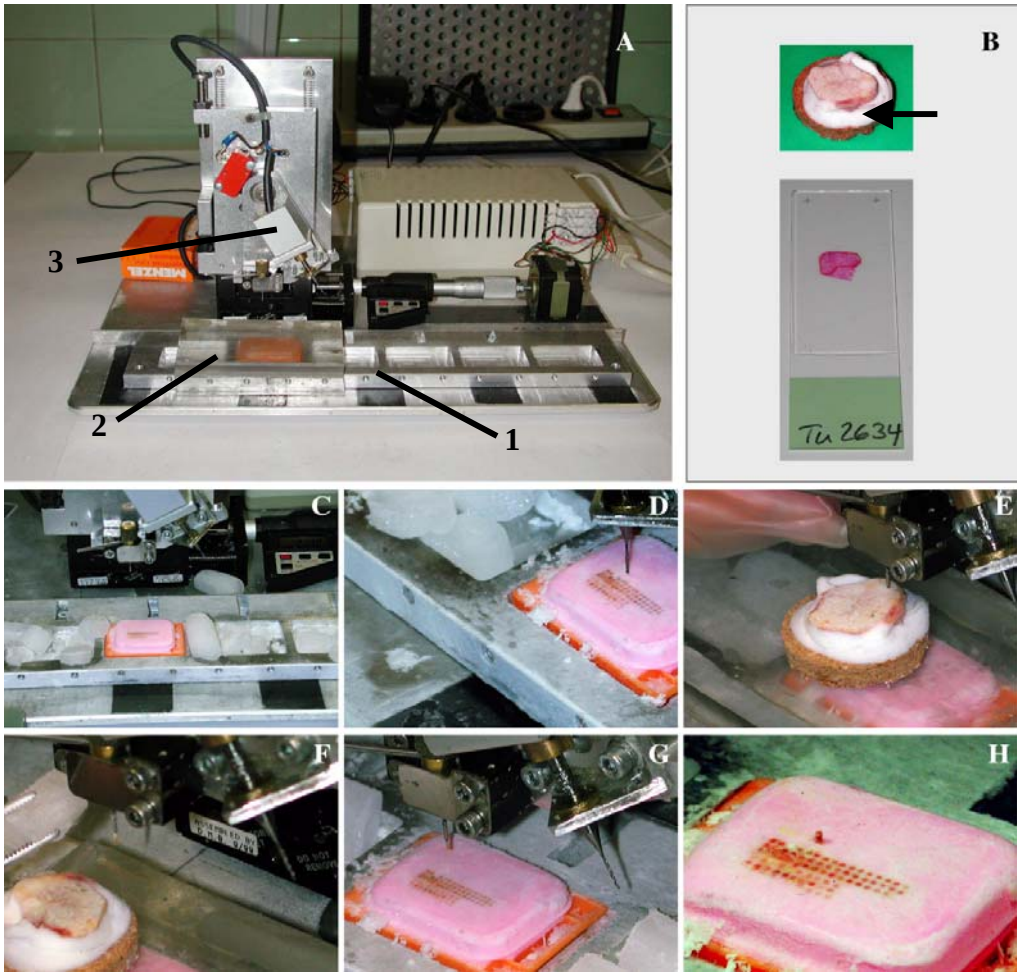

Figure 3: Construction of frozen TMA.

(A) Front view of the tissue arrayer. 1 = receptacle for the recipient (array) block; 2 = donor block bridge; 3 = turret for switching needle/drill between donor and recipient block. (B) Piece of frozen tissue placed on Tissue-Tek (arrow) to facilitate sectioning and handling. H&E stained sections were prepared to assign representative tissue areas. (C-H) Individual TMA production steps: (C) recipient block is fixed in the receptacle and permanently cooled with dry-ice; (D) drilling of the recipient whole; (E) retrieving the tissue sample using a hollow needle; (F) tissue core biopsy is cooled with dry-ice; (G-H) tissue is transferred into the pre-made whole of the recipient block.

Design of antisense oligonucleotide probes

For each gene to be analyzed by RISH 2-4 oligonucleotides were designed using the Vector NTI software package (InforMax Inc., Frederick, MD, USA). All oligonucleotides consisted of 35 to 55 nucleotides, had a guanosine-cytosine content of 50 to 60%, and had no palindromic sequences. Specificity of the probes was confirmed using the BLAST® program (http//www.ncbi.nlm.nih.gov). Oligonucleotide sequences showing more than 25 successive nucleotides that were homologous to any other gene than the target gene were discarded.

Labelling of oligonucleotide probes

Oligonucleotides were labeled separately with (α-^{33}P)dATP (Amersham Pharmacia) using terminal deoxynucleotidyl transferase (TdT; Promega). Twenty ng oligonucleotide were combined with 1 µl nuclease free water, 1 µl 5 X TdT buffer (500 mM cacodylate buffer, pH 6.8; 5 mM $CoCl_2$; 0.5 mM DTT), 20 µCi (α-^{33}P)dATP, and 1 µl TdT (15-30 units). The reaction was performed at 37°C for 2 h. After labelling, oligonucleotides concerning to one gene were pooled. Unincorporated nucleotides were removed using the QIAquick nucleotide removal (Qiagen). The activity of the radiolabeled probes was determined by pipetting 1 µl of the purified probe into 10 ml of Ultima Gold MV solution (Packard). The mixture was transferred into a liquid scintillation counter. Probes suitable for RISH had an activity of at least 1 x 10^8 counts per minute (cpm) per ml.

RISH

Radiolabeled probes (activity $\geq 10^8$ cpm/ml) were combined with 6 µl DTT (5 M) and RISH hybridization mix (Appendix) to a total volume of 200 µl. The mixture was vortexed and incubated at 42°C for 1 h prior addition of 10 µg heat-denatured Human Cot-1 DNA. After adding the hybridization mixtures, the TMA sections were covered with a spacer-coverslip and incubated in a moist chamber at 42°C for 36 h. After hybridization, slides were washed in 1 X SSC (prepared from 20 X SSC stock solution, see Appendix) at 55°C for 15 min (4 times), in 1 X SSC at room temperature for 1 h, and in distilled water at room temperature for 30 s. Afterwards, slides were dehydrated in 60% and 90% ethanol (30 s each) and air-dried. The dried slides were exposed to high resolution Phosphorimager screens (Packard) for 48 h prior scanning using a Cyclone Phosphorimager (Packard).

Image analysis

ArrayVision software (Imaging Research Inc., St. Catharines, Ontario, Canada) was employed to measure signal density (sDens) values of the array spots. To address possible heterogeneity of a given tissue spot, signal densities were measured over the whole area of each spot. The mean value from these sDens values (mean sDens) was than calculated for every single tissue spot. RCC and normal renal tissue spots were considered positive for gene expression if the mean

sDens was at least twice as high as the mean background sDens of the TMA section. The other spots were considered negative for gene expression.

Specificity of RISH was evaluated by direct autoradiograpy of the TMA slide using Hypercoat™ LM-1 emulsion (Amersham Pharmacia) according to the instructions of the manufacturer. After development of the emulsion, slides were counterstained with Harris‘ hematoxylin (122) and were analyzed under a conventional light microscope to identify those spots, which were completely or partly lost during the sectioning, hybridization, and washing process. Only spots containing more than 60% tumor or normal tissue, respectively, cells were included in further statistical analysis.

Statistical evaluation of RISH results

Only primary cRCCs and normal renal tissues were included in statistical analysis since the numbers of the other RCC subtypes on the TMA were to low. All statistical analysis were done using StatView 5.0.1 software package (SAS institue Inc.) RISH results were evaluated for each analyzed gene in two ways:

(1) **Expression frequency**. Contingency table (Chi Square) analysis was performend to search for differences in the percentage of tissue spots positive for gene expression (mean sDens ≥ 2-fold background sDens) between normal renal tissue and cRCC and also within the subset of cRCC.

(2) **Expression level.** Anova analysis was applied to compare gene expression levels (mean sDens values) of spots with positive gene expression between normal renal tissue and cRCC and also within the subset of cRCC.

2.5 Cloning of *BTG2* and *G3PDH* sequences

BTG2 and *G3PDH* sequences were cloned for two purposes:

- Generation of single stranded DNA probes for Northern analysis (section 2.6).

- Generation of *in vitro* transcribed RNA to establish standard curves for quantitative RT-PCR (section 2.7.2).

The pGEM®-T Easy Vector system (Promega), which is especially suited to clone PCR products and which contains SP6 and T7 RNA polymerase promoter sequences, was used.

Generation of inserts by PCR

BTG2 and *G3PDH* PCR products of about 1 kb were generated from reverse transcribed human lymphocyte RNA using 2.5 µl of AmpliTaq® Gold 10 X PCR buffer (1.5 mM Tris-HCl, pH 8.0; and 500 mM KCl), 0.2 mM dATP, dCTP, dGTP, and dTTP (Invitrogen), sequence-specific primer pairs for *BTG2* (forward: 5'-AGG GTA ACG CTG TCT TGT GG-3' and reverse: 5'-CAG GAG AGG CCT TTT CAC TC-3') and *G3PDH* (forward: 5'-ACA GTC AGC CGC ATC TTC TT-3' and reverse: 5'-AGG GGA GAT TCA GTG TGG TG-3') at a final concentration of 0.5 µM each, and 0.25 units of AmpliTaq® Gold polymerase (Applied Biosystems) in a total volume of 25 µl. Amplification was done for 10 min at 95°C, 35 cycles with 30 s at 95°C, 30 s at 58°C, and 1 min at 72°C. Subsequent incubation of the PCR reaction at 72°C for 10 min ensured sufficient generation of 3‘-Adenosin overhangs. PCR products were cleaned-up using the Quiaquick PCR purification kit (Quiagen). PCR products bound to the Quiaquick columns were eluted in 30 µl elution buffer, which was supplied in the kit.

Cloning and selection

Two µl of the purified PCR product were combined with 5 µl Rapid Ligation Buffer, 50 ng pGEM®-T Easy Vector DNA, 3 units T4 Ligase, and deionized water to a final volume of 10 µl. The reaction was incubated overnight at 4°C. Two µl of each ligation reaction were carefully mixed with 50 µl of JM109 High Efficiency Competent Cells (supplied with the pGEM®-T Easy Vector kit). The mixture was placed on ice for 20 min prior heat-shock at 42°C for exactly 50 s. Transformed cells were immediatly returned to ice for another 2 min.

Transformed cultures were mixed with 950 µl LB medium (Appendix) and incubated for 90 min at 37°C with shaking. One hundred µl of each culture were plated on LB/Agar plates supplemented with X-Gal and IPTG (Appendix). Plates were incubated at 37°C overnight.

Confirmation of cloned inserts

White colonies (containing the insert) were picked and transferred into microtiterplates containing 150 µl LB (Appendix) medium per well. Plates were incubated at 37°C for 2-3 h. PCR was done to confirm cloned inserts. In brief, 2-5 µl from each well of the microtiterplate was amplified using 2.5 µl of AmpliTaq® Gold 10 X PCR buffer (1.5 mM Tris-HCl, pH 8.0; 500 mM KCl), 0.2 mM dATP, dCTP, dGTP, and dTTP (Invitrogen), primers specific for SP6 (forward: 5'-GCC AAG CTA TTT AGG TGA CAC T-3') and T7 (reverse: 5'-ACG GCC AGT GAA TTG TAA TAC G-3') at a final concentration of 0.5 µM each, and 1.25 units of AmpliTaq® Gold polymerase (Roche) in a total volume of 25 µl for 10 min at 95°C and 35 cycles with 30 s at 95°C, 30 s at 60°C, and 1 min at 72°C. Five µl of each PCR product were analyzed by gel electrophoresis.

Gel electrophoresis

DNA was separated on conventional 1.2% agarose (Invitrogen) gels using 1 X TAE (prepared from 50 X TAE stock solution, see Appendix) as a running buffer (123). DNA molecular weight marker III (Roche) and a 100 bp-ladder (Invitrogen) were used as size standards.

Extraction of Plasmid DNA (Miniprep)

Twenty µl of each clone containing the appropiate insert were transferred into 5 ml LB medium (Appendix) and incubated at 37°C for 12-16 h. Plasmid-DNA was extracted using the QIAprep spin plasmid kit (Qiagen). Amount of plasmid DNA was assessed using a spectrophotometer (Genequant).

Sequencing

Direction of the cloned insert was determined by sequencing using the ABI 310 Prism sequencer (Applied Biosystems). PCR products were generated from 50 ng of each plasmid DNA according to the protocol described above (*Confirmation of cloned insert*). PCR products were purified using the Quiaquick PCR purification kit (Qiagen). PCR products bound to Quiaquick column

were eluted in 50 µl elution buffer supplied with the kit. Two µl of this eluate were combined with 8 µl BigDye Terminator v 2.0 (BigDye Terminator Cycle Sequencing v 2.0 kit; Applied Biosystems), SP6 sequencing primer (5'-ATT TAG GTG ACA CTA TAG AA-3') at a final concentration of 0.5 µM, and PCR grade water to a total volume of 20 µl. The reaction was incubated for 25 cycles with 96°C for 20 s, 50°C for 10 s, and 60°C for 4 min. Reaction products were pelleted by addition of 2.5 volumes of 100% ethanol and 1/10 volume of 3 M sodiumacetate (pH5.2) and incubation at –20°C overnight prior centrifugation at 14000 rpm for 30 min at 4°C. The pellet was washed in 75% ethanol and dried prior addition of 14 µl Template Suppression Reagent (Applied Biosystems). Before sequence analysis, the product was denatured at 95°C for 10 min and chilled on ice.

2.6 Northern blot analysis

Gel electrophoresis of RNA

RNA was separated under denaturing conditions using agarose/formaldehyde gels and 1 X MOPS (prepared from 10 X MOPS stock solution, see Appendix) as a running buffer (123). RNA Millenium™ Size Marker (Ambion) and the RNA Marker from Promega were used as size standards.

Blotting

Gels were rinsed in RNAse free water to remove formaldehyde prior blotting to Hybond™-N+ membranes (Amersham) using the capillary transfer method and 20 X SSC (Appendix) as a transfer buffer (123). To immobilize RNA, the membranes were incubated at 80°C for 1.5-2 h. RNA was visualized by incubating the membrane in methylene-blue staining solution (Appendix) for 30-60 s. The membrane was rinsed in RNAse free water to remove excess staining solution and airdried.

Northern analysis using (α-^{32}P)dATP labelled single-stranded DNA probes

To verify the results obtained for *BTG2* by cDNA microarray experiments (α-^{32}P)dATP labelled single-stranded DNA probes were hybridized to poly A^+ mRNA of cRCC cell lines, normal renal tissue, and human lymphocytes (positive control).

To generate sequence-specific probes for *BTG2* and *G3PDH* (reference), 50 ng plasmid DNA (preperation described in section 2.5) containing the cloned insert of *BTG2* or *G3PDH*, respectively, were amplified as described in section 2.5 (*Confirmation of cloned inserts*). PCR products were purified using the Qiaquick PCR purification kit (Qiagen).

For labeling, 25ng *BTG2* and *G3PDH* PCR product were combined with 25 ng *BTG2* reverse primer (5'-CAG GAG AGG CCT TTT CAC TC-3') or 25 ng *G3PDH* reverse primer (5'-AGG GGA GAT TCA GTG TGG TG-3'), respectively, denatured at 100°C for 10 min, and chilled on ice. Labelling reaction was performed in a total volume of 25 µl containing 2.5 µl 10 X Klenow Fragment buffer (500 mM Tris-HCl, pH7.2; 100 mM $MgSO_4$; 1 mM DTT), 0.5 M dCTP, dGTP, and dTTP (Invitrogen), 50 µCi (α-^{32}P)dATP (Amersham Pharmacia), and 5 units Klenow Fragment (Promega) for 1 h at 25°C. Reaction was stopped by adding 1 µl 0.5 M EDTA (pH8.0). QIAquick nucleotide removal kit was applied to remove unincorporated nucleotides (Qiagen).

Single-stranded DNA probes were hybridized to polyA$^+$ mRNA, which was extracted from 30 µg total RNA of each cRCC cell line (Caki-1, Caki-2, 786-O, and 769-P), normal renal tissue (Invitrogen), and human lymphocytes, respectively. Prehybridization and hybridization of the membrane was done at 42°C in formamide prehybridization/hybridization (FPH) solution (Appendix). To block unspecific binding of the probe, prehybridization was done with heat-denatured salmon sperm DNA (100 µg/ml FPH solution; Sigma) for 1 h prior addition of heat denatured *BTG2* and *G3PDH* probes. Hybridization was done overnight. Washing was done twice at 42°C in wash solution I (Appendix) for 15 min, twice at 42°C in wash solution II (Appendix) for 10 min, and also twice at 68°C in wash solution III (Appendix) for 5 min. The membrane was exposed to a high resolution Phosphorimager screen (Packard) for 6-12 h prior scanning using the Cyclone Phosphorimager (Packard).

Northern hybridization using (α-^{32}P)dATP labelled oligonucleotide probes

To verify the specificity of the *BTG2* oligonucleotides used in the RISH experiment, (α-^{32}P)dATP labelled oligonucleotides were hybridized to total RNA from human lymphocytes. In brief, *BTG2* oligonucleotide probes were generated and purified as described in section 2.4 (*Labelling of oligonucleotide probes*) with the exception that (α-^{32}P)dATP was used for labelling instead of (α-^{33}P)dATP.

BTG2 oligonucleotide probes were hybridized to 10 µg total RNA from human lymphocytes. Prehybridization and hybridization of the membrane was done as described in section 2.4 (*RISH on TMA*) with the exception that hybridization was done overnight only and the washing step in 1 X SCC at room temperature was reduced to 15 min. For signal detection, the membrane was exposed to a high resolution Phosphorimager screen (Packard) for 12 h prior scanning using the Cyclone Phosphorimager (Packard).

2.7 Quantification of *BTG2* mRNA copy numbers using the LightCycler

2.7.1 General aspects of quantitative PCR using the LightCycler system

Each PCR starts with a background phase followed by an exponential (or log) phase and ends in a plateau phase. By using the fluorochrome SYBR green, which binds to double stranded DNA, the increase of PCR product during an amplification reaction can be detected by the LightCycler system (figure 4).

During amplification, the number PCR products present at a certain PCR cycle is described by the equation:

$$N_n = N_0 \times E^n$$

Where N_n is number of products at PCR cycle n; N_0 is initial number of product (template); E is amplification efficiency; n is number of PCR cycle

Accurate DNA quantification is only possible in the log-phase of a PCR in which E is constant. In theory, the maximal amplification efficiency in log-phase is 2 so that every PCR product is

replicated once per cycle. In practice amplification efficiencies in this phase are generally less than 2 due to many factors that could inhibit PCR reactions (suboptimal primers, PCR inhibitors in sample material etc.).

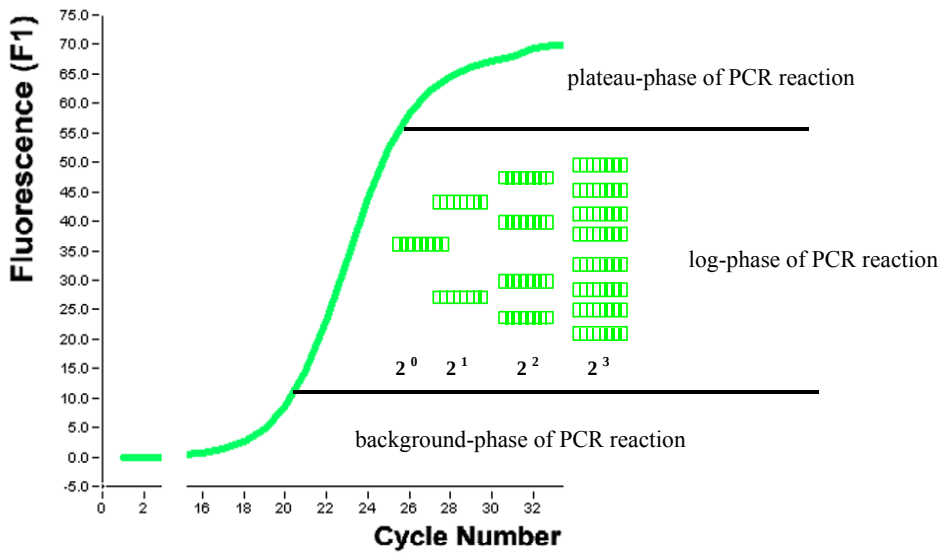

Figure 4: DNA amplification profile.

Increasing SYBR green emission is detected by the LightCycler system.

To determine amplification efficiencies for individual PCRs, serial template dilutions have to be amplified on the LightCycler instrument. Standard curves and their slopes are determined using the software provided by the LightCycler system. Amplification efficiencies are described by the equation:

$$E = 10^{-1/\text{slope}}$$

Where E is amplification efficiency; slope is slope of standard curve.

The easiest way to determine absolute mRNA copy numbers of a gene of interest is to use an external standard, which is prepared from serial dilutions of *in vitro* transcribed RNA with known concentrations. Standard curves can be generated by reverse transcription of this dilution series in a separate reaction followed by amplification of the obtained first strand cDNA products on the LightCycler system (two-step RT-PCR). Based on these standard curves, concentrations of a target sample can be determined. However, quantification of mRNA copy numbers using this method do not necessarily reflect the actual and physiological expression level of a gene since

faulty processing and storage of sample material as well as irregularities in extraction and improper storage of RNA might affect the abundance of a transcript. For these reasons, it makes sense to determine mRNA expression level of a gene of interest relative to a housekeeping/reference gene to adjust for alterations in mRNA copy numbers induced by experimental treatment. If this approach is used, separate standard curves have to be generated to determine the mRNA concentrations of the gene of interest and the reference gene in a given sample.

Guidelines for preparation of standard curves are (according to Roche):

- Standard sequences should differ only slightly by lenght and/or sequence from the target sequences so that amplification with the same pair of primers is possible.
- Size of the PCR products amplified from the gene of interest and the reference gene should be as similar as possible
- Amplification efficiency of gene of interest and reference gene should differ by no more than ± 0.05.
- At least 5 points for creation of a standard curve should be used, which should cover the expected concentration range of the gene of interest and the reference gene

2.7.2 Generation of standard curves from *BTG2* and *G3PDH in vitro* transcripts

Generation of plus strand RNA (in vitro transcription)

From both plasmids generated in section 2.5 plus strand run-off *in vitro* transcripts were synthesized. Therefore, the circular plasmid DNA had to be linearized using *Pst* I and *Sph* I restriction enzymes. As illustrated in figure 5, *Pst* I recognizes the site CTGCA↓G and cuts between the SP6 promoter and the insert whereas *Sph* I recognizes the site GCATG↓C and cuts between the T7 promoter and the insert.

Linearization of each plasmid DNA was done according to the instructions of the manufacturer of the restriction enzymes (Promega). Reactions were incubated at the appropriate temperatures for

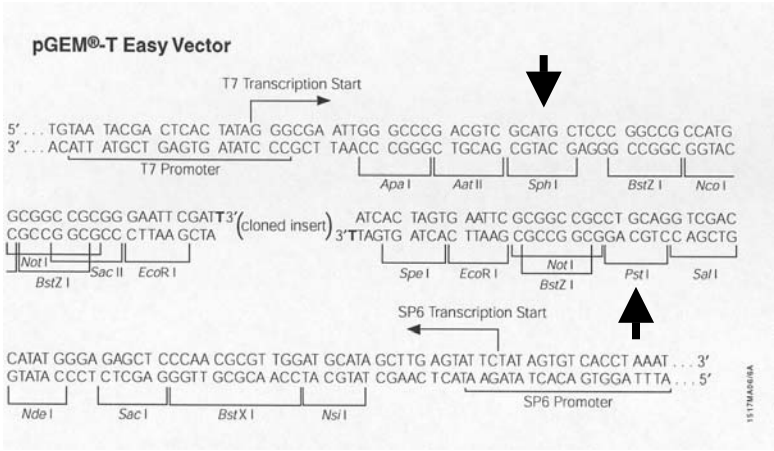

Figure 5: Restrictionsites of the pGEM®-T Easy Vector.
Restrictionsites for *Pst* I and *Sph* I are indicated by arrows.

4 h. To ensure completeness of the digestion, linearized DNA was analyzed by conventional gel electrophoresis as described in section 2.5.

In vitro transcription was done using the Riboprobe® *in vitro* Transcription System from Promega. Two µg linearized plasmid DNA were mixed with 20 µl Transcription Optimized 5 X Buffer, 10 µl DTT (100 mM), 29 µl nuclease free water, 2.5 µl RNAsin (40 units/µl), and 2.5 µl Klenow Fragment (5 units/µl; Promega) and incubated for 20 min at 22°C. This step converts the sticky ends, produced by *Pst* I and *Sph* I, into blunt ends thus avoiding initiation of transcription from the terminus of the template. After this step, 20 µl rNTP-Mix (2.5 mM of rATP, rCTP, rGTP, and rUTP), and 2.6 µl SP6 or T7 polymerase (10-20 units/µl) were added and the mixture was incubated at 30°C for 2 h. After *in vitro* transcription, plasmid DNA was degraded by addition of 2 µl RQ1 RNAse-free DNAse (1 unit/µl). RNA was purified using the RNeasy kit from Qiagen. Quality of *in vitro* transcripts was assessed using agarose/formaldehyde gels as described in section 2.6. Amount of *in vitro* transcripts was determined using a spectrophotometer (Genequant).

Generation of serial dilutions with known concentrations

The molecular weights (M_G) of *BTG2* and *G3PDH in vitro* transcripts were calculated as recommended by Ambion (http://www.ambion.com):

$$M_G\,(g/mol) = (A_n \times 328.2) + (U_n \times 305.2) + (C_n \times 304.2) + (G_n \times 344.2) + 159$$

Whereas n is the number of nucleotide within the RNA sequence.

The copy number (n) was determined by:

$$n = \frac{\text{concentration of in vitro transcript (g/l)} * 6.02 \times 10^{23}\ mol^{-1}}{M_G \text{ of in vitro transcript (g/mol)}}$$

Whereas n is in vitro transcript copy number, $6.02 \times 10^{23}\ mol^{-1}$ is the constant of Avogadro, and M_G is the molecular weight.

Serial dilutions of *BTG2* and *G3PDH in vitro* generated transcripts were mixed with ribosomal RNA from mice (Roche) to a final concentration of 0.5 µg/µl of ribosomal RNA.

Two-step RT-PCR

Reverse transcription. Two µl of each *in vitro* generated transcript (containing 1 µg of ribosomal RNA and the corresponding copy numbers of the in vitro transcripts) were combined with nuclease free water to a total volume of 9.5 µl. After incubation at 65°C for 10 min, RNA was chilled on ice. Fifty ng random hexamers (Invitrogen), 1 mM of dATP, dCTP, dGTP, and dTTP (Invitrogen), 5 mM $MgCl_2$, 1.5 mM Tris-HCl (pH 8.0), and 500 mM KCl, 100 units of M-MLV reverse transcriptase (Invitrogen), and 20 units of RNAsin (Roche) were added to a total volume of 19.5 µl. The reaction was incubated at 25°C for 10 min and 37°C for 60 min. After heat inactivation of the enzymes the remaining RNA in the reaction mixture was degraded for 20 min at 37°C with 0.5 µl (1 unit) of RNAse H (Invitrogen). A 1:2.5 dilution was prepared from each first strand cDNA synthesis product.

Quantitative PCR. Five µl of each first strand cDNA synthesis product generated above were combined with 2 µl of LightCycler-FastStart DNA Master SYBR Green I (Roche), primer-pairs for *BTG2* (forward: 5'-CTC ACC TGC AAG AAC CAA GTG-3'; reverse: 5'-AGT TCC CCA GGT TGA GGT ATG T-3') or *G3PDH* (forward:5'-GAA ATC CCA TCA CCA TCT TCC-3'; reverse: 5'-CAG AGA TGA TGA CCC TTT TGG-3') at a final concentration of 1 µM each, and $MgCl_2$ at a final concentration of 2 mM for *BTG2* and 3 mM for *G3PDH*. Amplification was

performed in a total volume of 20 µl for 10 min at 95°C and 40 cycles with 15 s at 95°C, 10 s at 58°C, and 7 s at 72°C.

Amplification efficiencies (E) were calculated as described in section 2.7.1. Melting curve analysis (LightCycler software package) was applied to ensure the specificity of the PCR reaction.

2.8 *BTG2* mRNA expression in primary cRCC and normal renal tissue

Tissue collective

Forty-two primary cRCCs and 12 normal renal tissues taken from the tumorbank of the Institute of Pathology in Basel were analyzed by quantitative RT-PCR. Histological grade and pT category were determined according to Thoenes and recommendations of the UICC, respectively (1, 30). Eight cRCCs were grade 1, 28 grade 2, and 6 grade 3. There were 20 pT1, 7 pT2, and 15 pT3 cRCC.

Quantification of BTG2 expression

To determine *BTG2*/*G3PDH* mRNA copy numbers, RT-PCR was done from 1 µg total RNA of each sample exactly following the protocol described in section 2.7.2 (*Two-step RT-PCR*).

Statistical analysis

All statistical analysis were done using StatView 5.0.1 software package (SAS institue Inc.).
In a first step, Anova analysis was applied to search for differences in *BTG2* and *G3PDH* mRNA copy numbers in cRCC and normal renal tissue.
In a second step, *BTG2* mRNA copy numbers were normalized to *G3PDH* mRNA copy numbers in each sample to correct for differences in the quality and quantity of RNA. Anova analysis was applied to search for differences in normalized *BTG2* mRNA expression. The association of *BTG2* mRNA expression with tumor grade and pT category was determined using Anova analysis.

2.9 Inducibility of *BTG2* mRNA expression in cRCC cell lines

Induction of BTG2 mRNA expression by 12-O-tetradecanoylphorbolester-13-acetate (TPA)

cRCC cell lines Caki-1, Caki-2, 786-O, 769-P and the positive control cell line Hela were plated at 5 x 10^5 cells/25 cm^2 culture vessel. Medium renewal was done 24 h after plating. RNA was extracted after 48 h from each cell line to determine the *BTG2* mRNA expression levels prior TPA treatment. The remaining cells were treated with various concentrations of TPA (25 ng, 50 ng, 75 ng, or 100 ng per ml culture medium, respectively) or DMSO alone (0.1% final concentration) and incubated for 70 min prior RNA extraction. To determine *BTG2*/*G3PDH* mRNA copy numbers, RT-PCR was done from 1 µg total RNA of each sample exactly following the protocol described in section 2.7.2 (*Two-step RT-PCR*).

BTG2 mRNA expression and cell density

Caki-1, Caki-2, 786-O, 769-P and Hela were plated at 1 x10^5, 2 x 10^5, and 5 x 10^5 cells/well in 6-well-plates. Medium renewal was done 24 h after plating. RNA was extracted after 48 h. At this time, cultures had - according to initial cell numbers - low, medium or high cell densities. To determine *BTG2*/*G3PDH* mRNA copy numbers, RT-PCR was done from 1 µg total RNA of each sample exactly following the protocol described in section 2.7.2 (*Two-step RT-PCR*).

3 Results

3.1 cDNA array analysis

To identify renal tumor relevant genes, gene expression profiles of four cRCC cell lines (Caki-1, Caki-2, 786-O, and 769-P) and one normal renal tissue were compared with each other. For this purpose, Atlas™ Human Cancer 1.2 cDNA microarrays, containing 1176 cDNA spots, were used. Microarray spots with sDens values ≥ 4500 were regarded as positive for gene expression. According to this threshold, expression of **748 genes** was not detectable in any of the analyzed samples (sDens value < 4500). sDens ratios were calculated for (i) genes which were expressed (sDens ≥ 4500) in normal renal tissue and cRCC cell line(s) and (ii) also for genes, which were not expressed (sDens < 4500) in normal renal tissue but strongly expressed (sDens ≥ 13500) in cRCC cell line(s) and vice versa. Genes with sDens ratios ≤ 0.5 and ≥ 2 in at least two cell lines were regarded as differentially expressed in cRCC cells compared to normal renal tissue. According to these definition, **36 genes** were stronger expressed in at least two cRCC cell lines compared to normal renal tissue. Of those cases, expression of 18 genes was not detectable in normal renal tissue but was very strong in at least two cRCC cell lines (sDens value ≥ 13500). In contrast, **35 genes** showed reduced expression levels in at least two cRCC cell lines. Fifteen of these genes were strongly expressed in normal renal tissue (sDens value ≥ 13500) but were undetectable in at least two cRCC cell lines.

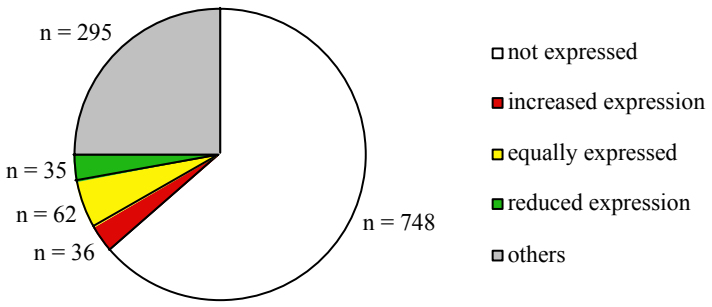

Figure 6: Overview of cDNA microarray hybridization results.

The expression patterns of 1176 cancer related genes have been analyzed in 4 cRCC cell lines and one normal renal tissue. not expressed = sDens < 4500 in all cRCC cell lines and normal renal tissue; increased expression = sDens ratio ≥ 2 in at least two cRCC cell lines compared to normal renal tissue; equally expressed = sDens ratio > 0.5 and < 2 in all cRCC cell lines and normal renal tissue; reduced expression = sDens ratio ≤ 0.5 in at least two cRCC cell lines compared to normal renal tissue; others = genes showing expression patterns different from those described above.

Sixty-two genes were equally expressed in normal renal tissue and in all cRCC cell lines because they had sDens ratios > 0.5 and < 2.The remaining **295 genes** did not fit into any of the above mentioned categories. Figure 6 gives an overview of the results from the cDNA microarray experiments. Only genes, showing at least 4-fold expression level differences in at least two cell lines (Table 4) were regarded as significantly differentially expressed. Those genes were selected as candidate genes for further studies by RISH. As an example, cDNA microarray results obtained from normal renal tissue and the cell line 769-P as an representative for all other analyzed cRCC cell lines are shown in figure 7.

Table 4: Candidate genes for further RISH experiments identified by cDNA array analysis.

	Position on cDNA microarray[1]	Gene name	Abbreviation in text[2]	Chromosomal locus	Gene bank accession number
increased expression in cRCC cell lines	1	Centromeric protein F	CENPF	1q32-q41	NM_016343
	2	CDC28 protein kinase regulatory subunit 1B	CKS1B	8q21	NM_001826
	3	Chondroitin sulfate proteoglycan 2	CSPG2	5q12-q14	NM_004385
	4	Fibronectin 1	FN1	2q34	NM_002026
	5	FOS-like antigene 1	FOSL1	11q13	NM_005438
	6	High mobility group AT-hook 1	HMGA1	6p21	NM_002131
	7	Integrin alpha 3	ITGA3	17	NM_002204
	8	Integrin beta 8	ITGB8	7p15.3	NM_002214
	9	Tubulin alpha ubiquitous	K-alpha-1	12q13.11	NM_006082
	10	Plasminogen activator inhibitor type 1	PAI1	7q21.3-q22	NM_000602
	11	Transforming growth factor beta induced	TGFB1	19q13.1	NM_000358
	12	Vimentin	VIM	10p13	NM_003380
reduced expression in cRCC cell lines	13	Basigin	BSG	19p13.3	NM_001728
	14	B-cell translocation gene 2	BTG2	1q32	NM_006763
	15	CD74 antigen	CD74	5q32	NM_004355
	16	CD9 antigen	CD9	12p13	NM_001769
	17	Checkpoint supppressor 1	CHES1	14q24.3-q31	NM_005197
	18	Cathepsin D	CTSD	11p15.5	NM_001909
	19	Early growth response 1	EGR1	5q31.1	NM_001964
	20	FC fragment of IgG, receptor transporter, alpha	FCGRT	19q13.3	NM_004107
	21	growth arrest-specific 6	GAS6	13q34	NM_000820
	22	Integrin alpha 6	ITGA6	2q31.1	NM_000210
	23	LPS-induced TNF alpha factor	LITAF	16p13.3-p12	NM_004862
	24	nuclear hormone receptor	NR0B2	1p36.1	NM_021969
	25	Tissue inhibitor of matrixmetalloproteinases 3	TIMP3	22q22.1-q13.2	NM_000362

[1] See figure 7.
[2] Abbreviation for gene name used in the text.

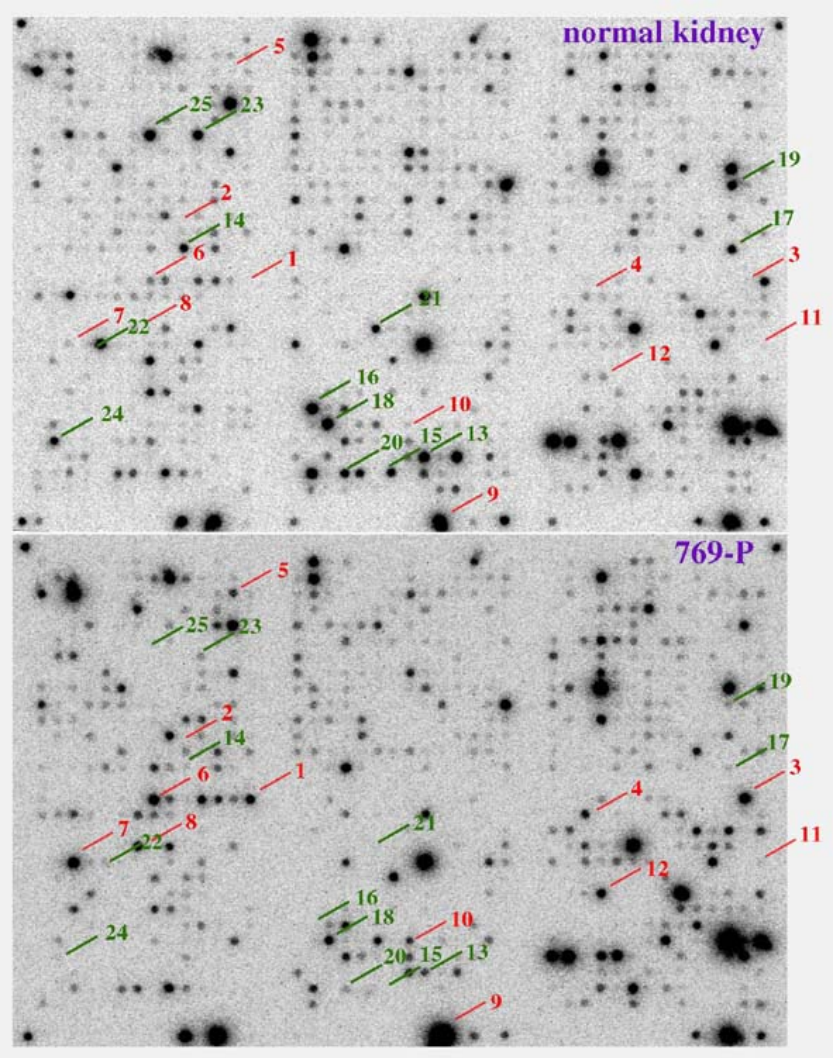

Figure 7: cDNA microarray hybridization of normal renal tissue and cRCC cell line 769-P.

3.2 RNA *in situ* hybridization

Twenty-five significantly differentially expressed genes (Table 4) identified by preceding cDNA microarray experiments were further studied by oligo-based RISH on primary RCCs to assess their impact on renal tumor biology.

The renal TMA

To study the expression patterns of the selected candidate genes by RISH, TMAs were generated from 61 snap-frozen primary RCCs and 12 normal renal tissues (Figure 8).

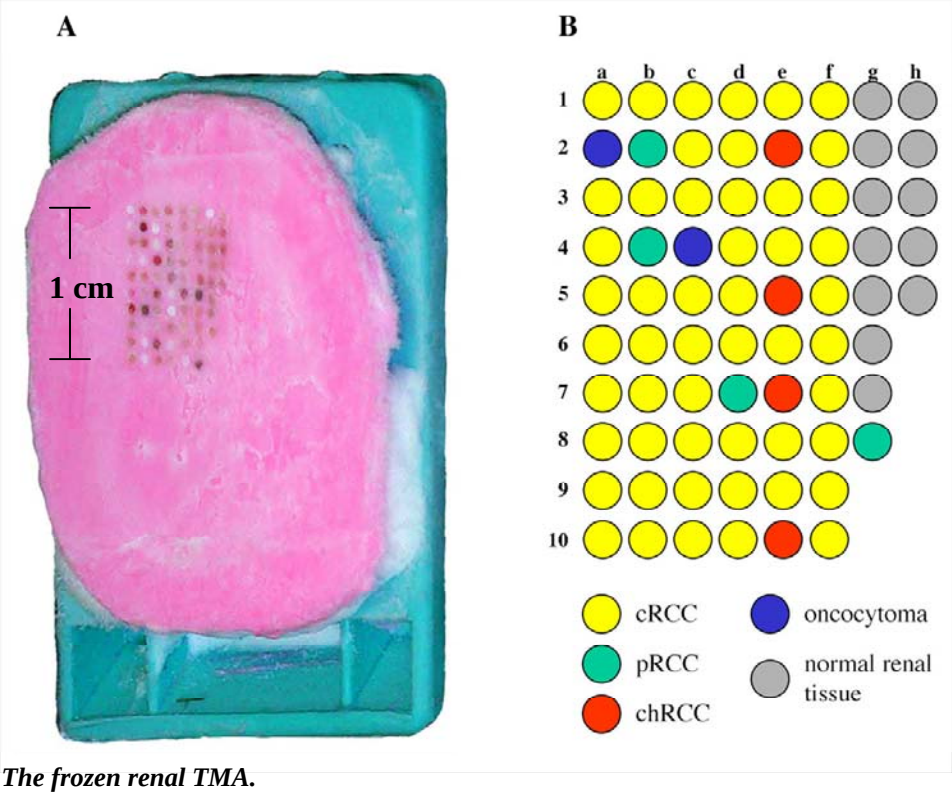

Figure 8: The frozen renal TMA.

(A) The frozen renal TMA composed of 73 different renal tissue core biopsies. (B) Localization and number of different RCC subtypes arranged in the renal TMA. There are 51 cRCCs, 4 pRCCs, 4 chRCCs, 2 oncocytomas and 12 normal renal tissues.

Certain experiments were done to control the quality of the TMA and the integrity of the tissue specimens:

- H&E-stained TMA sections were surveyed under the microscope to re-evaluate the quality and integrity of each tissue spot after generation of the TMA (Figure 9A).

- To analyze the RNA integrity in the tissue spots, *β-Actin* oligonucleotide probes were hybridized to a TMA section directly after preparation of the TMA (Figure 9B).

- Since the sectioning of the TMA and the hybridization process might lead to loss of tissue material, each TMA sections was counterstained with Harris‘ hematoxylin after hybridization of the oligonucleotide probes to exclude tissue spots containing less than 60% representative cells from further analysis (Figure 9C).

- To evaluate the specificity of the radioactive signal, slides were dipped into Hypercoat™ LM-1 emulsion, which allows direct autoradiography of the TMA section (Figure 9D).

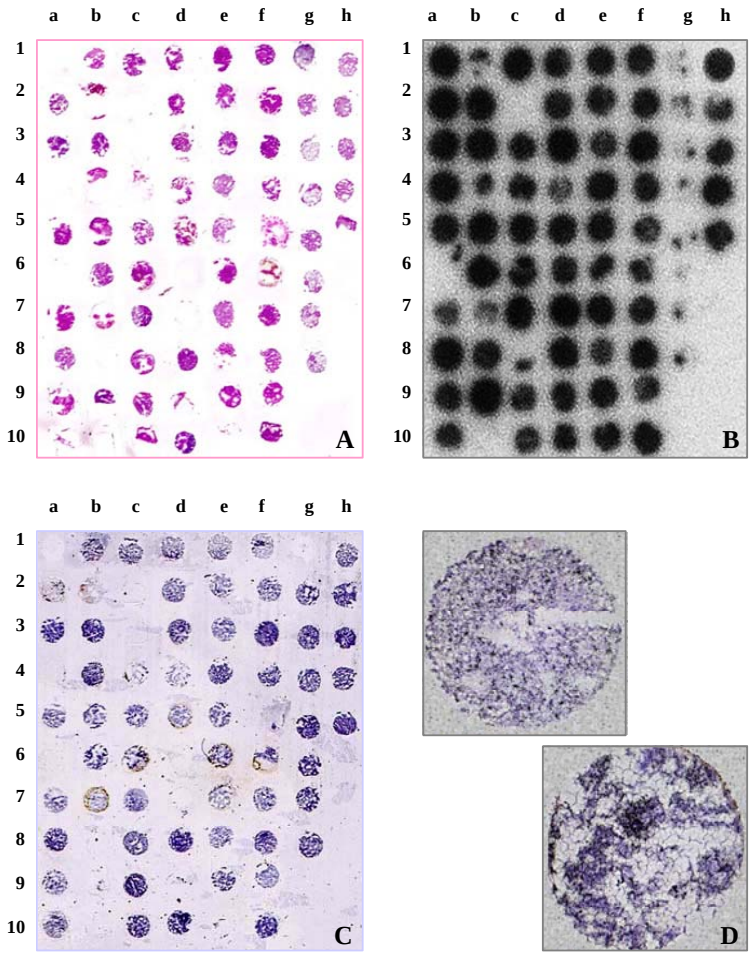

Figure 9: Control experiments to evaluate the quality of the tissues represented on the TMA and to assess the specificity of the hybridization signal .

H&E stained section of the TMA. (B) TMA hybridized with β-Actin probes. (C) TMA section counterstained with Harris‘ hematoxylin. (D) Magnification of TMA tissue spots after autoradiography using Hypercoat™ LM-1 solution. Black granules upon the cells are indicating the localization of the radioactive signals. Based on those control experiments, certain tissue spots were excluded from further analysis. For example, even though the morphology and amount of the tissue spots in row g was good (A and C) those samples had to be excluded from further analysis because the RNA quality was poor (B).

Based on these control experiments, the maximal number of evaluable tissue spots was 48 of originally 73 tissue specimens (Table 5). In brief, up to 36 (of originally 51) cRCCs, 3 (of 4) pRCCs, 3 (of 4) chRCCs, 1 (of 2) oncocytomas, and 5 (of 12) normal renal tissues were still analyzable.

Overview of RISH results

Only those tissue spots showing mean sDens values ≥ 2-fold mean background sDens values were considered positive for gene expression. Based on this threshold value, 19 of the 25 selected candidate genes were analyzable by RISH because they showed expression in at least three tissue spots (Table 5). Six genes (*CKS1B*, *CSPG2*, *FOSL1*, *HMGA1*, *TGFB1*, and *NR0B2*) did not show measurable sDens values in any of the evaluable tissue spots. Those genes were, even after repetition of the hybridization experiments, not analyzable by RISH.

Table 5: Gene expression frequencies in the subset of analyzable candidate genes.

Gene	**Positive tissue spots (n)** [1]	**Evaluable tissue spots (n)** [2]	**Gene expression frequency (%)** [3]
BSG	24	43	56
BTG2	8	46	17
CD74	42	43	98
CD9	12	39	31
CENPF	6	41	15
CHES1	12	47	26
CTSD	42	47	89
EGR1	26	46	57
FCGRT	7	48	15
FN1	18	47	38
GAS6	24	48	50
ITGA3	3	47	6
ITGA6	9	47	19
ITGB8	35	48	73
K-alpha-1	19	41	46
LITAF	20	46	43
PAI1	10	44	23
TIMP3	34	48	71
VIM	47	48	98

[1] Number of evaluable RCC and normal renal tissue spots with gene expression (mean sDens value ≥ mean 2-fold background value).
[2] Total number of evaluable RCC and normal renal tissue spots.
[3] Gene expression frequency: number of tissue spots positive for gene expression / total number of evaluable tissue spots.

As shown in table 5, the number of tissues displaying visible signals varied strongly within the set of analyzable genes. For example, *VIM* and *CD74* were expressed in almost 100% of the evaluable tissue spots whereas *ITGA3* expression was merely detectable in 6% of the analyzable cases (Table 5).

Figure 10 shows Phosphorimager displays of renal TMA sections after hybridization with oligonucleotide probes targeting different genes.

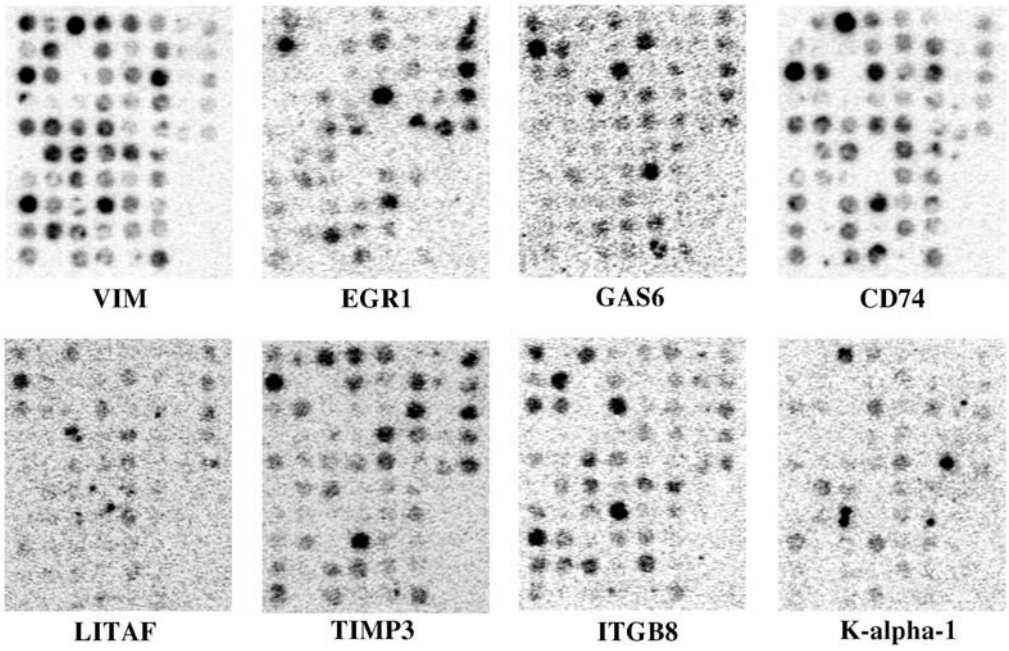

Figure 10: Phosphorimager displays of renal TMA sections after RISH.
Each hybridization results in individual expression patterns indicating the specificity of the used probes.

Gene expression frequencies in RCC subtypes and normal renal tissue

Since expression of some genes might be linked to certain RCC subtypes, gene expression frequencies of the 19 analyzable genes were compared between different RCC subtypes and normal renal tissue (Table 6). *FN1*, *ITGA3*, *PAI1*, and *BTG2* were expressed in cRCCs, the most common RCC subtype, but not in any of the other subtypes. However, the opposite case, not expressed in cRCC but expressed in any of the other RCC subtypes, has not been observed.

Table 6: Gene expression frequencies in RCC subtypes and normal renal tissue evaluated by RISH.

	Expression frequency [1]				
Gene	cRCC	pRCC	chRCC	onco-cytoma [2]	normal kidney
BSG	15/32	1/2	3/3	1/1	4/5
BTG2	4/35	0/2	0/3	0/1	4/5
CD74	33/33	1/2	3/3	na	5/5
CD9	6/29	0/2	3/3	na	3/5
CENPF	4/33	0/1	0/2	na	2/5
CHES1	5/35	0/3	3/3	1/1	3/5
CTSD	32/36	1/2	3/3	1/1	5/5
EGR1	19/35	0/3	2/3	1/1	4/4
FCGRT	6/36	1/3	0/3	0/1	0/5
FN1	16/36	0/2	0/3	0/1	2/5
GAS6	14/36	1/3	3/3	1/1	5/5
ITGA3	3/35	0/3	0/3	0/1	0/5
ITGA6	5/35	0/3	3/3	1/1	0/5
ITGB8	29/36	1/3	0/3	1/1	5/5
K-alpha-1	15/33	0/1	2/2	na	2/5
LITAF	10/35	1/2	3/3	1/1	5/5
PAI1	9/35	0/2	0/1	0/1	1/5
TIMP3	25/36	0/3	3/3	1/1	5/5
VIM	36/36	2/3	3/3	1/1	5/5

[1] Expression frequency: number of tissue spots positive for gene expression / total number of evaluable tissue spots.
[2] na: non of the tissue spots was analyzable.

Gene expression frequencies in cRCC and normal renal tissue

Statistical analysis was only done with the results obtained for cRCC and normal renal tissue. In a first step, gene expression frequencies (number of tissue spots positive for gene expression / total number of evaluable tissue spots) were compared between cRCC and normal renal tissue. As indicated in table 7, *ITGA3*, *FCGRT*, and *ITGA6* were detectable in cRCC tissue spots but not in normal renal tissue. In contrast, *BTG2*, *CHES1*, *GAS6*, and *LITAF* were significantly ($p < 0.05$) more frequently expressed in normal renal tissue than in cRCC. *CD9* and *EGR1* were also clearly more frequently expressed in normal renal tissue than in cRCC but this association did not reach significance ($p < 0.1$ but > 0.05).

In a second step, gene expression frequencies in cRCC were correlated with pT category and tumor grade in the subset of cRCC. Significant associations were found for *BTG2*, *CD9*, and *TIMP3*.

Expression of BTG2 and CD9 was associated with tumor extension (pT category). *BTG2* was merely expressed in organ-confined pT1/pT2 (4/24, 17%) cRCCs but not in advanced pT3 tumors (0/11, 0%). Expression of *CD9* was also only found in pT1/pT2 (6/20, 30%) lesions but not in any of the analyzable (0/9, 0%) pT3 tumors.

In contrast, expression of *TIMP3* was associated with tumor grade. *TIMP3* mRNA expression was less frequently found in grade 3 (1/5; 20%) than in grade 2 (17/23; 74%) and grade 1 cRCCs (7/8; 88%; $p = 0.03$).

Table 7: Gene expression frequencies in cRCC and normal renal tissue evaluated by RISH.

		Expression frequency [1]				
cDNA microarray [2]	Gene	**normal renal tissue (n) [3]**	**%**	**cRCC (n) [3]**	**%**	**p-value [4]**
increased expression in cRCC cell lines	CENPF	2/5	**40**	4/33	**12**	n.s.
	FN1	2/5	**40**	16/36	**44**	n.s.
	ITGA3	0/5	**0**	3/35	**9**	-
	ITGB8	5/5	**100**	29/36	**81**	n.s.
	K-alpha-1	2/5	**40**	15/33	**45**	n.s.
	PAI1	1/5	**20**	9/35	**26**	n.s.
	VIM	5/5	**100**	36/36	**100**	n.s.
reduced expression in cRCC cell lines	*BSG*	4/5	**80**	15/32	**47**	n.s.
	BTG2	4/5	**80**	4/35	**11**	*0.0003*
	CD74	5/5	**100**	33/33	**100**	n.s.
	CD9	3/5	**60**	6/29	**21**	*0.07*
	CHES1	3/5	**60**	5/35	**14**	*0.02*
	CTSD	5/5	**100**	32/36	**89**	n.s.
	EGR1	4/4	**100**	19/35	**54**	*0.08*
	FCGRT	0/5	**0**	6/36	**17**	-
	GAS6	5/5	**100**	14/36	**39**	*0.01*
	ITGA6	0/5	**0**	5/35	**14**	-
	LITAF	5/5	**100**	10/35	**29**	*0.002*
	TIMP3	5/5	**100**	25/36	**69**	n.s.

[1] Expression frequency: number of tissue spots positive for gene expression / total number of evaluable tissue spots.
[2] Gene expression pattern in preceding cDNA microarray experiments.
[3] Number of tissue spots with gene expression / total number of evaluable tissue spots.
[4] p-value was calculated using Chi-square analysis; n.s.: not significant.

Gene expression levels in cRCC and normal renal tissue

In order to quantitate mRNA expression levels in the tissues on the TMA, the raw sDens values (as measured by the Phosphor imager instrument) were utilized. Quantification is of particular

interest for those genes showing expression in both, tumor and normal tissues since the level of mRNA expression could be more important than the bare precence of the transcript. Here again, statistical analysis was done for the subset of cRCCs and normal renal tissues only.
Significant associations were found for *VIM* and CD74. VIM was stronger expressed in cRCC than in normal renal tissue ($p = 0.04$). CD74 was stronger expressed in advanced pT3 tumors than in organ-confined pT1/pT2 tumors ($p = 0.03$).

3.3 Molecular studies on *BTG2* to evaluate its importance for cRCC biology

In the second part of this thesis one gene was selected from preceding cDNA and tissue microarray experiments to further study its impact on cRCC biology.

BTG2 was chosen for further studies because:

- cDNA microarray analysis revealed significantly reduced *BTG2* mRNA expression levels in all analyzed cRCC cell lines compared to normal renal tissue (Figure 11A).

- RISH analysis showed that *BTG2* was significantly less frequently expressed in primary cRCCs than in normal renal tissue (Figure 11B) thus corroborating the findings of the cDNA microarray hybridizations.

- Melamed et al. (124) found strong *BTG2* protein expression in normal epithelial cells of renal proximal tubuli from which cRCC arise (1) strongly suggesting that loss of BTG2 expression might be of great importance for renal tumor biology.

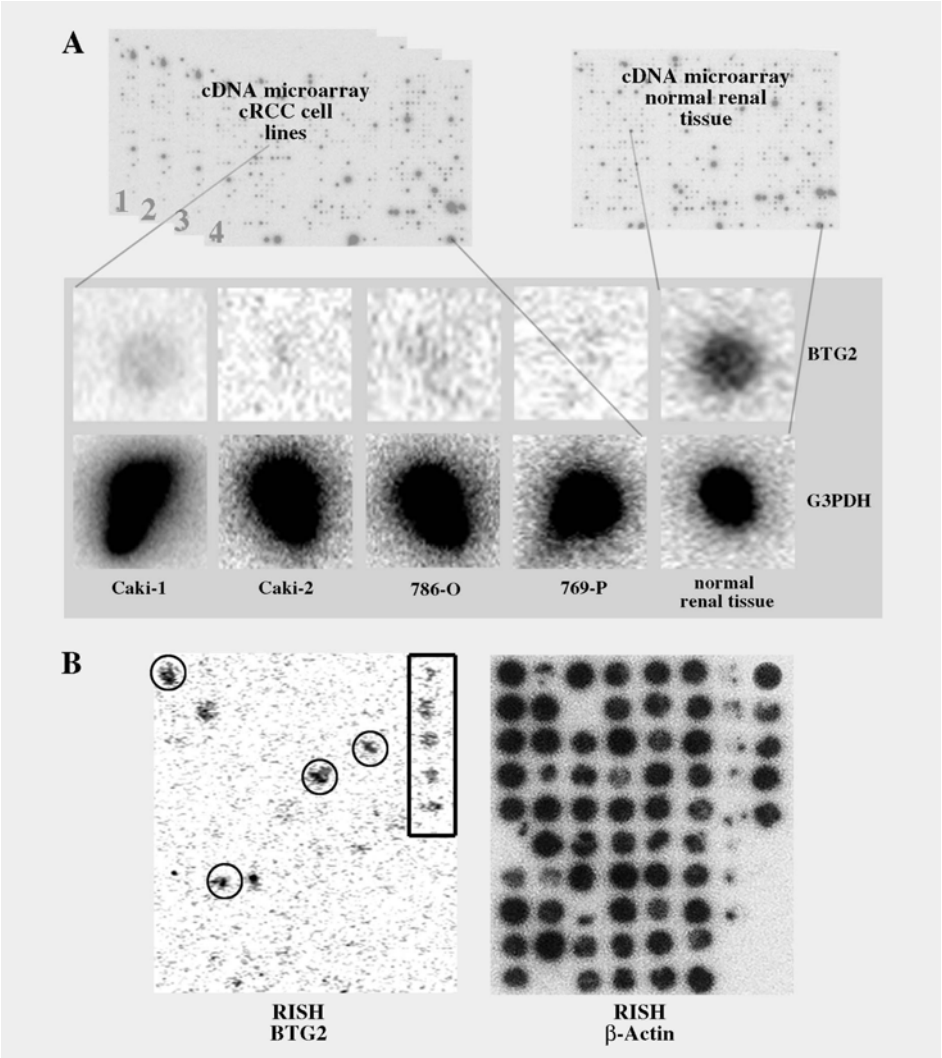

Figure 11: BTG2 mRNA expression on cDNA and tissue microarrays.

(A) *BTG2* mRNA expression in cRCC cell lines and in normal renal tissue as assessed by cDNA microarray analysis. Magnifications of the BTG2 and G3PDH (reference gene) cDNA spots after hybridization are shown in the lower pannel. BTG2 was strongly expressed in normal renal tissue but nearly undetectable in all analyzed cRCC cell lines. **(B)** *BTG2* mRNA expression in primary cRCC and in normal renal tissue evaluated by RISH. *BTG2* mRNA expression is detectable in 4 of 35 analyzable cRCCs (indicated by circles) and in 4 of 5 normal renal tissues (indicated by a rectangle). Reference genes G3PDH and β-Actin were used as positive controls (A, B).

3.3.1 Northern blot analysis

Confirmation of cDNA microarray results

To confirm the results obtained for *BTG2* with the cDNA microarray experiments, single-stranded ^{32}P labeled DNA probes for *BTG2* and *G3PDH* were hybridized to polyA^{+} mRNA of all four cRCC cell lines, normal renal tissue, and lymphocytes (positive control). *BTG2* transcripts were detected at the expected size of 2.7 kb (representative BTG2 mRNA sequence under gene bank accession number NM_006763 at the NCBI homepage) in normal renal tissue and the positive control but not in any of the analyzed cRCC cell lines (Figure 12). In contrast, G3PDH mRNA was found in all analyzed samples at the expected size of 1.3 kb (representative G3PDH mRNA sequence under gene bank accession number NM_002046 at the NCBI homepage).

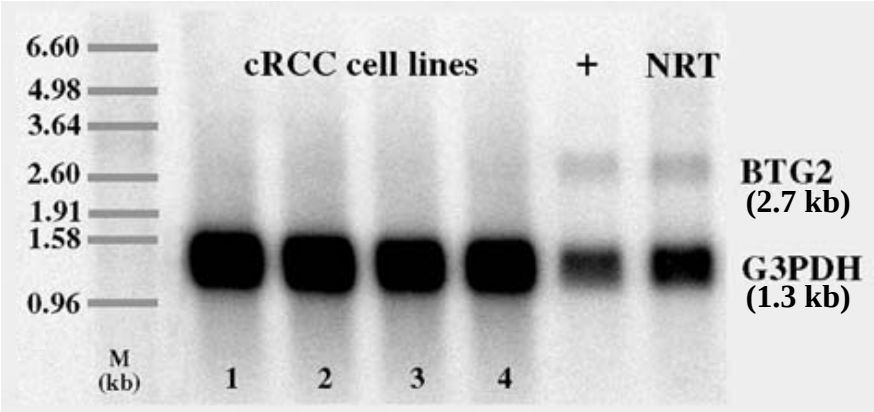

Figure 12: Northern blot analysis of BTG2 to confirm cDNA microarray results.

BTG2 mRNA expression was detectable as a single band at 2.7 kb in human lymphocytes (+) and normal renal tissue (NRT) but not in cRCC cell lines (1 = Caki-1, 2 = Caki-2, 3 = 786-O, and 4 = 769-P) after 4 h exposition. *G3PDH* was used as positive control.

Evaluating specificity of BTG2 oligonucleotide probes

To ensure the specificity of the *BTG2* oligonucleotide probe used on the renal TMA, ^{32}P labeled oligonucleotide probes for *BTG2* (the same that were used in the RISH experiments) were hybridized to total RNA from human lymphocytes. A single band at 2.7 kb (representative *BTG2* mRNA sequence under gene bank accession number NM_006763 at the NCBI homepage) confirmed the specificity of the oligonucleotides for the *BTG2* mRNA sequence (Figure 13).

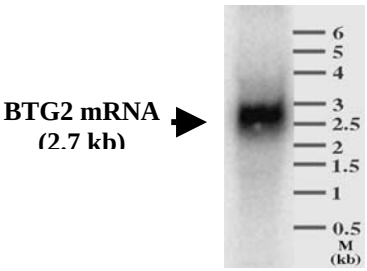

Figure 13: Northern blot analysis of BTG2 to confirm specificity of oligonucleotide probes used in the RISH experiment.

A strong and specific signal for BTG2 was obtained after an exposition time of 12 h.

3.3.2 *BTG2* mRNA expression in primary cRCC and normal renal tissue evaluated by quantitative RT-PCR

BTG2 mRNA amounts were determined in a subset of primary cRCC and normal renal tissues by quantitative RT-PCR using the LightCycler technology.

Calibration of RT-PCR

To calibrate RT-PCRs, standard curves for *BTG2* and *G3PDH* (reference) were established. For this purpose, serial dilutions of *in vitro* generated *BTG2* and *G3PDH* mRNA were prepared. *BTG2* and *G3PDH* PCR products were cloned into pGEM®-T easy vectors (Figure 14A). To generate run-off in vitro transcripts, plasmid DNA was digested with appropiate (*Sph*I or *Pst*I) restriction enzymes (Figure 14A). Run-off *in vitro* transcripts (sense strand) of *BTG2* and *G3PDH* were generated from the linearized plasmid DNA (Figure 14B).

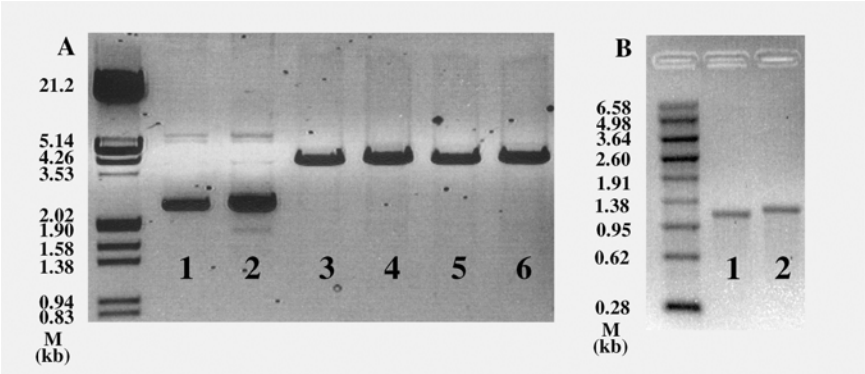

Figure 14: Generation of in vitro transcribed BTG2 and G3PDH mRNA using the pGEM Teasy vector.
(A) Gel electrophoresis of pGEM®-T easy plasmid DNA containing *BTG2* (1) and *G3PDH* (2) PCR products before (1 and 2) and after linearization with *Sph*I (3 and 4) and *Pst*I (5 and 6). M = DNA size marker. **(B)** *In vitro* generated run-off transcripts of *BTG2* (1) and *G3PDH* (2). M = RNA size marker.

Serial dilutions of both *in vitro* generated transcripts were reverse transcribed. First strand cDNA synthesis products were amplified on the LightCycler (Figure 15). Standard curve slopes were –3.718 for *BTG2* and –3.763 for *G3PDH* resulting in PCR efficiencies (E) of 1.86 and 1.84, respectively (Figure 15A).

Melting curve analysis confirmed specificity of PCR reactions. Melting of *BTG2* and *G3PDH* PCR products resulted in single melting-peaks for *BTG2* and *G3PDH* (Figure 15B).

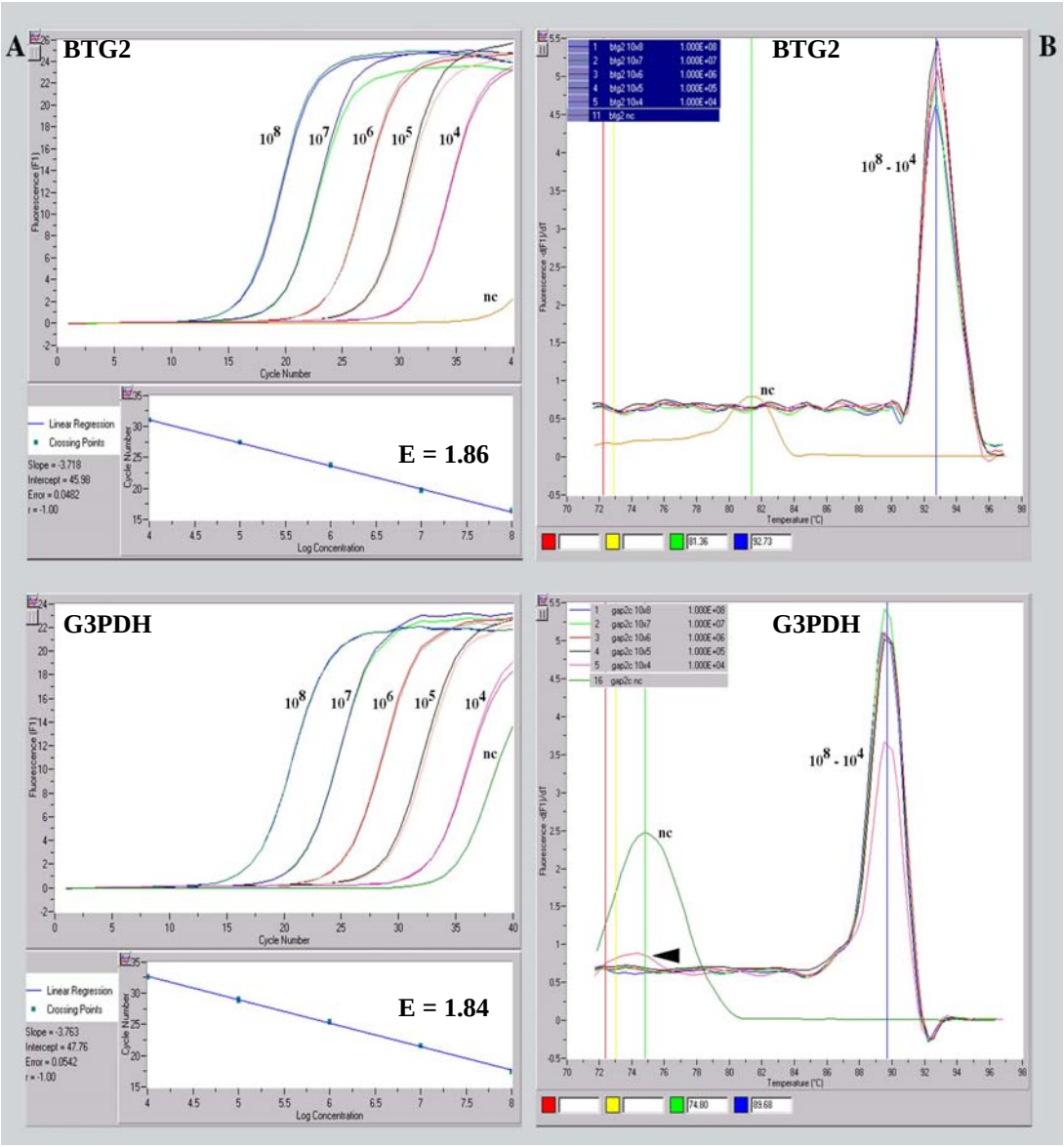

Figure 15: Calibration of quantitative RT-PCR.

(A) Standard curves for *BTG2* and *G3PDH*; nc = negative control. **(B)** Melting curve analysis of *BTG2* and *G3PDH* indicating the specifity of both PCR reactions. Unspecific primer-dimers occured in negative controls (nc) and in the lowest concentration of *G3PDH* template (indicated by arrowhead) only.

Quantification of BTG2 in primary cRCCs and normal renal tissues

BTG2 mRNA expression levels were analyzed in 42 fresh-frozen primary cRCC and 17 normal renal tissues. *BTG2* mRNA expression was significantly stronger in normal renal tissue than in cRCC. Mean *BTG2* mRNA copy numbers were 1.5 x 10^6 per µg total RNA (range:1.9 x 10^5 – 3.7 x 10^6) in cRCC and 9 x 10^6 per µg total RNA (range: 2.1 x 10^6 – 3.9 x 10^7) in normal renal tissue ($p < 0.0001$; Figure 16A). Mean *G3PDH* mRNA copy numbers were 42.6 x 10^6 per µg total RNA (range:9.5 x 10^6 – 9.8 x 10^7) in cRCC and 32.5 x 10^6 per µg total RNA (range: 8.3 x 10^6 – 4.9 x 10^7) in normal renal tissue ($p = 0.084$; Figure 16A). *BTG2*/*G3PDH* mRNA copy number ratios were calculated to normalize for differences in RNA quality and quantity. Mean *BTG2*/*G3PDH* ratios were 0.043 (range: 0.0065 – 0.18) in cRCC and 0.288 (range: 0.073 – 0.84) in normal renal tissue ($p<0.0001$; Figure 16B).

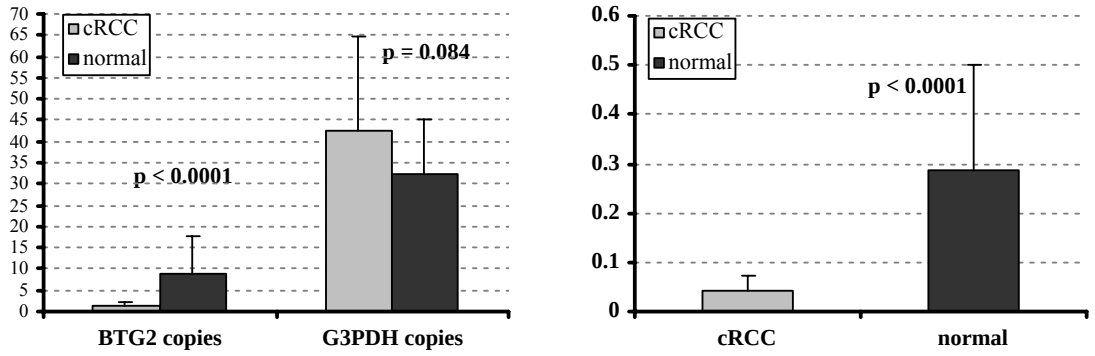

Figure 16: Quantitative mRNA expression analysis of BTG2 and G3PDH.

(A) Mean *BTG2* and *G3PDH* mRNA copy numbers in primary cRCCs and normal renal tissues. mRNA copy numbers are given in Mio copies per µg total RNA. **(B)** Mean *BTG2*/*G3PDH* mRNA copy number ratios in primary cRCCs and normal renal tissues.

BTG2 mRNA expression was also correlated with tumor extension (pT category) and tumor grade in the subset of cRCCs. There was no association between *BTG2* expression and pT category or tumor grade (Figure 17A and B).

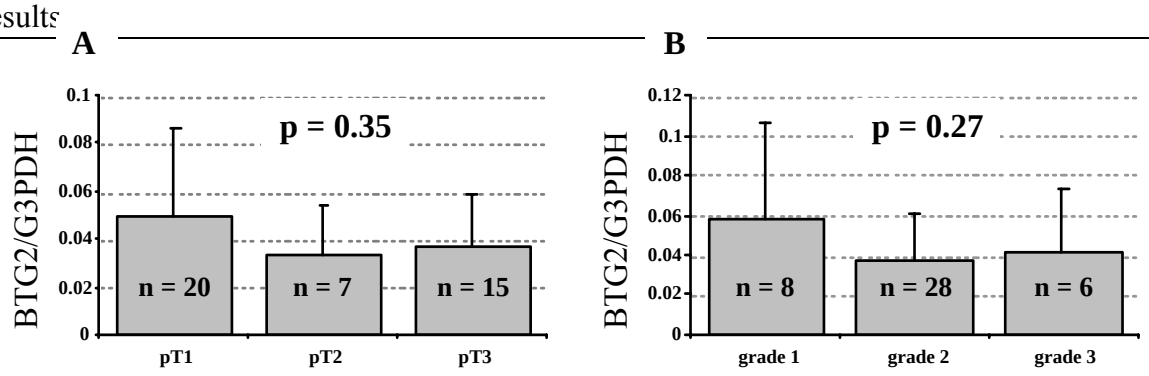

***Figure 17*: *BTG2* mRNA expression in association with pT category and tumor grade in cRCC.**

(A) *BTG2* mRNA expression and pT category. **(B)** *BTG2* mRNA expression and tumor grade. *BTG2* mRNA expression is given as *BTG2*/*G3PDH* mRNA copy number ratio.

3.3.3 Modulation of *BTG2* mRNA expression in cRCC cell lines

TPA treatment of cRCC cell lines

The phorbolester TPA has been shown by other groups (125, 126) to be a potent inducer of *BTG2* expression in HeLa cells and murine cell lines of different origin. Because *BTG2* mRNA expression is significantly reduced in cRCC cell lines and primary cRCC the question arises whether *BTG2* mRNA expression could be induced by TPA in cRCC cell lines.

Caki-1, Caki-2, 786-O, 769-P, and HeLa (positive control) cells were treated with various concentrations of TPA. *BTG2* and *G3PDH* mRNA copy numbers were determined by quantitative RT-PCR on the LightCycler. *BTG2* mRNA expression in untreated cRCC cell lines were comparable to those obtained for primary cRCC (Table 8). Expression of *G3PDH* mRNA was not significantly affected by TPA in any cell line (Figure 18). Therefore, *BTG2* to *G3PDH* mRNA copy number ratios were calculated to normalize for differences in RNA quality and amount (Table 8). According to these ratios, HeLa cells showed an up to 15-fold increase of *BTG2* mRNA expression after addition of TPA (Figure 19). In contrast, *BTG2* mRNA expression alterations upon TPA treatment were very weak or even not detectable in cRCC cell lines. Strongest response to TPA treatment was obtained for Caki-1 cells, which showed up to 2.4-fold increased *BTG2* mRNA expression levels. There was no association between TPA concentration and *BTG2* mRNA expression alteration in any cell line (Figure 19).

Table 8: BTG2 and G3PDH mRNA copy numbers in TPA treated cell lines.

Cell line	Treatment [1]	*BTG2* [2]	*G3PDH* [2]	Ratio [3]
HeLa	T0	0.52	128	0.0041
	25 ng TPA	6.58	106	0.0621
	50 ng TPA	6.92	110	0.0629
	75 ng TPA	7.26	121	0.0600
	100 ng TPA	6.76	109	0.0620
	0.01% DMSO	1.14	121	0.0094
Caki-1	T0	0.63	117	0.0054
	25 ng TPA	1.53	127	0.0120
	50 ng TPA	1.49	115	0.0130
	75 ng TPA	1.43	104	0.0138
	100 ng TPA	1.23	106	0.0116
	0.01% DMSO	0.33	103	0.0032
Caki-2	T0	0.78	229	0.0034
	25 ng TPA	0.85	174	0.0049
	50 ng TPA	0.89	171	0.0052
	75 ng TPA	1.12	216	0.0052
	100 ng TPA	0.98	173	0.0057
	0.01% DMSO	0.65	156	0.0042
786-O	T0	0.15	81.3	0.0019
	25 ng TPA	0.29	118	0.0024
	50 ng TPA	0.27	76.3	0.0036
	75 ng TPA	0.23	99.6	0.0023
	100 ng TPA	0.26	119	0.0022
	0.01% DMSO	0.15	108	0.0014
769-P	T0	0.60	143	0.0042
	25 ng TPA	0.50	119	0.0042
	50 ng TPA	0.55	126	0.0043
	75 ng TPA	0.86	182	0.0047
	100 ng TPA	0.70	147	0.0048
	0.01% DMSO	0.52	122	0.0042

[1] T0 = basal mRNA copy numbers (prior addition of TPA/DMSO).
[2] *BTG2* and *G3PDH* mRNA copy numbers are given in Mio copies/µg total RNA.
[3] *BTG2*/*G3PDH* mRNA copy number ratio.

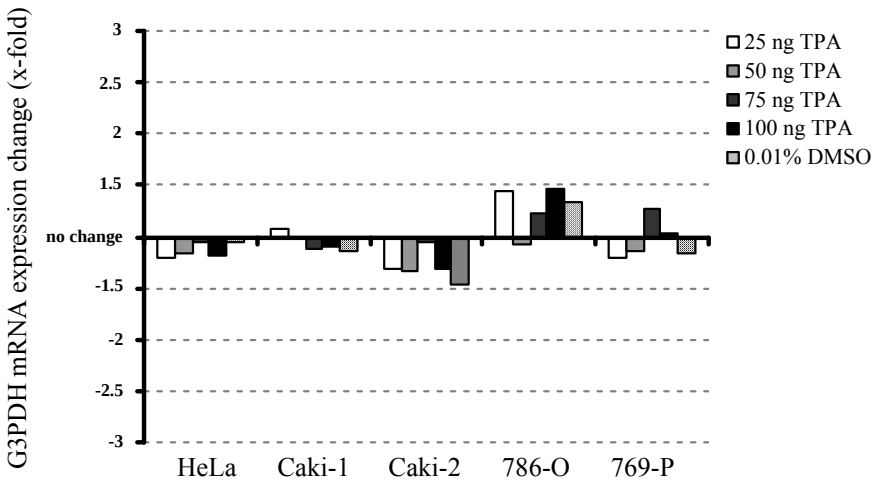

Figure 18: G3PDH mRNA expression alterations upon TPA treatment.

Expression alterations are given in ± x-fold relative to basal *G3PDH* mRNA expression (prior addition of TPA/DMSO) in the respective cell line. no change: *G3PDH* mRNA expression in TPA/DMSO treated culture equals basal *G3PDH* mRNA expression.

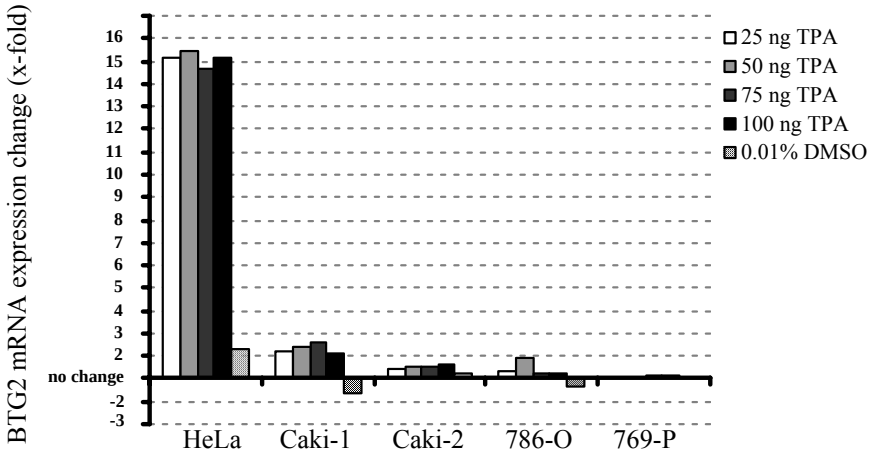

Figure 19: BTG2 mRNA expression change upon TPA treatment.

BTG2 mRNA copy numbers were normalized to *G3PDH* mRNA copy numbers. Expression alterations are given in ± x-fold relative to basal *BTG2*/*G3PDH* mRNA copy number ratios (prior addition of TPA/DMSO) in the respective cell line. no change: *BTG2* mRNA expression in TPA/DMSO treated culture equals basal *BTG2* mRNA expression.

BTG2 mRNA expression and cell density

BTG2 mRNA expression was found by other groups (127, 128) to be absent in exponentielly growing cell cultures but abundant in quiescent cells. For this reason, *BTG2* mRNA expression was analyzed in association with cell density in cRCC cell lines. Caki-1, Caki-2, 786-O, and 769-P cells were seeded at different densities and *BTG2* and *G3PDH* mRNA copy numbers were assessed by quantitative RT-PCR 48 h after plating (table 9). Since *G3PDH* mRNA expression was not significantly linked to cell density (figure 20), *BTG2* to *G3PDH* mRNA copy number ratios were calculated to normalize for differences in RNA quality and amount (table 9). *BTG2* mRNA expression was associated with increasing cell density in Caki-2, 786-O, and 769-P but not in Caki-1 cells (figure 21).

Table 9: BTG2 and G3PDH copy numbers in association with cell density.

Cell line	Cell density [1]	BTG2 [2]	G3PDH [2]	Ratio [3]
Caki-1	low	0.94 ± 0.01	189 ± 24	0.0050 ± 0.0001
	medium	1 ± 0.03	205 ± 1	0.0049 ± 0.0002
	high	0.97 ± 0.19	284 ± 60	0.0034 ± 0.0001
Caki-2	low	0.45 ± 0.09	191 ± 30	0.0023 ± 0.0001
	medium	0.65 ± 0.06	229 ± 29	0.0029 ± 0.0001
	high	0.9 ± 0.11	209 ± 14	0.0043 ± 0.0002
786-O	low	0.16 ± 0.01	119 ± 13	0.0014 ± 0.0001
	medium	0.23 ± 0.006	111 ± 1	0.0021 ± 0.0001
	high	0.61 ± 0.02	102 ± 2	0.0060 ± 0.0003
769-P	low	0.33 ± 0.05	145 ± 35	0.0023 ± 0.0002
	medium	0.45 ± 0.13	159 ± 27	0.0028 ± 0.0003
	high	0.59 0.07	154 ± 3	0.0038 ± 0.0004

[1] low = initial cell number 1 x 10^5/well; medium = initial cell number 2 x 10^5/well; high = initial cell number 5 x 10^5/well.
[2] BTG2 and G3PDH mRNA copy numbers are given in Mio copies/µg total RNA.
[3] BTG2/G3PDH mRNA copy number ratio.

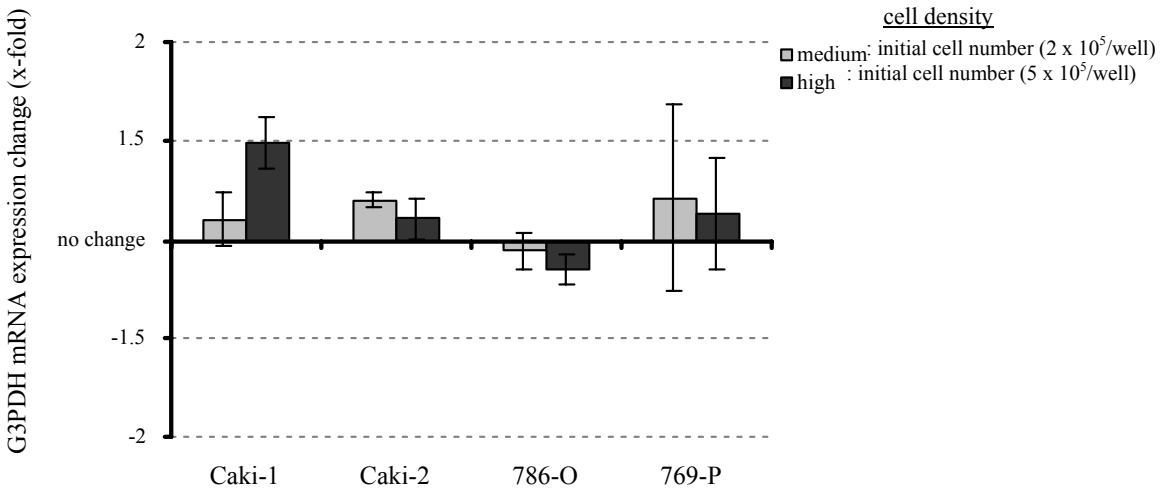

Figure 20: G3PDH mRNA expression and cell density.

G3PDH mRNA expression alterations are given in ± x-fold relative to cultures with lowest cell densities (initial cell number: 1 x 10^5 cells/well). no change: *G3PDH* mRNA expression in cultures with medium/high cell densities equals *G3PDH* mRNA expression in cultures with lowest densities.

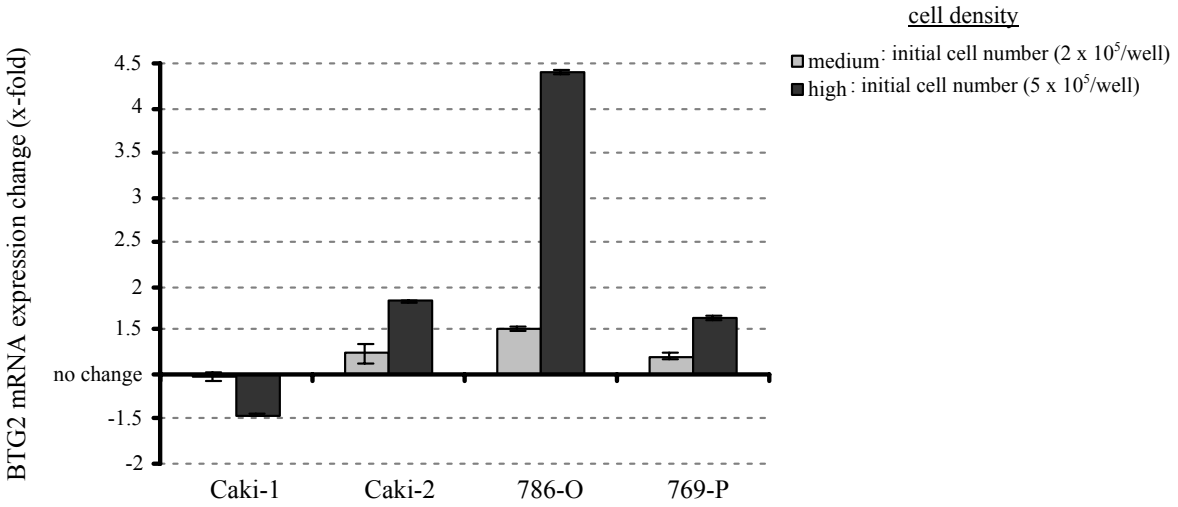

Figure 21: BTG2 mRNA expression and cell density.

BTG2 mRNA copy numbers were normalized to *G3PDH* mRNA copy numbers. Expression alterations are given in ± x-fold relative to normalized BTG2 mRNA expression levels in cultures with lowest cell densities (initial cell number: 1 x 10^5 cells/well). no change: *BTG2* mRNA expression in cultures with medium/high cell densities equals *BTG2* mRNA expression in cultures with lowest densities.

4 Discussion

4.1 Combination of cDNA and tissue microarray technologies for the identification of cRCC relevant genes

General and specific aspects of cDNA and tissue microarrays

DNA microarray technology has become one of the most popular platforms for performing global gene expression analysis in cancer. Commercially available cDNA microarrays mainly differ in the structure of the target sequences (e. g. cDNA or oligonucleotides), the support on which DNA targets are immobilized (nylon membrane, plastic, glass), and the mode of detection (radioactive or fluorescent). Although, the range of cDNA microarrays is diverse the advantages and disadvantages are very similar. Most advantageously features of cDNA microarrays are that they allow fast and quantitative expression profiling of thousands of genes in one experiment and that the identity of the arrayed genes is known a priori, in contrast to other expression screening methods (i. e. differential display RT-PCR), rendering time-consuming identification methods unnecessary. Disadvantages are (i) a possibly high number of false-positive signals due to unspecific hybridization reactions, (ii) requirement of large amounts of high quality RNA and (iii) high costs. Due to the vast number of arrayed gene sequences, cDNA microarrays produce large amounts of data which have to be handeled using bioinformatic tools. One of the major challenges of DNA microarray technology is to distinguish between „real“ and „false“ signals. This problem is addressed by applying stringent criteria for identifying gene expression alterations and confirming cDNA microarray results by independent approaches, e. g. Northern blot and quantitative RT-PCR (129, 130).

In this study, Atlas™ Human Cancer 1.2 arrays (BD Clontech) were used. Compared to other microarrays, these arrays are rather small since they contain „only“ 1176 different cDNA sequences. However, Atlas™ cDNA microarrays have considerable advantages:

- The selection of the arrayed sequences by the manufacturer was done with the focus on genes suggested to be involved in tumorigenic pathways. Thus, Atlas™ cDNA microarrays enable to concentrate on human cancer relevant genes.

- The use of ^{32}P labeled cDNAs offers the most sensitive method for measuring gene expression (129).

- The size of target gene cDNA fragments varies between 200-600 bp resulting in a high hybridization efficiency.

- cDNA probes are generated with sequence specific primers leading to a high signal specificity.

- In contrast to glass microarrays, Atlas cDNA microarrays are reusable (up to three times) and less expensive.

Using Atlas™ Human Cancer 1.2 microarrays, a total number of 71 differentially expressed genes (at least 2-fold expression changes in at least two cRCC cell lines compared to normal renal tissue) were determined. The number of identified genes is comparable with those published by other groups using the same arrays for studying expression alterations in squamous cell carcinoma of head and neck, papillary thyroid carcinoma, and gastric cancer (131-133). Importantly, the set of isolated genes are differing in all studies indicating that uncovered expression alterations are tumor specific and thus are argueing for the reliability of Atlas™ cDNA microarrays.

One of the bottle necks in cancer research is determining the clinical relevance of candidate genes uncovered by cDNA microarray analysis. Our recently developed TMA technology, which allows simultanous analysis of genes of interest in a large sample collective, has been designed to facilitate such studies (115). It has already been demonstrated by different groups that TMAs are optimally suited to evaluate the clinical significance of genes identified by cDNA microarray experiments (117-120).

However, TMAs generated from archival, paraffin embedded tissue material have limitations. Processing of tissues in a routine histopathological laboratory often takes many hours causing partial or complete degradation of particularly RNA. Furthermore, formalin, which is routinously

used for tissue fixation, chemically modifies proteins and nucleic acids (134, 135) impeding the binding of antibodies and hybridization probes to their target molecules. As consequence, gene expression analysis using formalin-fixed, paraffin-embedded tissue is often very difficult or even impossible.

Unfixed, fresh-frozen tissues would generally be superior for molecular analysis since quality and quantity of target molecules remain rather unaffected. Using a technology where tissues and recipient blocks are permanently kept below –20°C during TMA construction we were able to generate TMAs from snap frozen tissue specimens. A similar method was published at the same time when we were establishing this procedure at our institute two years ago (116).

The use of frozen TMAs enabled us to perform mRNA gene expression analysis in numerous tissue specimens. Twenty-five genes, which were significantly differentially expressed (at least 4-fold expression alteration in at least two cRCC cell lines compared to normal renal tissue) on the cDNA microarrays, were further studied by RISH on TMAs generated from frozen primary RCCs and normal renal tissues. It is of note, in comparison to paraffin TMAs, manufacturing and sectioning of frozen TMA is much more problematic since the tissue has to be kept frozen during the whole process to avoid RNA degradation. Furthermore, a special adhesive-coated tape system, which improves the sectioning of the TMA and helps to keep the tissue spots on the TMA section, was not applied for our “first generation” frozen TMAs. This lead to a rather high percentage (in average 38%) of tissue spots, which were lost during the sectioning and hybridization process. Despite these unwanted side effects 19 of 25 genes were successfully analyzed by RISH. Only six genes (*CKS1B*, *CSPG2*, *FOSL1*, *HMGA1*, *TGFB1*, and *NR0B2*) did not show any expression neither in the primary tumors nor in the normal renal tissues. Possible explanations for the observed discrepancies are:

- Human cancer cell lines are frequently used as model for neoplastic disease. The high amount of high-quality RNA, yielded from cell lines, makes them superior to tissue material for expression analysis using cDNA microarrays. However, it has been shown that gene expression patterns of cell lines may differ more or less from those obtained for primary tumors since some genes become activated or deactivated through the culturing process,

growth factors in the medium, and adaption to culture enviroment (136-138). Thus, some gene alterations uncovered in this study might be cell culture artefacts.

- Since the absolute number of mRNA target sequences in a 0.6 mm diameter tissue spot on the TMA is below the number of specific cDNA sequences present in a cDNA microarray spot some genes showing weak expression on the cDNA microarray remain undetected by RISH.

Using a combination of cDNA and frozen tissue microarray analysis, five genes (*VIM*, *CD74*, *CHES1*, *LITAF*, and *BTG2*) have been identified which might be cRCC associated. The possible roles of *VIM*, *CD74*, *CHES1*, and *LITAF* in cRCC biology will be discussed in the following sections. *BTG2*, which appeared to be the most interesting candidate gene, was chosen for further studies. These results will be discussed in sectiom 4.2.

VIM

VIM (*Vimentin*), which is coding for an intermediate filament protein of the cytoskeleton, was clearly stronger expressed in cRCC cell lines and primary cRCC compared to normal renal tissue. Overexpression of *VIM* in cRCC cell lines and tissues was recently described by two other groups who also used cDNA microarrays for identification of renal tumor relevant genes (117, 139). Using paraffin TMA technology it was furthermore demonstrated that *VIM* protein expression is significantly associated with poor patient prognosis independent of tumor grade and stage (117). These data clearly show that potential prognostic tumor markers may be identified with cDNA microarrays.

CHES1

Reduced *CHES1* mRNA expression was seen in cRCC cell lines and primary cRCCs. *CHES1* is a member of the family of forkhead/winged transcription factors. Although, the biological function of *CHES1* is yet unclear, certain lines of evidence indicate that this gene might be involved in DNA damage induced cell cycle arrest (140). Thus, reduced expression levels of *CHES1* might result in genomic instability, which is one of the hallmarks of human cancer (141, 142). Recently, a homozygous missense mutation in *CHES1* in a colon cancer cell line (143) and reduced

expression of *CHES1* mRNA in gastric cancer (133) have been described indicating an important role of this gene in some human cancers.

LITAF

Similar to *CHES1*, *LITAF* showed reduced expression levels in cRCC cell lines and primary cRCCs. *LITAF* is involved in the activation of the human *TNF-alpha* gene (144) which encodes a multifunctional cytokine capable of inducing apoptosis by binding to TNF receptors (145, 146). Impaired mRNA expression of LITAF might contribute to renal tumorigenesis by delaying cell death.

CD74

Interestingly, *CD74* mRNA expression was absent in cRCC cell lines but was detectable in primary cRCCs with expression levels similar to normal renal tissue. *CD74* plays an important role in processing/maturation of MHC class II molecules. Through association with the latter, *CD74* prevents untimely peptide loading of the premature MHC class II molecule and ensures correct trafficking to the intracellular peptide loading compartement. In contrast to MHC class I, which is expressed on almost all cell types, MHC class II was originally thought to be predominantly expressed on cells that present antigenes to CD4+ T cells like macrophages, monocytes, dendritic cells, and B lymphocytes (reviewed in (147)) suggesting that CD74 is also exclusively expressed in these cells.

However, recent reports demonstrated that both, MHC class II and *CD74*, are also expressed in various primary human cancers, e. g. colorectal, head and neck, stomach, and renal tumors (148-153). By IHC, Young et al. (139) recently found strong *CD74* expression in primary cRCC cells and tumor associated stromal and endothelial cells in 65% of the analyzed primary cRCCs.

As shown by RISH analysis on primary cRCCs, high *CD74* expression levels were significantly associated with high pT category. This observation suggests a potential role of *CD74* for tumor progression. Due to the biological function of *CD74* one might speculate that increased expression of *CD74* may help tumor cells to escape from the immune system by blocking peptide loading of MHC class II, thus preventing tumor antigen presentation on the cell surface. Results from other studies are supporting the theory that *CD74* might have “oncogenic” properties in cRCC biology: (i) *CD74* is localized on chromosome 5q, which is frequently gained in cRCC

(56, 154, 155); (ii) strong and frequent *CD74* protein expression in primary cRCC was recently described (139, 149), and (iii) increased *CD74* protein expression is also associated with tumor progression in colon and gastric cancers (153, 156). Therefore, *CD74* is a potential candidate gene for cRCC biology and further studies would be worthwhile.

4.2 *BTG2* – a new candidate gene for renal tumor biology?

cDNA and tissue microarray experiments demonstrated strong *BTG2* mRNA expression in normal renal tissue but reduced or absent expression in cRCC cell lines and primary tumors. Recently, Melamed et al. (124) showed that *BTG2* protein is strongly expressed in epithelial cells of the proximal tubulus of the kidney from which cRCC arise (1). These findings strongly suggest that *BTG2* is important for renal tumorigenesis.

Biological function of BTG2

BTG2 (also known as *TIS21* or *PC3*) was first described in 1991 and belongs to a gene family consisting of six members (*BTG1*, *BTG2*, *PC3B*, *ANA*, *TOB*, and *TOB2*), all of which having antiproliferative properties (reviewed in (157)). *BTG2* was cloned *from nerve growth factor* (*NGF*) treated PC12 cells suggesting that this gene might be of importance for neuronal differentiation (126). Further studies revealed that the impact of *BTG2* on neurogenesis is through cell cycle control since forced expression of *BTG2* in PC12 resulted in G1/S arrest (158) and *BTG2* is expressed in neuroblasts undergoing the last proliferation before differentiating into postmitotic neurons (159, 160). The cell cycle regulatory function of *BTG2* is not restricted to neuronal cells. Forced expression of *BTG2* resulted in cell cycle arrest at G1/S in NIH3T3 and 293 cells (158, 161, 162). Furthermore, *BTG2* is capable of inducing cell cycle arrest at the G1/S and also the G2/M checkpoint upon DNA damage in a p53 dependent manner (127, 163, 164).
Besides *p53* and *NGF* also *fibroblast-* and *epidermal growth factor* (*FGF* and *EGF*), the phorbolester TPA, *Interleukin-6*, and cAMP are able to induce *BTG2* expression (125, 126, 158). It is therefore concluded that a number of different signal transduction pathways turn on or enhance transcription of this gene.

In accordance, by sequencing the *BTG2* gene putative binding sites for several transcription factors including *AP-1*, *GATA-1*, *NFkappaB*, *CREB*, and *p53* were identified (Figure 22; (164)).

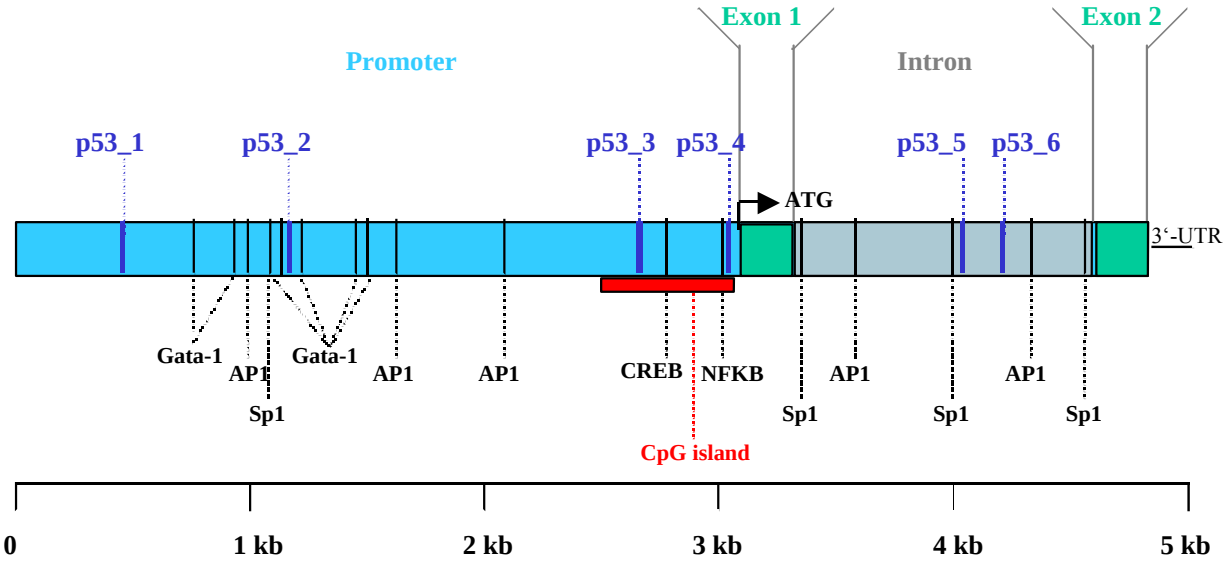

Figure 22: Genomic sequence of BTG2 (Duriez et al. 2002)

The molecular mechanisms how *BTG2* exerts its cell cycle regulatory function are not well understood. *BTG2* has been shown to interact with transcription factors like *Hoxb9* (165), *hCAF1* and *CALIF* (166) and modulate their activity indicating that *BTG2* functions as a transcriptional regulator. It was also demonstrated that *BTG2* binds to *protein-arginine N-methyltransferase 1* (*PRMT1*) resulting in enhanced activity of *PRMT1* (167, 168). Many of the target proteins of *PRMT1* are involved in RNA processing, metabolism and transport (e.g. *SPT5* (169), *poly(A) binding protein II* (170), *ILF3* (171), *hnRNP A2* (172), and *Sam68* (173)) and also in chromatin organization (174) suggesting that *BTG2* also plays a role in „pre-transcriptional" and post-transcriptional regulation steps.

Thus, by interacting with various partners, *BTG2* appears to have influence on almost all steps of transcription strongly suggesting that *BTG2* excerts its cell cycle regulatory function by controlling transcription of the respective genes (Figure 23).

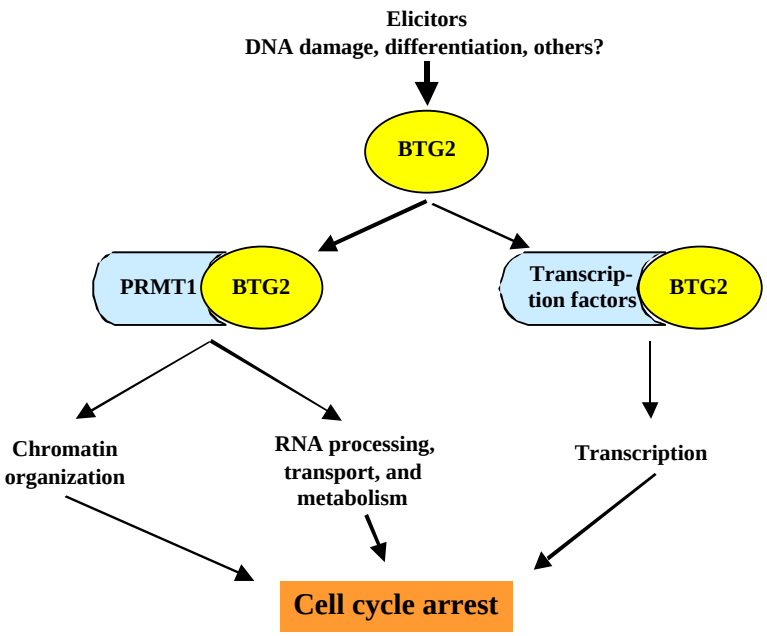

Figure 23: Probable mode of action of the negative cell cycle regulator BTG2.

Recent findings are supporting the theory that BTG2 is involved in cell cycle arrest through its involvement in transcriptional regulation :

- Guardavaccaro et al. demonstrated that cell cycle arrest at G1/S induced by forced *BTG2* expression relies on inhibition of *cyclin D1* transcription and consequently accumulation of hypophosphorylated *Rb* protein (162).

- Growth inhibition of wild-type *p53* containing MCF-7 cells after genotoxic treatment was accompanied by increased methylation of *histone IIA* and enhanced *BTG2* mRNA expression. In contrast, MCF-7 cells stably transfected with a dominant negative form of *p53* that abrogates sequence-specific DNA binding of *p53* did not show increasing *BTG2* mRNA expression levels and enhanced methylation of *histone IIA* upon adriamycin treatment. These cells were unable to arrest cell cycle (163).

- The negative cell cycle regulatory function of *BTG2* is an important tumor suppressive property, which has been described for well known tumor suppressor genes, e. g. *p53* (175),

pRB (176) or *p16* (177). In addition, *BTG2* participates in at least two cellular pathways (p53 and pRb), which are of great importance for tumorigenesis (178, 179).

BTG2 - a tumor suppressor candidate for cRCC?

In an attempt to study the possible tumor suppressive role of *BTG2* in renal tumorigenesis, the clinical impact of *BTG2* expression alterations in primary cRCC was analyzed in a first step. In a second step, the expression regulation and cell cycle regulatory function of *BTG2* were examined in cRCC cell lines.

Because commercially available antibodies for *BTG2* are not existing to date, correlation of *BTG2* protein expression with pathological and clinical parameters in cRCC using our large paraffin renal TMA (contains more than 500 archival RCC tissues) was unfortunatly not possible. For this reason, *BTG2* expression was studied on the mRNA level in 42 primary cRCCs and 17 normal renal tissues using quantitative RT-PCR. Using this approach, the results obtained from cDNA microarray, RISH, and Northern blot experiments were confirmed. Normal renal tissues showed significantly stronger *BTG2* mRNA expression levels than primary cRCCs. Although *BTG2* expression was detectable in all tumor samples, primary cRCCs showed - compared to the mean, normalized *BTG2* mRNA copy number of normal renal tissue - 6.7-fold (1.6-fold to 44-fold) reduced *BTG2* mRNA expression. Reduced *BTG2* mRNA expression levels were not associated with high tumor grade or pT category suggesting that impaired *BTG2* expression is rather an early event in renal tumorigenesis.

To address the possible tumor suppressive function of *BTG2* in renal cancer, the regulation of *BTG2* mRNA expression was studied in cRCC cell lines. It has been shown that *BTG2* is an immediate early response gene, whose transcription can be induced by the phorbolester TPA in human HeLa cells and also in a variety of rodent cell lines of different origin (125, 126). According to this, serveral *AP-1* binding sites (which are also known as TPA response elements; TREs), are located in the promotor region of *BTG2* ((164); Figure 22). These findings prompted us to investigate the inducibility of *BTG2* expression by TPA in the cRCC cell lines Caki-1, Caki-2, 786-O, and 769-P. Among all tested cRCC cell lines, merely Caki-1 cells showed a response to TPA. However, compared to HeLa, the increase of *BTG2* mRNA expression was

very weak (15-fold versus 2.3-fold). There are different explanations for the inability of cRCC cell lines to induce *BTG2* expression upon TPA treatment:

- Phorbolesters like TPA mainly excert their effects in cells by activating members of the *protein kinase C* (*PKC*) family (180, 181) but also by activating certain other receptors lacking kinase activity (reviewed in (182, 183)). Given the large number of *PKC* isotypes, which frequently show tissue specific expression patterns (184-188) and which have plenty of cellular substrates involved in many different biological processes (189), the reaction of cells upon phorbolester treatment may largely depend on the expression pattern of *PKCs* in this cell type. According to this, phorbolesters have been reported to enhance proliferation but also induce growth arrest, differentiation, and apoptosis in a variety of human cancer cell lines (190-193). Therefore, it is possible that discrepancies in the ability to induce *BTG2* expression upon TPA treatment in cervix carcinoma and cRCC cells are due to different TPA-target expression patterns in the respective cell lines.

- The effect of TPA on *BTG2* transcription activation is indirect and requires a signaling cascade acting as an intermediary. Alterations in this signaling cascade might occure in cRCC but not in cervix carcinoma cells resulting in impaired activation of *BTG2* gene transcription in cRCC cell lines upon TPA treatment.

- The *BTG2* gene might directly be affected by inactivating mutations, hypermethylation of CpG islands located in the promoter (164), or deletion leading to constricted gene activity in cRCC cell lines.

Whether the inability to induce *BTG2* mRNA expression upon TPA treatment in cRCC cell line but not in cervix carcinoma cells is caused by natural physiological differences in both cell types or by pathological alterations in the analyzed cRCC cell lines remains to be clarified.

Based on recent observations of other groups who showed that *BTG2* expression is low in exponentially growing cell lines, whereas quiescent cells showed high *BTG2* expression levels (127, 128) *BTG2* mRNA expression was quantitatively analyzed in cRCC cultures with different cell densities. *BTG2* mRNA expression was linked to increasing cell densities in Caki-2, 786-O,

and 769-P. The strongest association was found in 786-O cells, which showed slightly more than 4-fold increased *BTG2* mRNA expression in cultures with highest cell densities. Compared to this, the increase of *BTG2* mRNA expression was rather weak in Caki-2 and 769-P (both less than 2-fold).

It is of note that, although some of the cRCC cell lines are able to induce *BTG2* upon certain stimuli, neither TPA nor high cell densities were able to raise *BTG2* expression to the level observed in normal renal tissues. Downregulation of *BTG2* mRNA expression might therefore be an important mechanism driving renal cancer development.

The question arises, whether *BTG2* is a new tumor suppressor gene candidate or whether reduced expression of *BTG2* is merely a downstream-effect of impaired function of a signalling cascade. The inability of cRCC cell lines to enhance *BTG2* mRNA expression upon cellular cues (TPA and cell density) to the levels obtained in normal renal tissue are a strong argument for a tumor suppressive function of *BTG2* in cRCC.

Already in 1971 Knudson postulated (194) - based on his studies on hereditary retinoblastoma - that two independent events, loss of one allele and mutation of the remaining allele, were needed to inactivate a given tumor suppressive gene resulting in malignant transformation. To date, this „two-hit“ hypothesis is generally accepted and indeed many tumor suppressor genes are inactivated by deletion of one allel and mutation or (more recently acknowledged) epigenetic silencing of the other allel (reviewed in (195-197)).

A common deleted region was described in breast cancer spanning 1q23-32 (198), the latter including the *BTG2* locus (127). Duriez et al. (164) has analyzed primary breast tumors and breast cancer cell lines for LOH at 1q32 and mutations in the two exons of the BTG2 gene to study whether the “two-hit” hypothesis for inactivation of a tumor suppressor gene holds true for *BTG2* as well. They found LOH at 1q32 in 4 of 18 primary breast tumors. However, they were not able to identify any mutation in the *BTG2* sequence argueing against the “classical” modus of a tumor suppressor gene inactivation.

In this context, it is noteworthy that for some tumor suppressor genes impaired function of merely one allele may also be enough to drive tumorigenesis (reviewed in (195)). This new class of so-called haploinsufficient tumor suppressor genes has been inferred from mouse models of human cancer. Recently it has been demonstrated that mice hemizygous (+/-) for tumor suppressor genes like *p27*^{Kip1} (199), *p18(INK4c)* (200), *transforming growth factor-beta 1* (201), and also *p53* (202), show a higher spontanous tumor rate than their homozygous (+/+) littermates and rapidly develop tumors when challenged with carcinogens. In all cases the remaining wild-type allele remained unaffected.

In accordance, *FUS1*, a candidate tumor suppressor gene, which was identified from a 630 kb deletion region in lung cancer (203), is infrequently mutated or methylated in lung cancer cell lines and primary lung tumors (204). Kondo et al. (204) recently demonstrated that forced expression of *FUS1* leads to G1 arrest and growth inhibition in lung cancer cells suggesting that *FUS1* is also a candidate for a haploinsufficient tumor suppressor gene.

Another example for a potential haploinsufficient tumor suppressor gene is the transcription factor *KLF5* at 13q21. Forced expression of *KLF5* in breast and prostate carcinoma cell lines significantly inhibited growth of these cells. Although *KLF5* is frequently deleted at one allele in breast and prostate carcinoma cell lines inactivating mutations or hypermethylation of the remaining allel are uncommon (205, 206).

Current reports suggest that haploinsufficiency of tumor suppressor genes is caused by deletion of one allel whereas the other allel remains unaffected. As shown by CGH analysis, loss of 1q is a rare event in cRCC (see figure 2 (56)) speaking against the theory of a haploinsufficient tumor suppressor gene. However, one should take in account that CGH is a rather insensitive method detecting only those DNA sequence losses spanning more than 10 Mb (207). Using LOH analysis it would be possible to uncover very small deleted chromosomal segments at 1q.
But even if BTG2 is not deleted at one allele in renal cancer, the loss of tumor suppressive properties of this gene due to haploinsufficiency is still an attractive model for cRCC. One might speculate that expression of some potential haploinsufficient tumor suppressor genes might be decreased not due to deletion but due to mutation or hypermethylation of one allele. Those genes

would remain undetected by CGH and LOH analysis but would attract attention in cDNA microarray experiments.

Analyzing the mutation, methylation and LOH status of the *BTG2* gene in renal cancer would clarify whether this gene is directly affected by inactivating events at one or even both alleles and could thus be regarded as a new potential tumor suppressor gene for renal carcinogenesis.

Outlook

In this thesis a combination of cDNA and tissue microarray technology was used to identify potential RCC relevant genes. The negative cell cycle regulator and potential tumor suppressor *BTG2* was one of the most interesting candidate genes and we decided to further study the impact of this antiproliferative gene on renal carcinogenesis. As already mentioned, the experiments done in this thesis only allow to speculate about the role of *BTG2* in cRCC biology. The impaired ability of cRCC cell lines to significantly enhance expression of *BTG2* in response to increasing cell density strongly indicates that impaired function of this gene is of importance for renal tumorigenesis and that *BTG2* might be a tumor suppressor for cRCC. As discussed above, tumor suppressor genes are generally inactivated by loss of function of both alleles (by deletion and mutation/hypermethylation or by deletion of both alleles) or, if they are haploinsufficient, by deletion of merely one allele. Thus, to prove whether *BTG2* is a tumor suppressor for cRCC or not, the following experiments would be helpfull:

- Methylation analysis of the *BTG2* promotor in RCC cell lines and primary RCCs would show whether impaired BTG2 mRNA expression is a result of epigenetic silencing of the *BTG2* gene.

- Sequence analysis of the *BTG2* gene in RCC cell lines and primary RCC might show whether the function of this antiproliferative gene is impaired in renal tumors.

- LOH analysis would show whether reduced *BTG2* mRNA expression is based on deletion of one or even both alleles.

- Forced expression of *BTG2* using appropiate vectors transfected into cRCC cell lines followed by monitoring the proliferation rate in transfected and non-transfected cells will show whether *BTG2* is necessary for negative cell cycle regulation in cRCC cells as well.

The large number of fresh frozen and formalin fixed renal tumors, which are stored in the tumorbanks of our institute can be used for the above mentioned experiments (Methylation- and mutation assays, LOH analysis) and will enable us to uncover potential associations between the obtained results and tumor related and clinical follow-up data.

Generation of antibodies against *BTG2* would allow us to study *BTG2* protein expression levels and the distribution of *BTG2* protein within malignant and normal renal tissue by IHC and Western blot analysis. Here again the large number of renal tissues stored in our tumorbanks and also the availability of a large renal TMA containing more than 500 different RCC and normal renal tissues will significantly facilitate the correlation of protein expression data with tumor and patient related information.

Most tumor suppressor genes are not linked to a certain tumor type. Our group has constructed „multi-tumor“ TMAs containing thousands of different tissue core biopsies of almost all human cancers and corresponding normal tissues. RISH and IHC analysis on those TMAs might uncover other tumor types for which *BTG2* might be of importance.

4.3 Conclusion

In this thesis, combined cDNA and tissue microarray analysis was performed to screen for genes differentially expressed in cRCC and normal renal tissue. Although, the cDNA microarrays were rather small (1176 genes) and the TMAs generated from frozen tissue specimens belonged to our first-generation TMA set, five genes (*VIM*, *CD74*, *CHES1*, *LITAF*, and *BTG2*) were uncovered, which might be of importance for cRCC biology.

The identification of *VIM* and *CD74*, which have already been associated with renal cancer in previous reports, are corroborating the reliability of the cDNA and tissue microarray analysis in

this study. In contrast, *CHES1*, *LITAF*, and *BTG2* have never been linked to renal cancer before and are thus new potential renal tumor relevant genes.

Further experiments on the negative cell cycle regulator *BTG2* strongly indicate that this gene might have tumor suppressor properties in cRCC biology because (i) cRCC cell lines and primary cRCCs showed significantly reduced *BTG2* expression levels compared to normal renal tissue as assessed by quantitative RT-PCR; (ii) cRCC cell lines were unable to raise *BTG2* mRNA expression to the levels obseved in normal renal tissue upon certain cues (TPA and increasing cell density). Allelic deletion, mutation and methylation analysis of the *BTG2* gene and also re-expression of *BTG2* in cRCC cell lines will show whether *BTG2* is a new renal tumor suppressor gene.

5 Appendix

10 X MOPS:
0.2 M 3-*N*-morpholino-propanesulfonic acid (MOPS)
0.5 M sodium acetate
0.01 M Ethylenediamine tetraacetic acid (EDTA)
adjust pH to 7.0 with NaOH and autoclave

20 X SSC:
3 M NaCl
0.3 M $Na_3citrate \cdot 2H_2O$
adjust pH to 7.0 with NaOH/HCl and autoclave

50 X TAE (per liter):
242 g Tris base
57.1 ml glacial acetic acid
37.2 g $Na_2EDTA \cdot 2H_2O$

LB/Agar plates supplemented with X-Gal and IPTG (per liter):
15 g Agar
10 g Bacto®-tryptone
5 g Bacto®-yeast extract
5 g NaCl
adjust pH to 7.0 with NaOH and autoclave
allow the medium to cool to 50°C before adding
100 µg/ml Ampicillin
80 µg/ml X-Gal (5-bromo-4-chloro-3-indolyl-β-D-galactoside)
0.5 mM IPTG (Isopropylthio-β-D-galactoside)
pour 30-35 ml into 85 mm petri dishes

LB-medium (per liter):
10 g Bacto®-tryptone
5 g Bacto®-yeast extract
5 g NaCl
adjust pH to 7.0 with NaOH and autoclave
allow the medium to cool to 50°C before adding
100 µg/ml Ampicillin

Methylene-blue staining solution:
0.03% methylene-blue
0.3 M sodium acetate, pH5.2

Northern blot wash solution I-III:
prepared from 20 X SSC and 10% SDS stock solutions
I: 2 X SSC/0.1 % SDS
II: 0.2 X SSC/0.1 % SDS

III: 0.1 X SSC/0.1 % SDS

Formamide prehybridization/hybridization (FPH) solution:
25 ml 20 X SSC
5 ml 100 X Denhardt solution (*100 X Denhardt is: 10 g Ficoll 400, 10 g polyvinylpyrrolidone, 10 g bovine serum albumin (BSA), H_2O to 500 ml*)
50 ml Formamide
10 ml Sodium dodecyl sulphate (SDS) 10%
H_2O to 100 ml

RISH hybridization mix:
50 ml Formamide
20 ml 20 X SSC
1 ml 100 X Denhardt solution (*100 X Denhardt is: 10 g Ficoll 400, 10 g polyvinylpyrrolidone, 10 g bovine serum albumin (BSA), H_2O to 500 ml*)
10 ml 0.2 M $NaPO_4$, pH 7.0
10 g Dextran sulphate
5 ml 20% N-Lauroylsarcosine Sodium salt (Sarcosyl)
H_2O to 100 ml

Trypan blue:
150 mM NaCl
0.5% trypan blue

6 Literature

1. Thoenes, W., Stoerkel, S., and Rumpelt, H. Histopathology and classification of renal cell tumors (adenomas, oncocytomas, and carcinomas): the basic cytological and histopathological elements and their use for diagnostics, Pathol Res Pract. *181:* 125-143, 1986.

2. Kovacs, G., Akhtar, M., Beckwith, B. J., Bugert, P., Cooper, C. S., Delahunt, B., Eble, J. N., Fleming, S., Ljungberg, B., Medeiros, L. J., Moch, H., Reuter, V. E., Ritz, E., Roos, G., Schmidt, D., Srigley, J. R., Storkel, S., van den Berg, E., and Zbar, B. The Heidelberg classification of renal cell tumours, J Pathol. *183:* 131-3., 1997.

3. Moch, H., Gasser, T., Amin, M. B., Torhorst, J., Sauter, G., and Mihatsch, M. J. Prognostic utility of the recently recommended histologic classification and revised TNM staging system of renal cell carcinoma: a Swiss experience with 588 tumors, Cancer. *89:* 604-614, 2000.

4. Skinner, D., Colvin, R., Vermillion, C., Pfister, R., and Leadbetter, W. Diagnosis and management of renal cell carcinoma- a clinical and pathological study of 309 cases, Cancer. *28:* 1165-1177, 1971.

5. Konnak, J. W. and Grossman, H. B. Renal cell carcinoma as an incidental finding, J Urol. *134:* 1094-6., 1985.

6. Jayson, M. and Sanders, H. Increased incidence of serendipitously discovered renal cell carcinoma, Urology. *51:* 203-5., 1998.

7. Dhote, R., Pellicer-Coeuret, M., Thiounn, N., Debre, B., and Vidal-Trecan, G. Risk factors for adult renal cell carcinoma: a systematic review and implications for prevention, BJU Int. *86:* 20-7., 2000.

8. Ljungberg, B., Alamdari, F. I., Rasmuson, T., and Roos, G. Follow-up guidelines for nonmetastatic renal cell carcinoma based on the occurrence of metastases after radical nephrectomy, BJU Int. *84:* 405-11., 1999.

9. Sandock, D. S., Seftel, A. D., and Resnick, M. I. A new protocol for the followup of renal cell carcinoma based on pathological stage, J Urol. *154:* 28-31., 1995.

10. Ritchie, A. W. and Chisholm, G. D. The natural history of renal carcinoma, Semin Oncol. *10:* 390-400., 1983.

11. McNichols, D., Segura, J., and DeWeerd, J. Renal cell carcinoma: long-term survival and late recurrence, J Urol. *126:* 17-23, 1981.

12. Vogelzang, N. J. and Stadler, W. M. Kidney cancer, Lancet. *352:* 1691-6., 1998.

13. Guinan, P. D., Vogelzang, N. J., Fremgen, A. M., Chmiel, J. S., Sylvester, J. L., Sener, S. F., and Imperato, J. P. Renal cell carcinoma: tumor size, stage and survival. Members of the Cancer Incidence and End Results Committee, J Urol. *153:* 901-3., 1995.

14. Motzer, R. J. and Russo, P. Systemic therapy for renal cell carcinoma, J Urol. *163:* 408-17., 2000.

15. Schomburg, A., Kirchner, H., Fenner, M., Menzel, T., Poliwoda, H., and Atzpodien, J. Lack of therapeutic efficacy of tamoxifen in advanced renal cell carcinoma, Eur J Cancer. *29A:* 737-40., 1993.

16. Gershanovich, M. M., Moiseyenko, V. M., Vorobjev, A. V., Kapyla, H., Ellmen, J., and Anttila, M. High-dose toremifene in advanced renal-cell carcinoma, Cancer Chemother Pharmacol. *39:* 547-51., 1997.

17. Onufrey, V. and Mohiuddin, M. Radiation therapy in the treatment of metastatic renal cell carcinoma, Int J Radiat Oncol Biol Phys. *11:* 2007-9., 1985.

18. Mickisch, G., Bier, H., Bergler, W., Bak, M., Tschada, R., and Alken, P. P-170 glycoprotein, glutathione and associated enzymes in relation to chemoresistance of primary human renal cell carcinomas, Urol Int. *45:* 170-6., 1990.

19. Bukowski, R. M. Natural history and therapy of metastatic renal cell carcinoma: the role of interleukin-2, Cancer. *80:* 1198-220., 1997.

20. Yuba, H., Okamura, K., Ono, Y., and Ohshima, S. Growth fractions of human renal cell carcinoma defined by monoclonal antibody Ki-67. Predictive values for prognosis, Int J Urol. *8:* 609-14., 2001.

21. Minasian, L. M., Motzer, R. J., Gluck, L., Mazumdar, M., Vlamis, V., and Krown, S. E. Interferon alfa-2a in advanced renal cell carcinoma: treatment results and survival in 159 patients with long-term follow-up, J Clin Oncol. *11:* 1368-75., 1993.

22. Pyrhonen, S., Salminen, E., Ruutu, M., Lehtonen, T., Nurmi, M., Tammela, T., Juusela, H., Rintala, E., Hietanen, P., and Kellokumpu-Lehtinen, P. L. Prospective randomized trial of interferon alfa-2a plus vinblastine versus vinblastine alone in patients with advanced renal cell cancer, J Clin Oncol. *17:* 2859-67., 1999.

23. Fyfe, G. A., Fisher, R. I., Rosenberg, S. A., Sznol, M., Parkinson, D. R., and Louie, A. C. Long-term response data for 255 patients with metastatic renal cell carcinoma treated with high-dose recombinant interleukin-2 therapy, J Clin Oncol. *14:* 2410-1., 1996.

24. Negrier, S., Maral, J., Drevon, M., Vinke, J., Escudier, B., and Philip, T. Long-term follow-up of patients with metastatic renal cell carcinoma treated with intravenous recombinant interleukin-2 in Europe, Cancer J Sci Am. *6 Suppl 1:* S93-8., 2000.

25. Rosenberg, S. A., Yang, J. C., Topalian, S. L., Schwartzentruber, D. J., Weber, J. S., Parkinson, D. R., Seipp, C. A., Einhorn, J. H., and White, D. E. Treatment of 283 consecutive patients with metastatic melanoma or renal cell cancer using high-dose bolus interleukin 2, Jama. *271:* 907-13., 1994.

26. Henson, D. E., Fielding, L. P., Grignon, D. J., Page, D. L., Hammond, M. E., Nash, G., Pettigrew, N. M., Gorstein, F., and Hutter, R. V. College of American Pathologists Conference XXVI on clinical relevance of prognostic markers in solid tumors. Summary. Members of the Cancer Committee, Arch Pathol Lab Med. *119:* 1109-12., 1995.

27. Srigley, J. R., Hutter, R. V., Gelb, A. B., Henson, D. E., Kenney, G., King, B. F., Raziuddin, S., and Pisansky, T. M. Current prognostic factors--renal cell carcinoma: Workgroup No. 4. Union Internationale Contre le Cancer (UICC) and the American Joint Committee on Cancer (AJCC), Cancer. *80:* 994-6., 1997.

28. Störkel, S. Tumoren der Niere. *In:* R. W. (ed.) Pathologie, Zweite, neubearbeitete Auflage edition, Vol. 5, pp. 173-192: Springer Verlag, 1997.

29. Robson, C., Churchill, B., and Anderson, W. The results of radical nephrectomy for renal cell carcinoma, J Urol. *101:* 297-303, 1969.

30. UICC TNM Classification of malignant tumours, 5th ed. edition. New York, Chichester, Weinheim, Brisbane, Singapore, Toronto: Wiley-Liss, 1997.

31. Ficarra, V., Righetti, R., Pilloni, S., D'Amico, A., Maffei, N., Novella, G., Zanolla, L., Malossini, G., and Mobilio, G. Prognostic factors in patients with renal cell carcinoma: retrospective analysis of 675 cases, Eur Urol. *41:* 190-8., 2002.

32. Fuhrman, S., Lasky, L., and Limas, C. Prognostic significance of morphologic parameters in renal cell carcinoma, Am J Surg Path. *6:* 655-663, 1982.

33. Hafez, K. S., Novick, A. C., and Campbell, S. C. Patterns of tumor recurrence and guidelines for followup after nephron sparing surgery for sporadic renal cell carcinoma, J Urol. *157:* 2067-70., 1997.

34. Nativ, O., Sabo, E., Raviv, G., Madjar, S., Halachmi, S., and Moskovitz, B. The impact of tumor size on clinical outcome in patients with localized renal cell carcinoma treated by radical nephrectomy, J Urol. *158:* 729-32., 1997.

35. Eschwege, P., Saussine, C., Steichen, G., Delepaul, B., Drelon, L., and Jacqmin, D. Radical nephrectomy for renal cell carcinoma 30 mm. or less: long-term follow results, J Urol. *155:* 1196-9., 1996.

36. Scholzen, T. and Gerdes, J. The Ki-67 protein: from the known and the unknown, J Cell Physiol. *182:* 311-22., 2000.

37. MacCallum, D. E. and Hall, P. A. Biochemical characterization of pKi67 with the identification of a mitotic-specific form associated with hyperphosphorylation and altered DNA binding, Exp Cell Res. *252:* 186-98., 1999.

38. Endl, E. and Gerdes, J. Posttranslational modifications of the KI-67 protein coincide with two major checkpoints during mitosis, J Cell Physiol. *182:* 371-80., 2000.

39. Delahunt, B., Bethwaite, P. B., Thornton, A., and Ribas, J. L. Proliferation of renal cell carcinoma assessed by fixation-resistant polyclonal Ki-67 antibody labeling, Cancer. *75:* 2714-2719, 1995.

40. Aaltomaa, S., Lipponen, P., Ala-Opas, M., Eskelinen, M., and Syrjanen, K. Prognostic value of Ki-67 expression in renal cell carcinomas, Eur Urol. *31:* 350-5., 1997.

41. Rioux-Leclercq, N., Turlin, B., Bansard, J., Patard, J., Manunta, A., Moulinoux, J. P., Guille, F., Ramee, M. P., and Lobel, B. Value of immunohistochemical Ki-67 and p53 determinations as predictive factors of outcome in renal cell carcinoma, Urology. *55:* 501-5., 2000.

42. Papadopoulos, I., Weichert-Jacobsen, K., Wacker, H. H., and Sprenger, E. Correlation between DNA ploidy, proliferation marker Ki-67 and early tumor progression in renal cell carcinoma. A prospective study, Eur Urol. *31:* 49-53., 1997.

43. Egeblad, M. and Werb, Z. New functions for the matrix metalloproteinases in cancer progression, Nat Rev Cancer. *2:* 161-74., 2002.

44. Curran, S. and Murray, G. I. Matrix metalloproteinases in tumour invasion and metastasis, J Pathol. *189:* 300-8., 1999.

45. Kallakury, B. V., Karikehalli, S., Haholu, A., Sheehan, C. E., Azumi, N., and Ross, J. S. Increased expression of matrix metalloproteinases 2 and 9 and tissue inhibitors of metalloproteinases 1 and 2 correlate with poor prognostic variables in renal cell carcinoma, Clin Cancer Res. *7:* 3113-9., 2001.

46. Murashige, M., Miyahara, M., Shiraishi, N., Saito, T., Kohno, K., and Kobayashi, M. Enhanced expression of tissue inhibitors of metalloproteinases in human colorectal tumors, Jpn J Clin Oncol. *26:* 303-9., 1996.

47. Ree, A. H., Florenes, V. A., Berg, J. P., Maelandsmo, G. M., Nesland, J. M., and Fodstad, O. High levels of messenger RNAs for tissue inhibitors of metalloproteinases (TIMP-1 and TIMP-2) in primary breast carcinomas are associated with development of distant metastases, Clin Cancer Res. *3:* 1623-8., 1997.

48. Fong, K. M., Kida, Y., Zimmerman, P. V., and Smith, P. J. TIMP1 and adverse prognosis in non-small cell lung cancer, Clin Cancer Res. *2:* 1369-72., 1996.

49. Carroll, P. R., Murty, V. V., Reuter, V., Jhanwar, S., Fair, W. R., Whitmore, W. F., Chaganti, R. S., and Bukowski, R. M. Abnormalities at chromosome region 3p12-14 characterize clear cell renal carcinoma, Cancer Genet Cytogenet. *26:* 253-9. RCC are incurable., 1987.

50. Zbar, B., Brauch, H., Talmadge, C., and Linehan, M. Loss of alleles of loci on the short arm of chromosome 3 in renal cell carcinoma, Nature. *327:* 721-727, 1987.

51. Kovacs, G. and Frisch, S. Clonal chromosome abnormalities in tumor cells from patients with sporadic renal carcinomas, Cancer Res. *49:* 651-659, 1989.

52. Presti, J., Rao, H., Chen, Q., Reuter, V., Li, F., Fair, W., and Jhanwar, S. Histopathological, cytogenetic, and molecular characterization of renal cortical tumors, Cancer Res. *51:* 1544-1552, 1991.

53. Maloney, K., Norman, R., Lee, C., Millard, O., and Welch, J. Cytogenetic abnormalities associated with renal cell carcinoma, J Urol. *146:* 692-696, 1991.

54. Kallioniemi, A., Kallioniemi, O., Sudar, D., Rutovitz, D., Gray, J., Waldman, F., and Pinkel, D. Comparative genomic hybridization for molecular cytogenetic analysis of solid tumors, Science. *258:* 818-821, 1992.

55. Kallioniemi, O., Kallioniemi, A., Sudar, D., Rutovitz, D., Gray, J., Waldman, F., and Pinkel, D. Comparative genomic hybridization: a rapid new method for detecting and mapping DNA amplification in tumors, Semin Cancer Biol. *4:* 41-46, 1993.

56. Moch, H., Presti, J. C., Jr., Sauter, G., Buchholz, N., Jordan, P., Mihatsch, M. J., and Waldman, F. M. Genetic aberrations detected by comparative genomic hybridization are associated with clinical outcome in renal cell carcinoma, Cancer Res. *56:* 27-30, 1996.

57. Jiang, F., Desper, R., Papadimitriou, C. H., Schaffer, A. A., Kallioniemi, O. P., Richter, J., Schraml, P., Sauter, G., Mihatsch, M. J., and Moch, H. Construction of evolutionary tree models

for renal cell carcinoma from comparative genomic hybridization data, Cancer Res. *60:* 6503-9., 2000.

58. Reutzel, D., Mende, M., Naumann, S., Storkel, S., Brenner, W., Zabel, B., and Decker, J. Genomic imbalances in 61 renal cancers from the proximal tubulus detected by comparative genomic hybridization, Cytogenet Cell Genet. *93:* 221-7., 2001.

59. Kovacs, G., Erlandsson, R., Boldog, F., Ingvarsson, S., Muller, B. R., Klein, G., and Sumegi, J. Consistent chromosome 3p deletion and loss of heterozygosity in renal cell carcinoma, Proc Natl Acad Sci U S A. *85:* 1571-5, 1988.

60. Schraml, P., Muller, D., Bednar, R., Gasser, T., Sauter, G., Mihatsch, M. J., and Moch, H. Allelic loss at the D9S171 locus on chromosome 9p13 is associated with progression of papillary renal cell carcinoma, J Pathol. *190:* 457-461, 2000.

61. Wu, S., Hafez, G., Xing, W., Newton, M., Chen, X., and Messing, E. The correlation between the loss of chromosome 14q with histologic tumor grade, pathologic stage, and outcome of patients with nonpapillary renal cell carcinoma, Cancer. *77:* 1154-1160, 1996.

62. Anglard, P., Tory, K., Brauch, H., Weiss, G. H., Latif, F., Merino, M. J., Lerman, M. I., Zbar, B., and Linehan, W. M. Molecular analysis of genetic changes in the origin and development of renal cell carcinoma, Cancer Res. *51:* 1071-1077, 1991.

63. Presti, J., Reuter, V., Cordon-Cardo, C., Mazumdar, M., Fair, W., and Jhanwar, S. Allelic deletions in renal tumors: Histopathological correlations, Cancer Res. *53:* 5780-5783, 1993.

64. Kok, K., Naylor, S. L., and Buys, C. H. Deletions of the short arm of chromosome 3 in solid tumors and the search for suppressor genes, Adv Cancer Res. *71:* 27-92., 1997.

65. Zabarovsky, E. R., Lerman, M. I., and Minna, J. D. Tumor suppressor genes on chromosome 3p involved in the pathogenesis of lung and other cancers, Oncogene. *21:* 6915-35., 2002.

66. Martinez, A., Walker, R. A., Shaw, J. A., Dearing, S. J., Maher, E. R., and Latif, F. Chromosome 3p allele loss in early invasive breast cancer: detailed mapping and association with clinicopathological features, Mol Pathol. *54:* 300-6., 2001.

67. Matsumoto, S., Kasumi, F., Sakamoto, G., Onda, M., Nakamura, Y., and Emi, M. Detailed deletion mapping of chromosome arm 3p in breast cancers: a 2-cM region on 3p14.3-21.1 and a 5-cM region on 3p24.3-25.1 commonly deleted in tumors, Genes Chromosomes Cancer. *20:* 268-74., 1997.

68. Fullwood, P., Marchini, S., Rader, J. S., Martinez, A., Macartney, D., Broggini, M., Morelli, C., Barbanti-Brodano, G., Maher, E. R., and Latif, F. Detailed genetic and physical mapping of tumor suppressor loci on chromosome 3p in ovarian cancer, Cancer Res. *59:* 4662-7., 1999.

69. Latif, F., Fivash, M., Glenn, G., Tory, K., Orcutt, M. L., Hampsch, K., Delisio, J., Lerman, M., Cowan, J., Beckett, M., and et al. Chromosome 3p deletions in head and neck carcinomas: statistical ascertainment of allelic loss, Cancer Res. *52:* 1451-6., 1992.

70. Tory, K., Brauch, H., Linehan, M., Barba, D., Oldfield, E., Filling-Katz, M., Seizinger, B., Nakamura, Y., White, R., and Marshall, F. Specific genetic change in tumors associated with von Hippel-Lindau disease, J Natl Cancer Inst. *81:* 1097-1101, 1989.

71. Bergerheim, U., Nordenskjöld, M., and Collins, V. Deletion mapping in human renal cell carcinoma, Cancer Res. *49:* 1390-1398, 1989.

72. van der Hout, A. H., van der Vlies, P., Wijmenga, C., Li, F. P., Oosterhuis, J. W., and Buys, C. H. The region of common allelic losses in sporadic renal cell carcinoma is bordered by the loci D3S2 and THRB, Genomics. *11:* 537-542, 1991.

73. Yamakawa, K., Morita, R., Takahashi, E., Hori, T., Ishikawa, J., and Nakamura, Y. A detailed deletion mapping of the short arm of chromosome 3 in sporadic renal cell carcinoma, Cancer Res. *51:* 4707-4711, 1991.

74. Lubinski, J., Hadaczek, P., Podolski, J., Toloczko, A., Sikorski, A., McCue, P., Druck, T., and Huebner, K. Common regions of deletion in chromosome regions 3p12 and 3p14.2 in primary clear cell renal carcinomas, Cancer Res. *54:* 3710-3, 1994.

75. Druck, T., Kastury, K., Hadaczek, P., Podolski, J., Toloczko, A., Sikorski, A., Ohta, M., LaForgia, S., Lasota, J., McCue, P., and et al. Loss of heterozygosity at the familial RCC t(3;8) locus in most clear cell renal carcinomas, Cancer Res. *55:* 5348-53, 1995.

76. Latif, F., Tory, K., Gnarra, J., Yao, M., Duh, F. M., Orcutt, M. L., Stackhouse, T., Kuzmin, I., Modi, W., Geil, L., and et al. Identification of the von Hippel-Lindau disease tumor suppressor gene, Science. *260:* 1317-20., 1993.

77. Chen, F., Kishida, T., Duh, F. M., Renbaum, P., Orcutt, M. L., Schmidt, L., and Zbar, B. Suppression of growth of renal carcinoma cells by the von Hippel-Lindau tumor suppressor gene, Cancer Res. *55:* 4804-7, 1995.

78. Schraml, P., Struckmann, K., Hatz, F., Sonnet, S., Kully, C., Gasser, T., Sauter, G., Mihatsch, M. J., and Moch, H. VHL mutations and their correlation with tumour cell

proliferation, microvessel density, and patient prognosis in clear cell renal cell carcinoma, J Pathol. *196:* 186-93., 2002.

79. Gnarra, J. R., Tory, K., Weng, Y., Schmidt, L., Wei, M. H., Li, H., Latif, F., Liu, S., Chen, F., Duh, F. M., and et al. Mutations of the VHL tumour suppressor gene in renal carcinoma, Nat Genet. *7:* 85-90, 1994.

80. Brauch, H., Weirich, G., Brieger, J., Glavac, D., Rodl, H., Eichinger, M., Feurer, M., Weidt, E., Puranakanitstha, C., Neuhaus, C., Pomer, S., Brenner, W., Schirmacher, P., Storkel, S., Rotter, M., Masera, A., Gugeler, N., and Decker, H. J. VHL alterations in human clear cell renal cell carcinoma: association with advanced tumor stage and a novel hot spot mutation, Cancer Res. *60:* 1942-1948, 2000.

81. Herman, J. G., Latif, F., Weng, Y., Lerman, M. I., Zbar, B., Liu, S., Samid, D., Duan, D. S., Gnarra, J. R., Linehan, W. M., and et al. Silencing of the VHL tumor-suppressor gene by DNA methylation in renal carcinoma, Proc Natl Acad Sci U S A. *91:* 9700-4, 1994.

82. Harris, A. L. Hypoxia--a key regulatory factor in tumour growth, Nat Rev Cancer. *2:* 38-47., 2002.

83. Koong, A. C., Denko, N. C., Hudson, K. M., Schindler, C., Swiersz, L., Koch, C., Evans, S., Ibrahim, H., Le, Q. T., Terris, D. J., and Giaccia, A. J. Candidate genes for the hypoxic tumor phenotype, Cancer Res. *60:* 883-7., 2000.

84. Wykoff, C. C., Pugh, C. W., Maxwell, P. H., Harris, A. L., Ratcliffe, P. J., Kok, K., Naylor, S. L., and Buys, C. H. Identification of novel hypoxia dependent and independent target genes of the von Hippel-Lindau (VHL) tumour suppressor by mRNA differential expression profiling, Oncogene. *19:* 6297-305., 2000.

85. Lal, A., Peters, H., St Croix, B., Haroon, Z. A., Dewhirst, M. W., Strausberg, R. L., Kaanders, J. H., van der Kogel, A. J., Riggins, G. J., Kok, K., Naylor, S. L., and Buys, C. H. Transcriptional response to hypoxia in human tumors, J Natl Cancer Inst. *93:* 1337-43., 2001.

86. Maxwell, P. H., Wiesener, M. S., Chang, G. W., Clifford, S. C., Vaux, E. C., Cockman, M. E., Wykoff, C. C., Pugh, C. W., Maher, E. R., and Ratcliffe, P. J. The tumour suppressor protein VHL targets hypoxia-inducible factors for oxygen-dependent proteolysis [see comments], Nature. *399:* 271-5, 1999.

87. Cockman, M. E., Masson, N., Mole, D. R., Jaakkola, P., Chang, G. W., Clifford, S. C., Maher, E. R., Pugh, C. W., Ratcliffe, P. J., and Maxwell, P. H. Hypoxia inducible factor-alpha

binding and ubiquitylation by the von Hippel-Lindau tumor suppressor protein, J Biol Chem. *275:* 25733-41., 2000.

88. Ohh, M., Park, C. W., Ivan, M., Hoffman, M. A., Kim, T. Y., Huang, L. E., Pavletich, N., Chau, V., Kaelin, W. G., Ratcliffe, P. J., and Maxwell, P. H. Ubiquitination of hypoxia-inducible factor requires direct binding to the beta-domain of the von Hippel-Lindau protein, Nat Cell Biol. *2:* 423-7., 2000.

89. Wiesener, M. S., Munchenhagen, P. M., Berger, I., Morgan, N. V., Roigas, J., Schwiertz, A., Jurgensen, J. S., Gruber, G., Maxwell, P. H., Loning, S. A., Frei, U., Maher, E. R., Grone, H. J., and Eckardt, K. U. Constitutive activation of hypoxia-inducible genes related to overexpression of hypoxia-inducible factor-1alpha in clear cell renal carcinomas, Cancer Res. *61:* 5215-22., 2001.

90. Turner, K. J., Moore, J. W., Jones, A., Taylor, C. F., Cuthbert-Heavens, D., Han, C., Leek, R. D., Gatter, K. C., Maxwell, P. H., Ratcliffe, P. J., Cranston, D., and Harris, A. L. Expression of hypoxia-inducible factors in human renal cancer: relationship to angiogenesis and to the von Hippel-Lindau gene mutation, Cancer Res. *62:* 2957-61., 2002.

91. Dammann, R., Li, C., Yoon, J. H., Chin, P. L., Bates, S., and Pfeifer, G. P. Epigenetic inactivation of a RAS association domain family protein from the lung tumour suppressor locus 3p21.3, Nat Genet. *25:* 315-9., 2000.

92. Dreijerink, K., Braga, E., Kuzmin, I., Geil, L., Duh, F. M., Angeloni, D., Zbar, B., Lerman, M. I., Stanbridge, E. J., Minna, J. D., Protopopov, A., Li, J., Kashuba, V., Klein, G., and Zabarovsky, E. R. The candidate tumor suppressor gene, RASSF1A, from human chromosome 3p21.3 is involved in kidney tumorigenesis, Proc Natl Acad Sci U S A. *98:* 7504-9., 2001.

93. Morrissey, C., Martinez, A., Zatyka, M., Agathanggelou, A., Honorio, S., Astuti, D., Morgan, N. V., Moch, H., Richards, F. M., Kishida, T., Yao, M., Schraml, P., Latif, F., and Maher, E. R. Epigenetic inactivation of the RASSF1A 3p21.3 tumor suppressor gene in both clear cell and papillary renal cell carcinoma, Cancer Res. *61:* 7277-81., 2001.

94. Dammann, R., Yang, G., and Pfeifer, G. P. Hypermethylation of the cpG island of Ras association domain family 1A (RASSF1A), a putative tumor suppressor gene from the 3p21.3 locus, occurs in a large percentage of human breast cancers, Cancer Res. *61:* 3105-9., 2001.

95. Dammann, R., Takahashi, T., and Pfeifer, G. P. The CpG island of the novel tumor suppressor gene RASSF1A is intensely methylated in primary small cell lung carcinomas, Oncogene. *20:* 3563-7., 2001.

96. Liu, L., Yoon, J. H., Dammann, R., and Pfeifer, G. P. Frequent hypermethylation of the RASSF1A gene in prostate cancer, Oncogene. *21:* 6835-40., 2002.

97. Yoon, J. H., Dammann, R., Pfeifer, G. P., Liu, L., Tommasi, S., Wilczynski, S. P., Li, C., Chin, P. L., and Bates, S. Hypermethylation of the CpG island of the RASSF1A gene in ovarian and renal cell carcinomas

Methylation of the RASSF1A gene in human cancers

Epigenetic inactivation of a RAS association domain family protein from the lung tumour suppressor locus 3p21.3, Int J Cancer. *94:* 212-7., 2001.

98. Spugnardi, M., Tommasi, S., Dammann, R., Pfeifer, G. P., and Hoon, D. S. Epigenetic inactivation of RAS association domain family protein 1 (RASSF1A) in malignant cutaneous melanoma, Cancer Res. *63:* 1639-43., 2003.

99. Vavvas, D., Li, X., Avruch, J., and Zhang, X. F. Identification of Nore1 as a potential Ras effector, J Biol Chem. *273:* 5439-42., 1998.

100. Sanchez, Y., el-Naggar, A., Pathak, S., and Killary, A. M. A tumor suppressor locus within 3p14-p12 mediates rapid cell death of renal cell carcinoma in vivo, Proc Natl Acad Sci U S A. *91:* 3383-7., 1994.

101. Lott, S. T., Lovell, M., Naylor, S. L., and Killary, A. M. Physical and functional mapping of a tumor suppressor locus for renal cell carcinoma within chromosome 3p12, Cancer Res. *58:* 3533-7, 1998.

102. Lovell, M., Lott, S. T., Wong, P., El-Naggar, A., Tucker, S., and Killary, A. M. The genetic locus NRC-1 within chromosome 3p12 mediates tumor suppression in renal cell carcinoma independently of histological type, tumor microenvironment, and VHL mutation, Cancer Res. *59:* 2182-9, 1999.

103. Barrans, J. D., Allen, P. D., Stamatiou, D., Dzau, V. J., and Liew, C. C. Global gene expression profiling of end-stage dilated cardiomyopathy using a human cardiovascular-based cDNA microarray, Am J Pathol. *160:* 2035-43., 2002.

104. Wang, G., Zhang, Y., Chen, B., and Cheng, J. Preliminary studies on Alzheimer's disease using cDNA microarrays, Mech Ageing Dev. *124:* 115-24., 2003.

105. Jazaeri, A. A., Yee, C. J., Sotiriou, C., Brantley, K. R., Boyd, J., and Liu, E. T. Gene expression profiles of BRCA1-linked, BRCA2-linked, and sporadic ovarian cancers, J Natl Cancer Inst. *94:* 990-1000., 2002.

106. Takahashi, M., Fujita, M., Furukawa, Y., Hamamoto, R., Shimokawa, T., Miwa, N., Ogawa, M., and Nakamura, Y. Isolation of a novel human gene, APCDD1, as a direct target of the beta-Catenin/T-cell factor 4 complex with probable involvement in colorectal carcinogenesis, Cancer Res. *62:* 5651-6., 2002.

107. Udtha, M., Lee, S. J., Alam, R., Coombes, K., and Huff, V. Upregulation of c-MYC in WT1-mutant tumors: assessment of WT1 putative transcriptional targets using cDNA microarray expression profiling of genetically defined Wilms' tumors, Oncogene. *22:* 3821-6., 2003.

108. Alizadeh, A. A., Eisen, M. B., Davis, R. E., Ma, C., Lossos, I. S., Rosenwald, A., Boldrick, J. C., Sabet, H., Tran, T., Yu, X., Powell, J. I., Yang, L., Marti, G. E., Moore, T., Hudson, J., Jr., Lu, L., Lewis, D. B., Tibshirani, R., Sherlock, G., Chan, W. C., Greiner, T. C., Weisenburger, D. D., Armitage, J. O., Warnke, R., Staudt, L. M., and et al. Distinct types of diffuse large B-cell lymphoma identified by gene expression profiling, Nature. *403:* 503-11., 2000.

109. Bittner, M., Meltzer, P., Chen, Y., Jiang, Y., Seftor, E., Hendrix, M., Radmacher, M., Simon, R., Yakhini, Z., Ben-Dor, A., Sampas, N., Dougherty, E., Wang, E., Marincola, F., Gooden, C., Lueders, J., Glatfelter, A., Pollock, P., Carpten, J., Gillanders, E., Leja, D., Dietrich, K., Beaudry, C., Berens, M., Alberts, D., and Sondak, V. Molecular classification of cutaneous malignant melanoma by gene expression profiling, Nature. *406:* 536-40., 2000.

110. Heighway, J., Knapp, T., Boyce, L., Brennand, S., Field, J. K., Betticher, D. C., Ratschiller, D., Gugger, M., Donovan, M., Lasek, A., and Rickert, P. Expression profiling of primary non-small cell lung cancer for target identification, Oncogene. *21:* 7749-63., 2002.

111. Leung, S. Y., Chen, X., Chu, K. M., Yuen, S. T., Mathy, J., Ji, J., Chan, A. S., Li, R., Law, S., Troyanskaya, O. G., Tu, I. P., Wong, J., So, S., Botstein, D., and Brown, P. O. Phospholipase A2 group IIA expression in gastric adenocarcinoma is associated with prolonged survival and less frequent metastasis, Proc Natl Acad Sci U S A. *99:* 16203-8., 2002.

112. Iacobuzio-Donahue, C. A., Maitra, A., Olsen, M., Lowe, A. W., van Heek, N. T., Rosty, C., Walter, K., Sato, N., Parker, A., Ashfaq, R., Jaffee, E., Ryu, B., Jones, J., Eshleman, J. R., Yeo, C. J., Cameron, J. L., Kern, S. E., Hruban, R. H., Brown, P. O., and Goggins, M. Exploration of global gene expression patterns in pancreatic adenocarcinoma using cDNA microarrays, Am J Pathol. *162:* 1151-62., 2003.

113. Dan, S., Tsunoda, T., Kitahara, O., Yanagawa, R., Zembutsu, H., Katagiri, T., Yamazaki, K., Nakamura, Y., and Yamori, T. An integrated database of chemosensitivity to 55 anticancer

drugs and gene expression profiles of 39 human cancer cell lines, Cancer Res. *62:* 1139-47., 2002.

114. Ohno, R. and Nakamura, Y. Prediction of response to imatinib by cDNA microarray analysis, Semin Hematol. *40:* 42-9., 2003.

115. Kononen, J., Bubendorf, L., Kallioniemi, A., Barlund, M., Schraml, P., Leighton, S., Torhorst, J., Mihatsch, M. J., Sauter, G., and Kallioniemi, O. P. Tissue microarrays for high-throughput molecular profiling of tumor specimens, Nat Med. *4:* 844-847, 1998.

116. Schoenberg Fejzo, M. and Slamon, D. J. Frozen tumor tissue microarray technology for analysis of tumor RNA, DNA, and proteins, Am J Pathol. *159:* 1645-50., 2001.

117. Moch, H., Schraml, P., Bubendorf, L., Mirlacher, M., Kononen, J., Gasser, T., Mihatsch, M. J., Kallioniemi, O. P., and Sauter, G. High-throughput tissue microarray analysis to evaluate genes uncovered by cDNA microarray screening in renal cell carcinoma, Am J Pathol. *154:* 981-986, 1999.

118. Sallinen, S. L., Sallinen, P. K., Haapasalo, H. K., Helin, H. J., Helen, P. T., Schraml, P., Kallioniemi, O. P., and Kononen, J. Identification of differentially expressed genes in human gliomas by DNA microarray and tissue chip techniques., Cancer Res. *60:* 6617-6622, 2000.

119. Sanchez-Carbayo, M., Socci, N. D., Charytonowicz, E., Lu, M., Prystowsky, M., Childs, G., and Cordon-Cardo, C. Molecular profiling of bladder cancer using cDNA microarrays: defining histogenesis and biological phenotypes, Cancer Res. *62:* 6973-80., 2002.

120. Giordano, T. J., Thomas, D. G., Kuick, R., Lizyness, M., Misek, D. E., Smith, A. L., Sanders, D., Aljundi, R. T., Gauger, P. G., Thompson, N. W., Taylor, J. M., and Hanash, S. M. Distinct transcriptional profiles of adrenocortical tumors uncovered by DNA microarray analysis, Am J Pathol. *162:* 521-31., 2003.

121. Freshney, R. I. Culture of Animal Cells-A Manual of Basic Technique: Wiley-Liss, 1987.

122. Romeis B., D. H., Künzle H., Plenk H. jr., and Sellner W. Mikroskopische Technik, p. 179-249. München: Urban & Schwarzenberg, 1989.

123. Ausubel Frederick M, B. R., Kingston Robert E., Moore David D., Seidman J. G., Smith John A., Struhl Kevin Current Protocols in Molecular Biology, Vol. 1: Current Protocols: Greene Publishing Associates, Inc. and John Wiley & Sons, Inc., 1994.

124. Melamed, J., Kernizan, S., and Walden, P. D. Expression of B-cell translocation gene 2 protein in normal human tissues, Tissue Cell. *34:* 28-32., 2002.

125. Fletcher, B. S., Lim, R. W., Varnum, B. C., Kujubu, D. A., Koski, R. A., and Herschman, H. R. Structure and expression of TIS21, a primary response gene induced by growth factors and tumor promoters, J Biol Chem. *266:* 14511-8., 1991.

126. Bradbury, A., Possenti, R., Shooter, E. M., and Tirone, F. Molecular cloning of PC3, a putatively secreted protein whose mRNA is induced by nerve growth factor and depolarization, Proc Natl Acad Sci U S A. *88:* 3353-7., 1991.

127. Rouault, J. P., Falette, N., Guehenneux, F., Guillot, C., Rimokh, R., Wang, Q., Berthet, C., Moyret-Lalle, C., Savatier, P., Pain, B., Shaw, P., Berger, R., Samarut, J., Magaud, J. P., Ozturk, M., Samarut, C., and Puisieux, A. Identification of BTG2, an antiproliferative p53-dependent component of the DNA damage cellular response pathway, Nat Genet. *14:* 482-6., 1996.

128. Walden, P. D., Lefkowitz, G. K., Ficazzola, M., Gitlin, J., and Lepor, H. Identification of genes associated with stromal hyperplasia and glandular atrophy of the prostate by mRNA differential display, Exp Cell Res. *245:* 19-26., 1998.

129. Duggan, D. J., Bittner, M., Chen, Y., Meltzer, P., and Trent, J. M. Expression profiling using cDNA microarrays, Nat Genet. *21:* 10-4., 1999.

130. Fryer, R. M., Randall, J., Yoshida, T., Hsiao, L. L., Blumenstock, J., Jensen, K. E., Dimofte, T., Jensen, R. V., Gullans, S. R., Ouchida, M., Fukushima, K., Gunduz, E., Ito, S., Sakai, A., Nagai, N., Nishizaki, K., and Shimizu, K. Global analysis of gene expression: methods, interpretation, and pitfalls, Exp Nephrol. *10:* 64-74., 2002.

131. Hanna, E., Shrieve, D. C., Ratanatharathorn, V., Xia, X., Breau, R., Suen, J., and Li, S. A novel alternative approach for prediction of radiation response of squamous cell carcinoma of head and neck, Cancer Res. *61:* 2376-80., 2001.

132. Wasenius, V. M., Hemmer, S., Kettunen, E., Knuutila, S., Franssila, K., and Joensuu, H. Hepatocyte growth factor receptor, matrix metalloproteinase-11, tissue inhibitor of metalloproteinase-1, and fibronectin are up-regulated in papillary thyroid carcinoma: a cDNA and tissue microarray study, Clin Cancer Res. *9:* 68-75., 2003.

133. El-Rifai, W., Frierson, H. F., Jr., Harper, J. C., Powell, S. M., and Knuutila, S. Expression profiling of gastric adenocarcinoma using cDNA array, Int J Cancer. *92:* 832-8., 2001.

134. Masuda, N., Ohnishi, T., Kawamoto, S., Monden, M., and Okubo, K. Analysis of chemical modification of RNA from formalin-fixed samples and optimization of molecular biology applications for such samples, Nucleic Acids Res. *27:* 4436-43., 1999.

135. Werner, M., Chott, A., Fabiano, A., and Battifora, H. Effect of formalin tissue fixation and processing on immunohistochemistry, Am J Surg Pathol. *24:* 1016-9., 2000.

136. Ross, D. T., Scherf, U., Eisen, M. B., Perou, C. M., Rees, C., Spellman, P., Iyer, V., Jeffrey, S. S., Van de Rijn, M., Waltham, M., Pergamenschikov, A., Lee, J. C., Lashkari, D., Shalon, D., Myers, T. G., Weinstein, J. N., Botstein, D., and Brown, P. O. Systematic variation in gene expression patterns in human cancer cell lines, Nat Genet. *24:* 227-35., 2000.

137. Ross, D. T. and Perou, C. M. A comparison of gene expression signatures from breast tumors and breast tissue derived cell lines, Dis Markers. *17:* 99-109., 2001.

138. Dangles, V., Lazar, V., Validire, P., Richon, S., Wertheimer, M., Laville, V., Janneau, J. L., Barrois, M., Bovin, C., Poynard, T., Vallancien, G., and Bellet, D. Gene expression profiles of bladder cancers: evidence for a striking effect of in vitro cell models on gene patterns, Br J Cancer. *86:* 1283-9., 2002.

139. Young, A. N., Amin, M. B., Moreno, C. S., Lim, S. D., Cohen, C., Petros, J. A., Marshall, F. F., and Neish, A. S. Expression profiling of renal epithelial neoplasms: a method for tumor classification and discovery of diagnostic molecular markers, Am J Pathol. *158:* 1639-51., 2001.

140. Pati, D., Keller, C., Groudine, M., and Plon, S. E. Reconstitution of a MEC1-independent checkpoint in yeast by expression of a novel human fork head cDNA, Mol Cell Biol. *17:* 3037-46., 1997.

141. Rouse, J. and Jackson, S. P. Interfaces between the detection, signaling, and repair of DNA damage, Science. *297:* 547-51., 2002.

142. Coleman William B., T. G. J. Genomic Instability in the Development of Human Cancer. *In:* G. J. T. William B. Coleman (ed.) The Molecular Basis of Human Cancer, pp. 115-142. Totowa: Humana Press Inc., 2002.

143. Ejima, Y., Yang, L., and Kazanietz, M. G. Determination of the genotype of a panel of human tumor cell lines for the human homologues of yeast cell cycle checkpoint control genes: identification of cell lines carrying homoallelic missense base substitutions, Somat Cell Mol Genet. *25:* 41-8., 1999.

144. Myokai, F., Takashiba, S., Lebo, R., and Amar, S. A novel lipopolysaccharide-induced transcription factor regulating tumor necrosis factor alpha gene expression: molecular cloning, sequencing, characterization, and chromosomal assignment, Proc Natl Acad Sci U S A. *96:* 4518-23., 1999.

145. Idriss, H. T. and Naismith, J. H. TNF alpha and the TNF receptor superfamily: structure-function relationship(s), Microsc Res Tech. *50:* 184-95., 2000.
146. Locksley, R. M., Killeen, N., and Lenardo, M. J. The TNF and TNF receptor superfamilies: integrating mammalian biology, Cell. *104:* 487-501., 2001.
147. Ting, J. P., Trowsdale, J., and Kazanietz, M. G. Genetic control of MHC class II expression, Cell. *109 Suppl:* S21-33., 2002.
148. Gastl, G., Ebert, T., Finstad, C. L., Sheinfeld, J., Gomahr, A., Aulitzky, W., and Bander, N. H. Major histocompatibility complex class I and class II expression in renal cell carcinoma and modulation by interferon gamma, J Urol. *155:* 361-7., 1996.
149. Saito, T., Kimura, M., Kawasaki, T., Sato, S., and Tomita, Y. MHC class II antigen-associated invariant chain on renal cell cancer may contribute to the anti-tumor immune response of the host, Cancer Lett. *115:* 121-7., 1997.
150. Vora, A. R., Rodgers, S., Parker, A. J., Start, R., Rees, R. C., Murray, A. K., and Kazanietz, M. G. An immunohistochemical study of altered immunomodulatory molecule expression in head and neck squamous cell carcinoma, Br J Cancer. *76:* 836-44., 1997.
151. Kunihiro, M., Tanaka, S., Haruma, K., Yoshihara, M., Sumii, K., Kajiyama, G., Shimamoto, F., and Kazanietz, M. G. Combined expression of HLA-DR antigen and proliferating cell nuclear antigen correlate with colorectal cancer prognosis, Oncology. *55:* 326-33., 1998.
152. Lovig, T., Andersen, S. N., Thorstensen, L., Diep, C. B., Meling, G. I., Lothe, R. A., Rognum, T. O., and Kazanietz, M. G. Strong HLA-DR expression in microsatellite stable carcinomas of the large bowel is associated with good prognosis, Br J Cancer. *87:* 756-62., 2002.
153. Ishigami, S., Natsugoe, S., Tokuda, K., Nakajo, A., Iwashige, H., Aridome, K., Hokita, S., and Aikou, T. Invariant chain expression in gastric cancer, Cancer Lett. *168:* 87-91., 2001.
154. Kenck, C., Bugert, P., Wilhelm, M., and Kovacs, G. Duplication of an approximately 1.5 Mb DNA segment at chromosome 5q22 indicates the locus of a new tumour gene in nonpapillary renal cell carcinomas, Oncogene. *14:* 1093-8, 1997.
155. Bugert, P., Von Knobloch, R., and Kovacs, G. Duplication of two distinct regions on chromosome 5q in non-papillary renal-cell carcinomas, Int J Cancer. *76:* 337-40., 1998.
156. Jiang, Z., Xu, M., Savas, L., LeClair, P., and Banner, B. F. Invariant chain expression in colon neoplasms, Virchows Arch. *435:* 32-6., 1999.

157. Tirone, F. The gene PC3(TIS21/BTG2), prototype member of the PC3/BTG/TOB family: regulator in control of cell growth, differentiation, and DNA repair?, J Cell Physiol. *187:* 155-65., 2001.

158. Montagnoli, A., Guardavaccaro, D., Starace, G., and Tirone, F. Overexpression of the nerve growth factor-inducible PC3 immediate early gene is associated with growth inhibition, Cell Growth Differ. *7:* 1327-36., 1996.

159. Iacopetti, P., Barsacchi, G., Tirone, F., Maffei, L., and Cremisi, F. Developmental expression of PC3 gene is correlated with neuronal cell birthday, Mech Dev. *47:* 127-37., 1994.

160. Iacopetti, P., Michelini, M., Stuckmann, I., Oback, B., Aaku-Saraste, E., and Huttner, W. B. Expression of the antiproliferative gene TIS21 at the onset of neurogenesis identifies single neuroepithelial cells that switch from proliferative to neuron-generating division, Proc Natl Acad Sci U S A. *96:* 4639-44., 1999.

161. Lim, I. K., Lee, M. S., Ryu, M. S., Park, T. J., Fujiki, H., Eguchi, H., and Paik, W. K. Induction of growth inhibition of 293 cells by downregulation of the cyclin E and cyclin-dependent kinase 4 proteins due to overexpression of TIS21, Mol Carcinog. *23:* 25-35., 1998.

162. Guardavaccaro, D., Corrente, G., Covone, F., Micheli, L., D'Agnano, I., Starace, G., Caruso, M., and Tirone, F. Arrest of G(1)-S progression by the p53-inducible gene PC3 is Rb dependent and relies on the inhibition of cyclin D1 transcription, Mol Cell Biol. *20:* 1797-815., 2000.

163. Cortes, U., Moyret-Lalle, C., Falette, N., Duriez, C., Ghissassi, F. E., Barnas, C., Morel, A. P., Hainaut, P., Magaud, J. P., and Puisieux, A. BTG gene expression in the p53-dependent and -independent cellular response to DNA damage, Mol Carcinog. *27:* 57-64., 2000.

164. Duriez, C., Falette, N., Audoynaud, C., Moyret-Lalle, C., Bensaad, K., Courtois, S., Wang, Q., Soussi, T., and Puisieux, A. The human BTG2/TIS21/PC3 gene: genomic structure, transcriptional regulation and evaluation as a candidate tumor suppressor gene, Gene. *282:* 207-14., 2002.

165. Prevot, D., Voeltzel, T., Birot, A. M., Morel, A. P., Rostan, M. C., Magaud, J. P., and Corbo, L. The leukemia-associated protein Btg1 and the p53-regulated protein Btg2 interact with the homeoprotein Hoxb9 and enhance its transcriptional activation, J Biol Chem. *275:* 147-53., 2000.

166. Prevot, D., Morel, A. P., Voeltzel, T., Rostan, M. C., Rimokh, R., Magaud, J. P., and Corbo, L. Relationships of the antiproliferative proteins BTG1 and BTG2 with CAF1, the human

homolog of a component of the yeast CCR4 transcriptional complex: involvement in estrogen receptor alpha signaling pathway, J Biol Chem. *276:* 9640-8., 2001.

167. Lin, W. J., Gary, J. D., Yang, M. C., Clarke, S., and Herschman, H. R. The mammalian immediate-early TIS21 protein and the leukemia-associated BTG1 protein interact with a protein-arginine N-methyltransferase, J Biol Chem. *271:* 15034-44., 1996.

168. Berthet, C., Guehenneux, F., Revol, V., Samarut, C., Lukaszewicz, A., Dehay, C., Dumontet, C., Magaud, J. P., and Rouault, J. P. Interaction of PRMT1 with BTG/TOB proteins in cell signalling: molecular analysis and functional aspects, Genes Cells. *7:* 29-39., 2002.

169. Kwak, Y. T., Guo, J., Prajapati, S., Park, K. J., Surabhi, R. M., Miller, B., Gehrig, P., and Gaynor, R. B. Methylation of SPT5 regulates its interaction with RNA polymerase II and transcriptional elongation properties, Mol Cell. *11:* 1055-66., 2003.

170. Smith, J. J., Rucknagel, K. P., Schierhorn, A., Tang, J., Nemeth, A., Linder, M., Herschman, H. R., and Wahle, E. Unusual sites of arginine methylation in Poly(A)-binding protein II and in vitro methylation by protein arginine methyltransferases PRMT1 and PRMT3, J Biol Chem. *274:* 13229-34., 1999.

171. Tang, J., Kao, P. N., and Herschman, H. R. Protein-arginine methyltransferase I, the predominant protein-arginine methyltransferase in cells, interacts with and is regulated by interleukin enhancer-binding factor 3, J Biol Chem. *275:* 19866-76., 2000.

172. Nichols, R. C., Wang, X. W., Tang, J., Hamilton, B. J., High, F. A., Herschman, H. R., and Rigby, W. F. The RGG domain in hnRNP A2 affects subcellular localization, Exp Cell Res. *256:* 522-32., 2000.

173. Cote, J., Boisvert, F. M., Boulanger, M. C., Bedford, M. T., and Richard, S. Sam68 RNA binding protein is an in vivo substrate for protein arginine N-methyltransferase 1, Mol Biol Cell. *14:* 274-87., 2003.

174. Strahl, B. D., Briggs, S. D., Brame, C. J., Caldwell, J. A., Koh, S. S., Ma, H., Cook, R. G., Shabanowitz, J., Hunt, D. F., Stallcup, M. R., and Allis, C. D. Methylation of histone H4 at arginine 3 occurs in vivo and is mediated by the nuclear receptor coactivator PRMT1, Curr Biol. *11:* 996-1000., 2001.

175. Dubrez, L., Coll, J. L., Hurbin, A., de Fraipont, F., Lantejoul, S., and Favrot, M. C. Cell cycle arrest is sufficient for p53-mediated tumor regression, Gene Ther. *8:* 1705-12., 2001.

176. Ookawa, K., Shiseki, M., Takahashi, R., Yoshida, Y., Terada, M., and Yokota, J. Reconstitution of the RB gene suppresses the growth of small-cell lung carcinoma cells carrying multiple genetic alterations, Oncogene. *8:* 2175-81., 1993.

177. Frizelle, S. P., Grim, J., Zhou, J., Gupta, P., Curiel, D. T., Geradts, J., and Kratzke, R. A. Re-expression of p16INK4a in mesothelioma cells results in cell cycle arrest, cell death, tumor suppression and tumor regression, Oncogene. *16:* 3087-95., 1998.

178. Smith, N. D., Rubenstein, J. N., Eggener, S. E., and Kozlowski, J. M. The p53 tumor suppressor gene and nuclear protein: basic science review and relevance in the management of bladder cancer, J Urol. *169:* 1219-28., 2003.

179. Hickman, E. S., Moroni, M. C., and Helin, K. The role of p53 and pRB in apoptosis and cancer, Curr Opin Genet Dev. *12:* 60-6., 2002.

180. Castagna, M., Takai, Y., Kaibuchi, K., Sano, K., Kikkawa, U., and Nishizuka, Y. Direct activation of calcium-activated, phospholipid-dependent protein kinase by tumor-promoting phorbol esters, J Biol Chem. *257:* 7847-51., 1982.

181. Mellor, H. and Parker, P. J. The extended protein kinase C superfamily, Biochem J. *332:* 281-92., 1998.

182. Kazanietz, M. G. Eyes wide shut: protein kinase C isozymes are not the only receptors for the phorbol ester tumor promoters, Mol Carcinog. *28:* 5-11., 2000.

183. Kazanietz, M. G. Novel "nonkinase" phorbol ester receptors: the C1 domain connection Eyes wide shut: protein kinase C isozymes are not the only receptors for the phorbol ester tumor promoters, Mol Pharmacol. *61:* 759-67., 2002.

184. Liu, W. S., Heckman, C. A., and Kazanietz, M. G. The sevenfold way of PKC regulation, Cell Signal. *10:* 529-42., 1998.

185. Zeidman, R., Pettersson, L., Sailaja, P. R., Truedsson, E., Fagerstrom, S., Pahlman, S., and Larsson, C. Novel and classical protein kinase C isoforms have different functions in proliferation, survival and differentiation of neuroblastoma cells, Int J Cancer. *81:* 494-501., 1999.

186. Pfaff, I. L., Wagner, H. J., and Vallon, V. Immunolocalization of protein kinase C isoenzymes alpha, beta1 and betaII in rat kidney, J Am Soc Nephrol. *10:* 1861-73., 1999.

187. Boczan, J., Boros, S., Mechler, F., Kovacs, L., and Biro, T. Differential expressions of protein kinase C isozymes during proliferation and differentiation of human skeletal muscle cells in vitro, Acta Neuropathol (Berl). *99:* 96-104., 2000.

188. Moriarty, P., Dickson, A. J., Erichsen, J. T., and Boulton, M. Protein kinase C isoenzyme expression in retinal cells, Ophthalmic Res. *32:* 57-60., 2000.

189. Jaken, S. Protein kinase C isozymes and substrates, Curr Opin Cell Biol. *8:* 168-73., 1996.

190. Barth, H., Kinzel, V., and Kazanietz, M. G. Phorbol ester TPA rapidly prevents activation of p34cdc2 histone H1 kinase and concomitantly the transition from G2 phase to mitosis in synchronized HeLa cells, Exp Cell Res. *212:* 383-8., 1994.

191. Detjen, K. M., Brembeck, F. H., Welzel, M., Kaiser, A., Haller, H., Wiedenmann, B., and Rosewicz, S. Activation of protein kinase Calpha inhibits growth of pancreatic cancer cells via p21(cip)-mediated G(1) arrest, J Cell Sci. *113:* 3025-35., 2000.

192. Garzotto, M., White-Jones, M., Jiang, Y., Ehleiter, D., Liao, W. C., Haimovitz-Friedman, A., Fuks, Z., and Kolesnick, R. 12-O-tetradecanoylphorbol-13-acetate-induced apoptosis in LNCaP cells is mediated through ceramide synthase, Cancer Res. *58:* 2260-4., 1998.

193. Zheng, X., Ravatn, R., Lin, Y., Shih, W. C., Rabson, A., Strair, R., Huberman, E., Conney, A., and Chin, K. V. Gene expression of TPA induced differentiation in HL-60 cells by DNA microarray analysis, Nucleic Acids Res. *30:* 4489-99., 2002.

194. Knudson, A. Mutation and cancer: Statistical study of retinoblastoma, Proc Natl Acad Sci USA. *68:* 820-823, 1971.

195. Macleod, K. Tumor suppressor genes, Curr Opin Genet Dev. *10:* 81-93., 2000.

196. Reinartz, J. J. Cancer genes. *In:* C. W. B. a. T. G. J. (ed.) The Molecular Basis of Human Cancer, pp. 45-64. Totowa: Humana Press, 2002.

197. Jones, P. A. and Laird, P. W. Cancer epigenetics comes of age, Nat Genet. *21:* 163-7., 1999.

198. Chen, L. C., Dollbaum, C., and Smith, H. S. Loss of heterozygosity on chromosome 1q in human breast cancer, Proc Natl Acad Sci U S A. *86:* 7204-7., 1989.

199. Fero, M. L., Randel, E., Gurley, K. E., Roberts, J. M., and Kemp, C. J. The murine gene p27Kip1 is haplo-insufficient for tumour suppression, Nature. *396:* 177-80., 1998.

200. Bai, F., Pei, X. H., Godfrey, V. L., and Xiong, Y. Haploinsufficiency of p18(INK4c) sensitizes mice to carcinogen-induced tumorigenesis, Mol Cell Biol. *23:* 1269-77., 2003.

201. Tang, B., Bottinger, E. P., Jakowlew, S. B., Bagnall, K. M., Mariano, J., Anver, M. R., Letterio, J. J., and Wakefield, L. M. Transforming growth factor-beta1 is a new form of tumor suppressor with true haploid insufficiency, Nat Med. *4:* 802-7., 1998.

202. Venkatachalam, S., Tyner, S. D., Pickering, C. R., Boley, S., Recio, L., French, J. E., and Donehower, L. A. Is p53 haploinsufficient for tumor suppression? Implications for the p53+/- mouse model in carcinogenicity testing, Toxicol Pathol. *29 Suppl:* 147-54., 2001.

203. Lerman, M. I. and Minna, J. D. The 630-kb lung cancer homozygous deletion region on human chromosome 3p21.3: identification and evaluation of the resident candidate tumor suppressor genes. The International Lung Cancer Chromosome 3p21.3 Tumor Suppressor Gene Consortium, Cancer Res. *60:* 6116-33., 2000.

204. Kondo, K., Yao, M., Kobayashi, K., Ota, S., Yoshida, M., Kaneko, S., Baba, M., Sakai, N., Kishida, T., Kawakami, S., Uemura, H., Nagashima, Y., Nakatani, Y., and Hosaka, M. PTEN/MMAC1/TEP1 mutations in human primary renal-cell carcinomas and renal carcinoma cell lines, Int J Cancer. *91:* 219-224., 2001.

205. Chen, C., Bhalala, H. V., Qiao, H., and Dong, J. T. A possible tumor suppressor role of the KLF5 transcription factor in human breast cancer, Oncogene. *21:* 6567-72., 2002.

206. Chen, C., Bhalala, H. V., Vessella, R. L., and Dong, J. T. KLF5 is frequently deleted and down-regulated but rarely mutated in prostate cancer, Prostate. *55:* 81-8., 2003.

207. Kallioniemi, O., Kallioniemi, A., Piper, J., Isola, J., Waldman, F., Gray, J., and Pinkel, D. Optimizing comparative genomic hybridization for analysis of DNA sequence copy number changes in solid tumors, Genes Chromosom Cancer. *10:* 231-243, 1994.

7 Curriculum vitae

Persönliche Daten

Geburtsdatum	19. November 1973
Geburtsort	Köln-Porz
Nationalität	Deutsche

Ausbildung

1980 - 1984 **Grundschule Köln-Porz und Otterberg (Rheinland-Pfalz)**

1984 – 1993 **Gymnasium an der Burgstrasse in Kaiserslautern (Rheinland-Pfalz)**

Abitur im Mai 1993

1993 - 1999 **Biologiestudium an der Universität in Kaiserslautern**

Diplom im August 1999

Titel der Diplomarbeit: „DNS-Sequenzanalyse des Tumorsuppressorgens p16 an klarzelligen Nierenzellkarzinomen“.

1999 – 2003 **Doktorarbeit am Institut für Pathologie der Universität Basel**

Promotion im November 2003

Titel der Doktorarbeit: „Differential gene expression screening uncovers downregulation of the cell cycle regulator BTG2 as an important step in renal tumor biology“.

An der Ausbildung beteiligte Dozenten:

- Prof. Dr. med. Christoph Moroni (Fakultätsverantwortlicher; Institut für Medizinische Mikrobiologie, Basel)
- Prof. Dr. Nancy Hynes (Korreferentin; FMI, Basel)
- Prof. Dr. med Holger Moch (direkter Betreuer; Institut für Pathologie Basel)

Besuch von Vorlesungen/Seminaren bei folgenden Dozenten:

- Prof. Dr. Max Burger (FMI, Basel)
- PD Dr. rer nat. Rolf Jessberger (Universität, Basel)

- Prof. Dr. R. Gisler (Institut für Immunologie, Basel)
- Prof. Dr. U. A. Meyer (Universität, Basel)
- Prof Dr. T. A. Bickle (Universität, Basel)
- PD Dr. R. G. Clerc (Biozentrum, Basel)
- PD Dr. Raija Lindberg (Pharmazentrum, Basel)
- PD Dr. Dieter Kunz (Universität, Basel)
- Sowie bei den an der Ausbildung beteiligten Dozenten

Berufserfahrung

5/1997 – 12/1998	Studienbegleitendes Arbeiten im Bereich der PCR-Diagnostik am Institut für Immunologie und Genetik des Westpfalsklinikums in Kaiserslautern
12/2003 – 4/2004	Anstellung als Post-Doc am Institut für Pathologie in Basel. Forschungsschwerpunkt: Nierentumorbiologie
seit 5/2004	Anstellung als Post-Doc am Institut für Klinische Pathologie des Universitätsspitals Zürich. Forschungsschwerpunkt: Nierentumorbiologie

Publikationen

1. **Schraml P., Struckmann K., Bednar R., Fu W., Gasser T., Wilber K., Kononen J., Sauter G., Mihatsch M.J., Moch H.**
   CDKN2A mutation analysis, protein expression, and deletion mapping of chromosome 9p in conventional clear-cell renal cell carcinomas: evidence for a second tumor suppressor gene proximal to CDKN2A.
   Am J Pathol. 2001 Feb(2): 593-601

2. **Schraml P., Struckmann K., Hatz F., Sonnet S., Gasser T., Sauter G., Mihatsch M. J., Moch H.**
   VHL mutations and their correlation with tumor cell proliferation, microvessel density, and patient prognosis in clear cell renal cell carcinoma.
   J Pathol. 2002 Feb; 196(2): 186-93

3. **Simon R., Struckmann K., Schraml P., Wagner U:; Forster T., Moch H., Fijan A., Bruderer J., Wilber K., Mihatsch M. J., Gasser T., Sauter G.**
   Amplification pattern of 12q13-q15 (MDM2, CDK4, GLI) in urinary bladder cancer.
   Oncogene. 2002 Apr 11; 21(16): 2476-83

4. **Struckmann K., Schraml P., Simon R., Elmenhorst K., Mirlacher M., Kononen J., Moch H.**
   Impaired expression of the cell cycler regulator BTG2 is common in clear cell renal cell carcinoma

Cancer Res. 2004Mar 1; 64(5):1632-8

5. **Bruder E., Passera O., Harms D., Leuschner I., Ladanyi M., Argani P., Eble J. N., Struckmann K., Schraml P., Moch H.**
   Morphologic and molecular characterization of renal cell carcinoma in children and young adults
   Am J Surg Pathol. 2004 Sep; 28(9): 1117-32